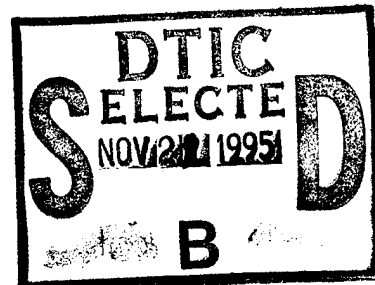


AN INVESTIGATION OF THE CAUSES OF OPTICAL AND INFRARED AIRGLOW STRUCTURES IN THE MESOSPHERE

Edmond M. Dewan

17 October 1994



APPROVED FOR PUBLIC RELEASE; DISTRIBUTION UNLIMITED.

19951120 093

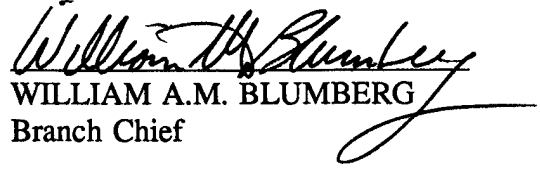
DTIC QUALITY INSPECTED 5

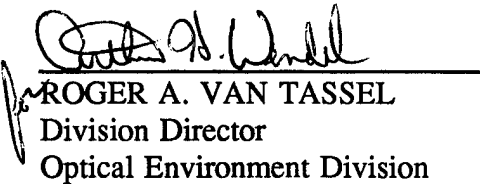


PHILLIPS LABORATORY
Directorate of Geophysics
AIR FORCE MATERIEL COMMAND
HANSCOM AIR FORCE BASE, MA 01731-3010

REPRODUCED BY AUTOMATIC PROCESS
FROM THE BEST COPY AVAILABLE
THIS WILL BE AN INKLESS AND
FADINGLESS COPY

"This technical report has been reviewed and is approved for publication"


WILLIAM A.M. BLUMBERG
Branch Chief


ROGER A. VAN TASSEL
Division Director
Optical Environment Division

This report has been reviewed by the ESC Public Affairs Office (PA) and is releasable to the National Technical Information Service (NTIS).

Qualified requestors may obtain additional copies from the Defense Technical Information Center.
All others should apply to the National Technical Information Service.

If your address has changed, or if you wish to be removed from the mailing list, or if the addressee is no longer employed by your organization, please notify PL/TSI, Hanscom AFB, MA 01731-3010. This will assist us in maintaining a current mailing list.

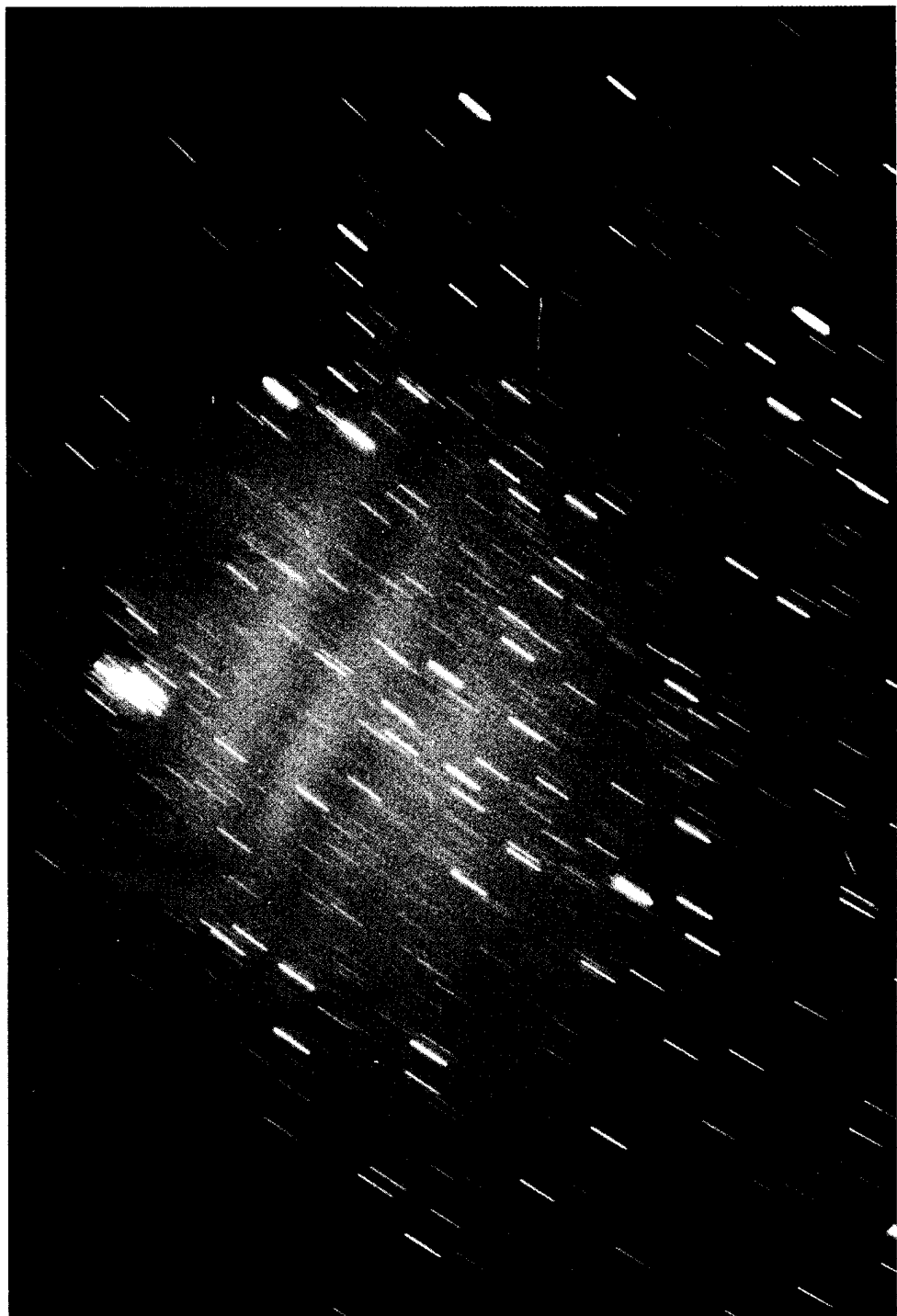
Do not return copies of this report unless contractual obligations or notices on a specific document requires that it be returned.

REPORT DOCUMENTATION PAGE

Form Approved
OMB No. 0704-0188

Public reporting burden for this collection of information is estimated to average 1 hour per response, including the time for reviewing instructions, searching existing data sources, gathering and maintaining the data needed, and completing and reviewing the collection of information. Send comments regarding this burden estimate or any other aspect of this collection of information, including suggestions for reducing this burden, to Washington Headquarters Services, Directorate for Information Operations and Reports, 1215 Jefferson Davis Highway, Suite 1204, Arlington, VA 22202-4302, and to the Office of Management and Budget, Paperwork Reduction Project (0704-0188), Washington, DC 20503.

1. AGENCY USE ONLY (Leave blank)			2. REPORT DATE 17 October 1994	3. REPORT TYPE AND DATES COVERED Scientific, Interim	
4. TITLE AND SUBTITLE An Investigation of the Causes of Optical and Infrared Airglow Structures in the Mesosphere			5. FUNDING NUMBERS PE 61102F 2310G504		
6. AUTHOR(S) Edmond M. Dewan					
7. PERFORMING ORGANIZATION NAME(S) AND ADDRESS(ES) PL/GPOS 29 Randolph Road Hanscom AFB, MA 01731-3010			8. PERFORMING ORGANIZATION REPORT NUMBER PL-TR-94-2261 ERP, No. 1163		
9. SPONSORING/MONITORING AGENCY NAME(S) AND ADDRESS(ES) AFOSR, Bolling AFB, Washington, D.C.			10. SPONSORING/MONITORING AGENCY REPORT NUMBER		
11. SUPPLEMENTARY NOTES					
12a. DISTRIBUTION / AVAILABILITY STATEMENT Approved for public release; Distribution unlimited			12b. DISTRIBUTION CODE		
13. ABSTRACT (Maximum 200 words) <p>The MAPSTAR program was both a theoretical and experimental investigation of airglow structure and its causes. We found that the most important cause of the structures is atmospheric gravity waves, and that thunderstorms are a clearly identified source of the waves responsible for such structure. We also studied many related issues. In addition, two new instruments were designed and fabricated during this program. These were the MAPSTAR infrared Michelson interferometer and the MAPSTAR radar imaging Doppler interferometer. The latter instrument has played the crucial role in removing discrepancies between different methods of radar wind profiling. Structures investigated under MAPSTAR give rise to system clutter; thus having direct impact upon Air Force surveillance operations from space.</p>					
14. SUBJECT TERMS Gravity waves, Airglow infrared clutter, Mesospheric dynamics			15. NUMBER OF PAGES 98		
16. PRICE CODE					
17. SECURITY CLASSIFICATION OF REPORT Unclassified	18. SECURITY CLASSIFICATION OF THIS PAGE Unclassified	19. SECURITY CLASSIFICATION OF ABSTRACT Unclassified	20. LIMITATION OF ABSTRACT SAR		



Example of a Time-lapse Photograph Showing (presumably) both OH (red) and Un-ionized Atomic Oxygen (green) Structures in the Airglows (Peterson).

Accession For	
NTIS GRA&I	<input checked="" type="checkbox"/>
DTIC TAB	<input type="checkbox"/>
Unannounced	<input type="checkbox"/>
Justification _____	
By _____	
Distribution/ _____	
Availability Codes	
Dist	Avail and/or Special
R	

Contents

1.	THE MAPSTAR PROGRAM	1
1.1	Air Force Relevance	1
1.2	Overview of Report	2
1.3	Airglow Structure	2
1.4	Gravity Waves and IR Structure	4
1.4.1	Geometry of Internal Gravity Wave Propagation	5
1.4.2	OH Infrared Airglow	5
2.	MAPSTAR FIELD CAMPAIGNS	8
2.1	The Sacramento Peak Campaign	9
2.2	Campaign at Book Lake, Colorado	11
2.3	MAPSTAR/MISTI Campaign at Poker Flat, Alaska	15
2.4	MAC/EPSILON Campaign in Northern Scandinavia	17
2.5	MAPSTAR Colorado Campaign	19
2.6	AIDA Campaign at Arecibo, Puerto Rico	25
2.7	The ALOHA-90 Campaign	25
2.8	Other MAPSTAR-related Campaigns	26
3.	IMAGING OF OH AIRGLOW WAVE STRUCTURE	26
3.1	Circular Waves in Airglow	26
3.2	Direct Comparison Between OH Wave Structure in Sky Images and in Interferometer Measurements	27
3.3	Structure Sky Cover and the Kink in the Radiometer Power Spectra-Relation to Bright Nights	28

Contents

3.4	The Question of Bright Nights	31
3.5	Ripple Waves and Their Origins	31
3.6	Horizon to Horizon Sinusoidal Waves	32
3.7	Simultaneous Color Imaging of OH, OI, and Na Airglow	34
4.	WAVE PROPAGATION, CRITICAL LAYERS, AND AIR PARCEL TRAJECTORIES	34
4.1	Wind-Profile Blockage of Upwelling Gravity Waves	34
4.2	Gravity-Wave Air Parcel Trajectories	35
4.3	Effects of Wave Orientation Upon Ground-Based Measurements of Airglow Temperature and Brightness Fluctuations	36
4.4	Gravity-wave Ducting	36
5.	THE POWER SPECTRAL DENSITIES (PSD'S) OF GRAVITY WAVES - THEORY AND EXPERIMENT	38
5.1	History of Gravity-Wave Saturation Studies	38
5.2	Gravity-Wave Frequency Spectra	40
5.3	Gravity-Wave-Induced Temperature Fluctuations	41
5.4	Potential Applications	41
6.	MAPSTAR OH AIRGLOW TEMPERATURE AND BRIGHTNESS FLUCTUATIONS	43
6.1	Temperature Power Spectra: Model Compared to Data	43
6.2	Processing of Data Having Gaps or Intervals of Missing Information	43
6.3	OH Airglow Brightness Power Spectra	43
6.4	OH Temperature-Brightness Cross-Spectra	47
6.5	Source of Brightness Fluctuations and Photochemical/Dynamical Models	47
7.	NEW INSTRUMENTATION	47
7.1	The MAPSTAR Radar and the IDI (Imaging Doppler Interferometer) Method of Adams and Brosnahan	47
7.2	Infra-Red Field Widened Interferometer (IRFWI)	49
7.3	The Infrared MAPSTAR Interferometer/Spectrometer	49
8.	EXPERIMENTAL FINDINGS OF MAPSTAR	50
8.1	Regarding Gravity-Wave-Driven OH Airglow Findings	50
8.1.1	Orographic Effects on OH Structure	50
8.1.2	<i>In-Situ</i> Gravity Wave Generation	51
8.1.3	Simultaneous Radar and Imager Observations	51
8.1.4	Co-Variation of the Temperature and Intensity of OH Airglow	51

Contents

8.1.5 Simultaneous Ground Measurements of OH Temperature by Means of Lidar and Interferometer/Spectrometer	52
8.2 Findings on Wind Measurements	52
8.2.1 PSDs of Stratospheric Wind Components	52
8.2.2 Definitive Mesospheric Radar Wind Profile Measurement Comparison	52
8.2.3 IDI Tidal Measurements	53
9. OH MOLECULAR SPECTROSCOPY AND MESOPAUSE-REGION TEMPERATURE MEASUREMENTS	53
10. RESPONSE OF AIRGLOW BRIGHTNESS TO WAVES	55
11. RESULTS ON NOCTILUCENT CLOUDS, AURORAS, SOLAR INFLUENCE, AND "BRIGHT NIGHTS"	56
11.1 Pulsating Auroras	56
11.2 Nightglow and Noctilucent Clouds (NLCs)	56
11.3 Bright Nights (BNs) and Thunderstorms	58
11.4 Noctilucent Clouds (NLCs) and Polar Mesospheric Summer Echoes (PMSEs)	58
11.5 Sunspot-Weather Correlations: Are They Real?	59
11.6 Sound Waves in Airglow Structure?	59
12. RESEARCH QUESTIONS RAISED BY MAPSTAR ON WAVE-DRIVEN AIRGLOW AND ASSOCIATED TOPICS	60
REFERENCES	81

Illustrations

<i>Frontispiece:</i> Example of a Time-Lapse Photograph showing (presumably) both OH (red) and Atomic Oxygen (green) structure in the Airglows	ii
1. Concentric Gravity Wave Patterns over the Matterhorn (from M. Taylor, Ph.D. Thesis).	3
2. Schematic Diagram of Phase Progression (up to down) Together with Group Velocity (lower left to upper right). The group velocity is in the phase plane.	6
3. Thunderstorm Induced Gravity Waves: Airglow Structure	7
4. Map of Campaign Instrument Location and an Example of OH Imager Results (Taylor)	21
5. OH TV Image with Crossed Circle Marking the Position of Co-Aligned Interferometer Field of View (Taylor). The dark region at the center is due to a defect in the camera tube.	22
6. Example of PSD of Brightness Variation of OH Layer Viewed at Zenith by Means of a Photometer (Espy).	29
7. Correlation Between the Frequency Position of the PSD "Break" (see Figure 6) and the Percent of Sky Covered with "Structure" (Espy).	30
8. Example of All-Sky Image of OH Brightness Showing a Train of Sine Waves Propagating from Horizon to Horizon (Peterson).	33
9. Simulated Orbit of an Air Parcel moved by a 6 Minute Period Gravity Wave. Longer periods would have more linear trajectories (Tuan).	37
10. Well Known Example of Universal PSD (vertical wave number, horizontal speeds) of Gravity Waves in the Lower Stratosphere (Dewan, Good, Grossbard et al).	39

Illustrations

11.	Scales of Turbulent Inner and Outer Scales as Well as Wave "Outer" Scales Estimated by Dewan for the Science Modeling Requirements Document (SMRD) for the Midcourse Space Experiment (MSX).	42
12.	Temperature Spectra (fitted line) Showing $\omega^{-5/3}$ Slopes (temporal frequency) and Amplitude in Agreement with Observed ϵ Values as Predicted by Cascade Scaling (Dewan, Pendleton, Espy, and Grossbard).	44
13.	(a) PSD of Brightness Variation in OH (Lowe et al), (b) PSD of Temperature Variation of OH (Lowe et al). These were obtained from Mt. Haleakela, Hawaii during the 1990 ALOHA Campaign.	45
14.	Results of a Cross-Spectral Analysis of the Signals (temperature and brightness) Shown in Figure 13. (a) Shows phase and (b) the coherence between the signals. The upper and lower curves were intended to represent "error bars" relating to plus or minus one standard deviation. The main conclusion is that for the main frequencies of interest (10^{-3} Hz to 5.5×10^{-4} Hz) or 5 min. (buoyancy period) to 1/2 hour there is a coherence around 0.1 and the phase is around 0°	46
15.	Plot of Zenith Intensity for Cycle 11 as Determined from the Video Records. The sketches show the all-sky auroral activity at several instances during this cycle. The hatched areas show the pulsating patches and the shaded areas the bright arcs to the north.	57

Tables

1.	Boot Lake Campaign; Instrumentation/Location	12
2.	Boot Lake Campaign; Observing Windows	24

Preface

This program was monitored at AFOSR by Lt. Col. James Koermer and Lt. Col. James Stobie. Major participants outside Phillips Laboratory included G. Adams, S. Avery, D. Baker, J. Brosnahan, P. Espy, D. Fritts, C. Hines, R. Lowe, A. Peterson, W. Pendleton, M. Taylor, T.-F. Tuan, D. Turnbull, J. Ulwick, G. Ware and numerous graduate students at their institutions (see Bibliography), many of whom have become well-known for these and subsequent accomplishments.

In its initial stages the MAPSTAR Program was managed by R. Armstrong, A. Ratkowski, R. O'Neil, and R. Picard.

I thank R. Picard and J. Winick for very many helpful suggestions regarding the MAPSTAR Program and R. Picard for many suggestions concerning the present manuscript.

Finally I thank R. Lowe, M. Taylor, W. Pendleton, P. Espy, and R. Picard for writing sections of the report. Gene Adams, the IDI principal investigator, died before publication of his reports, and the special issue of JATP devoted to AIDA was dedicated to his memory.

When MAPSTAR started, the imaging of airglow was in its infancy, and the only people doing it in the world (Taylor and Peterson) were members of our team. At present, Dr. M. Taylor is the most internationally prominent scientist in this area and much has been learned from his work.

In conclusion, the MAPSTAR project went beyond the reasonable expectations with which it started.

Executive Summary

Theater missiles (such as SCUDS in the Gulf War) continue to pose a threat to US interests in future conflicts. Surveillance from space is therefore necessary to detect missile launches. This has given rise to the "Brilliant Eyes" and "Alarm" systems, for example. Unfortunately, these systems can be severely hampered by highly structured infrared radiance emitted from the hydroxyl layer located at 85 km altitude in the earth's atmosphere. As a result the Air Force must cope with infrared (IR) "systems clutter" which can both create false targets and obscure real targets. The purpose of MAPSTAR was to obtain as much knowledge as possible about the causes of the IR structure. This was to enable the Air Force to cope as effectively as possible with clutter by designing the systems appropriate for this task.

Seven field campaigns were conducted under MAPSTAR, two new instruments were developed, approximately 50 scientific publications and 60 presentations came out as end products. This work is described in detail in this report.

The major question was "What in fact causes the structure in the hydroxyl airglow layer?" Our conclusion is that it is caused by temperature fluctuations induced by internal atmospheric gravity waves. These waves (sometimes seen in clouds) are generated by such things as thunderstorms and jet streams. They become more intense as they ascend in altitude; and, when they reach the 85 km region of the hydroxyl layer, they are large enough to cause significant height and temperature variations. These in turn give rise to brightness variations due to density variations (associated with the height variations) and also to temperature and density dependent photochemical reactions.

An important factor controlling whether or not the gravity waves generated in the troposphere ever reach the mesosphere (for example, 85 km) is the mean winds located at

Executive Summary

intermediate altitudes. Theory shows what kind of wind profiles can block waves of given properties, and one of the outcomes of the analysis was that in fact those sources (thunderstorms) that theory predicted would be isolated from the mesosphere indeed were, and vice versa. The theory also explained why mountain waves never appeared in the airglow during the campaigns. In short, theory and experiment were in complete agreement regarding this kind of "wind filtering" of gravity waves.

Part of the MAPSTAR project was to create an Imaging Doppler Interferometer (IDI) radar system. Unfortunately completion of this radar could not be funded. In spite of this unfortunate circumstance, the IDI radar receiver, which had been completed, was used in the AIDA campaign (which took place in Puerto Rico), together with other wind profiler instruments. The role of transmitter was played by the Arecibo "heater". The purpose of the campaign was to compare the results of differing techniques to measure winds as a function of altitude and to decide, at last, which altitudes gave mutual agreement and which did not. It was known that something was "wrong" ahead of time and the issue was considered to be of the greatest importance. It was learned that above 85 km the wind profilers diverged in their results in regard to gravity wave induced winds. As for tidal information, there was again, mutual agreement even above 85 km provided appropriate averaging was done.

The most important product of the MAPSTAR program was the combination of both the experimental and theoretical power spectral results. The agreement between measurement and theory is better than could have been anticipated. More specifically, the power spectra of temperature were studied. The AF relevance arises from the fact that temperature spectra (due to gravity waves) are directly related to the brightness variations (previously denoted "IR clutter" here). The connection is described by a parameter called "Krassovski Eta" (which is defined as the ratio of the fractional variation of brightness to that of temperature). Thus the MAPSTAR spectra can lead directly to the structure computer codes needed by the AF for system designs. In our experimental temperature-brightness spectral comparisons it was found that in contrast to some theories, the brightness variation is almost directly proportional to temperature variation and this would be a great simplification in appropriate circumstances.

An Investigation of the Causes of Optical and Infrared Airglow Structures in the Mesosphere

1. INTRODUCTION

MAPSTAR (Middle Atmosphere Periodic Structured Associated Radiance) was a coordinated experimental and theoretical investigation of upper atmospheric infrared and optical structure. Its primary goal was to find a scientific explanation for the observed patterns in the mesospheric and lower thermospheric visible airglow such as that emitted by O and Na, and in the OH infrared emissions in particular. It was conducted between 1985 and 1993 and was sponsored by AFOSR. In this report we summarize some of the MAPSTAR results on mesospheric optical structure.

1.1 Air Force Relevance

Surveillance from space of Infrared (IR) targets (such as rockets and rocket plumes) is hampered by spatial patterns in the infrared airglow. These patterns affect Air Force systems in the form of "IR clutter". The clutter is caused by the emissions from layers in the earth's mesosphere and lower thermosphere and it forms a structured background with which surveillance systems must cope. Thus the clutter can potentially cause false targets and obscure true targets. For this reason, the Air Force needs to understand as much as possible about the physical and chemical mechanisms causing the problem. This will allow designers to provide system specifications that will minimize clutter effects on system performance.

(Received for publication 26 October 1994)

1.2 Overview of Report

This report begins with a brief description of gravity waves, and then discusses a number of experimental field campaigns in which, to varying degrees, there was MAPSTAR participation. The main findings of MAPSTAR are then presented. These descriptions are quite brief, but they are organized by category to provide the context in which the findings fit together. The details will be found in existing reports, journal articles, and theses (PhD and Masters), plus presentations now being prepared for publication. These are all referenced. We also anticipate that the data obtained during the MAPSTAR campaigns will result in future publications in a new program known as SOAR (Structural Optical Atmospheric Radiance).

The MAPSTAR results are included in the following categories: (a) airglow imaging (as exemplified in Figure 1¹), (b) gravity wave propagation and associated velocity fluctuations, (c) gravity wave power spectral theory and its application to MAPSTAR data, (d) new radar and IR interferometer concepts and technology, (e) experimental findings concerning OH structure and radar winds (using the MAPSTAR radar), (f) basic findings in the molecular spectroscopy of OH emission, (g) findings in wave effects on airglow, and finally, (h) subjects related to airglow such as wave driven noctilucent clouds and aurora. The text concludes with a list of questions that are presently unanswered. These suggest directions for current and future research. At the report's conclusion will be found a list of publications (by categories) and presentations under MAPSTAR.

The following institutions were the principal collaborators with Phillips Laboratory in this program: Utah State University, University of Western Ontario, University of Cincinnati, and University of Southampton.

1.3 Airglow Structure

The MAPSTAR program is concerned mainly with airglow in the OH Meinel bands, which is emitted from an atmospheric layer approximately 7 km thick at 85 km altitude.^{*} The emitting species are excited states of the hydroxyl radical, OH. The Meinel bands of the OH free radical consist of a large set of rovibrational transitions that emit over a broad range of wavelengths from the visible to the near and mid infrared. Taken as a whole, they are the component of the nightglow containing the most energy, and they are observable from the ground in the visible region of the spectrum and again near 1.5 μm in the infrared.

The structure in the visible and infrared images of the sky (from TV, camera, CCDs) has been described for years in the literature, notably by Peterson, Kieffaber, and Taylor of the MAPSTAR team. The patterns were classified into categories such as: (a) broad bands, (b)

¹Taylor, M.J. (1985) *Observation and Analysis of Wave-like Structures in the Lower Thermospheric Nightglow Emissions*, Ph.D. Thesis, Southampton University, U.K.

*Airglow was first discovered around the turn of the century in the visible wavelengths (557.7 nm). The source of airglow was ultimately identified as electronic transitions of un-ionized atomic oxygen in a layer of atmosphere (about 95 km) in the lower thermosphere. The discoverer, the fourth Lord Rayleigh, called it "non-polar aurora."



**Figure 1. Concentric Gravity Wave Patterns Over the Matterhorn
(from M. Taylor, Ph.D. Thesis).**

narrow stripes, (c) curved structures, (d) ripples, and (e) diffuse patchy structures. As an example of (c) consider Figure 1. It is an image obtained by M. Taylor which, as will be described below, is circular because the source of the waves that made the pattern was at the center of the concentric circles.

One of the goals of MAPSTAR was to ascertain the cause of the IR and visible structures. Initially the list of possibilities included turbulence, acoustic compression waves, atmospheric gravity or buoyancy waves, and tides. At the completion of the program it was found that by far the dominant source was the gravity waves. For this reason this report will be dominated by the subject of atmospheric gravity waves.

1.4 Gravity Waves and IR Structure

Atmospheric gravity waves, like all waves, must have a "restoring force" acting in opposition to "inertia". For gravity waves, the restoring force is buoyancy (which is caused by the fact that the air is in a gravitational field). At almost all altitudes the atmosphere is stable. This means that, if a parcel of air is vertically displaced and then released, it will experience a buoyancy force causing it to accelerate toward its original altitude. Inertia will cause it to go beyond, or overshoot, that altitude and hence the parcel will oscillate about its (equilibrium) position. In some sense these waves are exactly like the waves on the surface of bodies of water, which waves, in fact, are also called gravity waves. (They are different in the sense that the change in density for surface waves is large and sudden (water to air) as opposed to small and gradual). In the troposphere (which extends from the ground up to 17 km, depending on location) the minimum period of the wave is on the order of 8 minutes; whereas above the troposphere this period is shorter and closer to 5 minutes (but varies with altitude). The maximum wave frequency goes by two names, the Brunt-Vaisala frequency and the buoyancy frequency. This frequency was first derived by the third Lord Rayleigh, father of the Lord Rayleigh who discovered airglow. Waves usually have longer periods than the minimum, and commonly are found with periods of tens of minutes to many hours. These longer periods result when the wave-induced air parcel trajectories have horizontal components. The more horizontal the fluid wave motion is, the longer its period becomes. There is an upper limit to the wave period known as the inertial period, which is due to the earth's rotation. At the poles the inertial period is 12 hours, but it increases toward the equator, reaching infinity there. (See Gossard and Hooke²). The sources of the waves include weather fronts, jet streams, thunderstorms, hurricanes, wind over mountains (mountain waves), tsunami ocean waves, seismic waves, and large explosions.

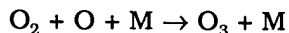
²Gossard, E., and Hooke, W. (1975) *Waves in the Atmosphere*, Amsterdam, Elsevier.

1.4.1 GEOMETRY OF INTERNAL GRAVITY WAVE PROPAGATION

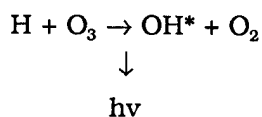
Gravity waves possess a unique and, at first sight, very surprising feature. This is shown in Figure 2 which depicts how the phase velocity and group velocity are mutually perpendicular. (The phase velocity is ω/k whereas the group velocity is $\partial\omega/\partial k$)². This is a surprise because in acoustic waves, waves upon fluid surfaces, electromagnetic waves in free space, and so forth, the group and phase velocities are in the same direction. As is well known (Gossard and Hooke, 1975) the energy of any wave travels in the direction of the group velocity. For this reason the energy propagates *along the phase fronts* of the gravity waves, *not* normal to them in the direction of the phase propagation. Figure 3 shows this more vividly for a wave launched by a thunderstorm. The direction of energy flow (or group velocity) is controlled by the wave frequency. Lower frequencies travel more horizontally while higher frequencies propagate energy in a direction closer to the vertical.

1.4.2 OH INFRARED AIRGLOW

As was mentioned in Section 1.3, the OH layer is at around 85 km altitude. Other airglow layers in this region are at 90 km (yellow sodium airglow) and 95 km (atomic oxygen green line). The OH airglow is due to chemiluminescence that commences with the production of ozone from ambient atomic oxygen:



This is followed by the production of vibrationally excited hydroxyl (OH)* by reaction with H, which then radiates a photon.



The gravity waves induce brightness variations in the OH airglow by a complicated process. The waves cause changes in temperature and total density. These, in turn, cause changes in the density of emitters as well as changes in the rates of chemical reactions. This interaction can be significantly nonlinear.

The gravity-wave-induced temperature changes, on the other hand, can be much more simply explained. They are caused by a combination of acoustic compressions and rarefactions, without the need for altitude change, together with compressions and rarefaction associated with buoyancy forces that are directly due to altitude changes. The simplification is in the fact that for the waves that one sees in the airglow, the temperature changes can be regarded as due *only* to the adiabatic expansions and contractions of parcel volumes as they go up and down in altitude. The acoustic compressions and rarefactions can be neglected.

THUNDERSTORM INDUCED GRAVITY WAVES

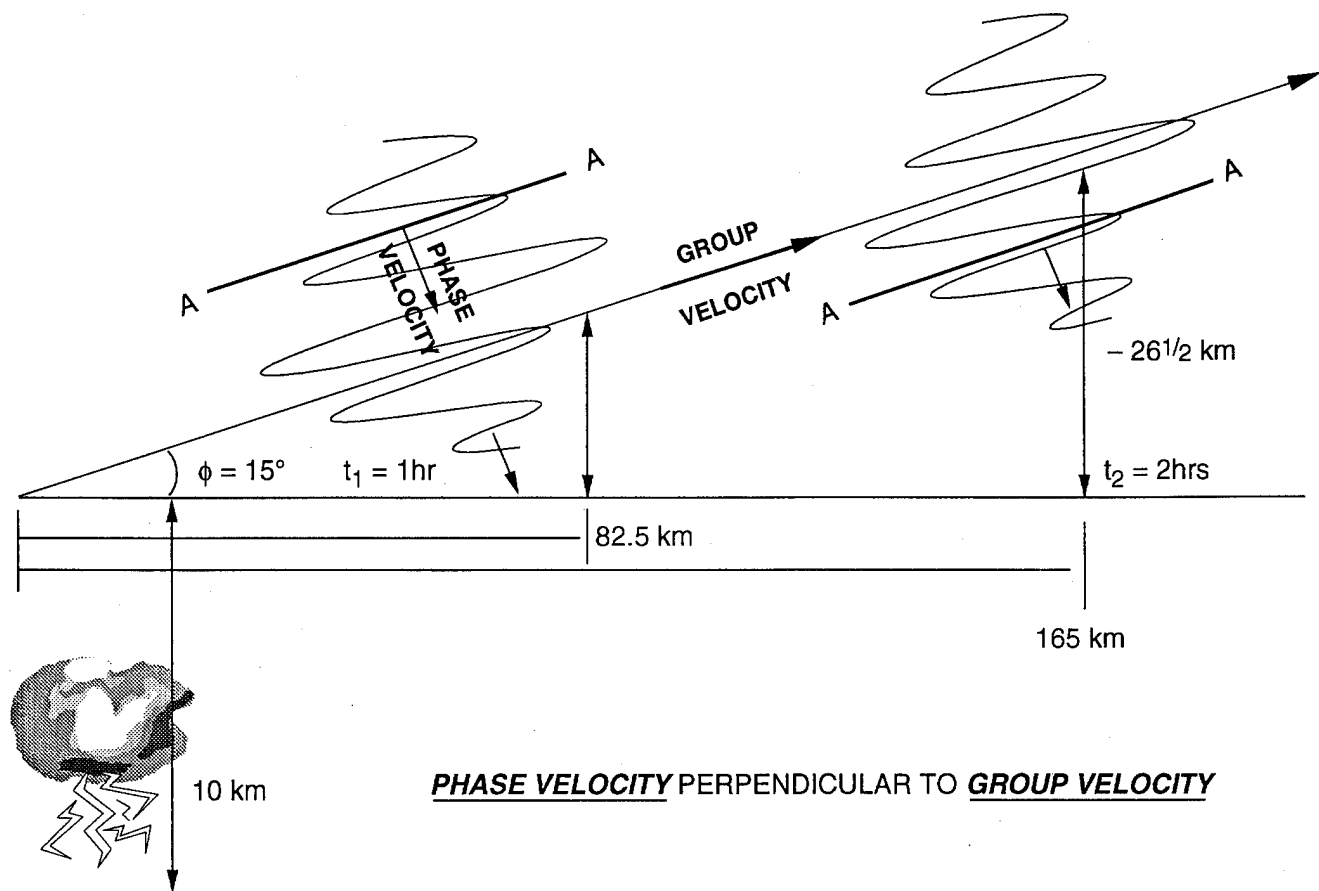


Figure 2. Schematic Diagram of Phase Progression (up to down), Together with Group Velocity (lower left to upper right). The group velocity is in the phase plane.

THUNDERSTORM INDUCED GRAVITY WAVES: AIRGLOW STRUCTURE

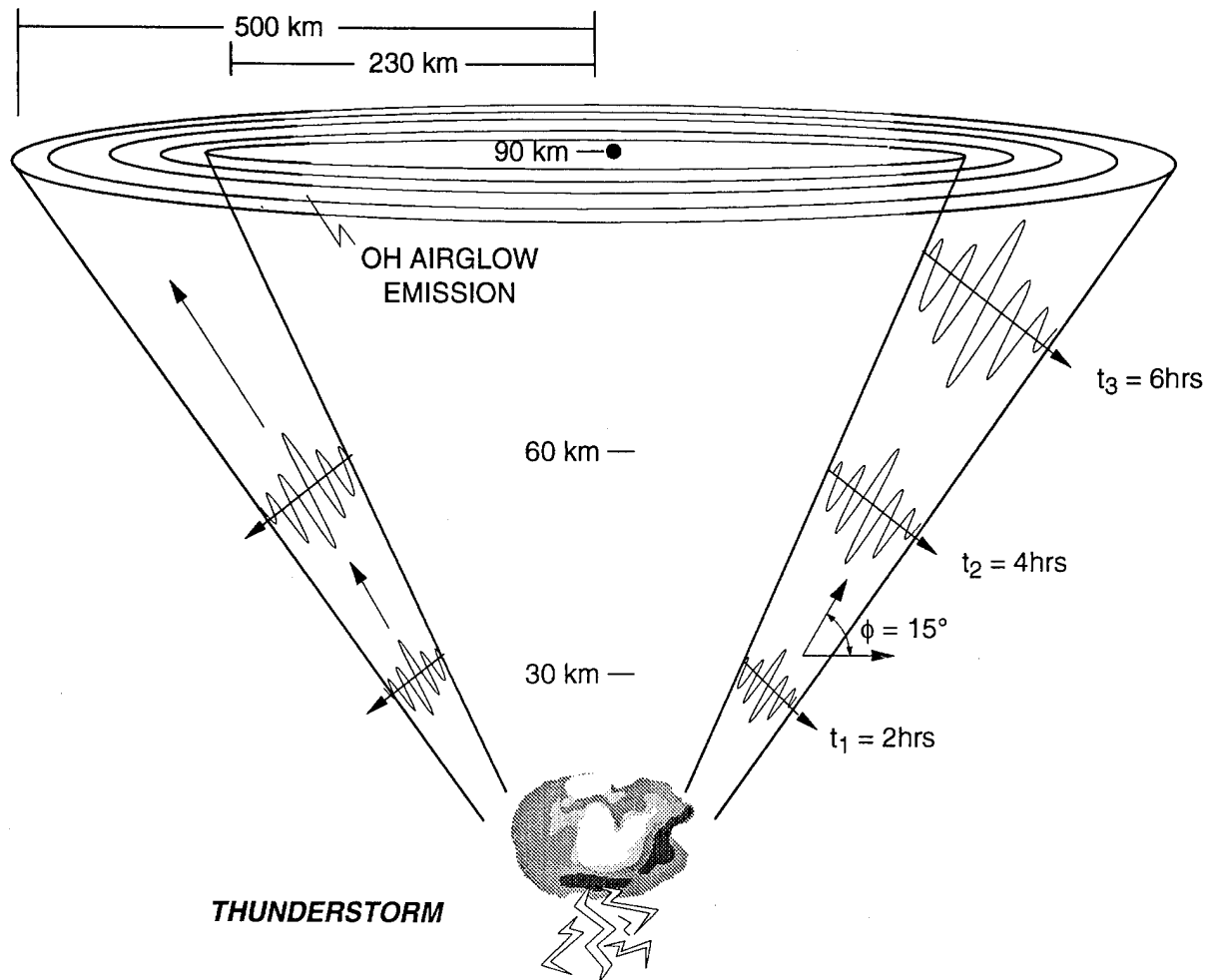


Figure 3. Schematic of Thunderstorm-Generated Wave Propagation of a Single Frequency.
In reality such waves have a preferential direction.

We have found (see Section 5) that the typical structures seen in the OH images are explained entirely by the altitude changes in air parcels caused by the waves. Unfortunately, both brightness and temperature, as measured from the ground, are influenced by line-of-sight effects. This means that the temperatures one measures are "brightness weighted" averages along the line of sight; and brightness measurements are due to an emitting column along this direction. Below, and in the publications, these factors are discussed in more detail.

2. MAPSTAR FIELD CAMPAIGNS

The MAPSTAR team either played a major role or were the sole participants in the following list of campaigns.

1. Sacramento Peak (New Mexico, June, 1983) (precursor, but data were analyzed during MAPSTAR)
2. Boot Lake (Colorado, June, 1984)
3. MAPSTAR/MISTI Campaign (Poker Flat, Alaska, August, 1986)
4. MAC/EPSILON (N. Scandinavia, October, 1987)
5. MAPSTAR Colorado Campaign '88 (May, June, and July, 1988)
6. AIDA (Puerto Rico, April, 1989)
7. ALOHA (Hawaii, April, 1990)

Objectives of the MAPSTAR campaigns:

1. Sacramento Peak
 - a. Test the concept of the use of an imager and Fourier spectrometer to get overlapping OH data that are mutually consistent.
 - b. Obtain information on OH behavior during the summer at a midlatitude location.
2. Boot Lake
 - a. Continue project under 1.b. above.
 - b. The main objective was to establish a "proof of concept" of the IDI prototype and its use in concert with imagers and the Fourier spectrometer.
3. MISTI
 - a. Measure high latitude airglow behavior.
 - b. Measure noctilucent cloud behavior in conjunction with airglow behavior.

(This experiment used, in addition to imagers and spectrometers, the Chatanika MST radar as well as rockets.)

4. Colorado

- a. It was configured to; (a) compare zenith looking as well as slant range looking imaging and spectroscopic observations, and (b) stereo viewing of the OH layer.
- b. Special attention was focused upon thunderstorm sources capable of generating waves with the appropriate parameters to have ray trajectories penetrating the airglow layer; which is to say, the effects of wind filtering on wave paths from the troposphere to mesopause were well documented and taken into account when source to OH image identifications were made.
- c. The most important goals of this campaign were; (a) to create a theory for the power spectra of the OH temperature variations over time, (b) to measure these variations in temperature in OH at 85 km by spectral means, and (c) to compare theory with experiment.

(This was a three month long campaign (midlatitude summer). It involved imagers, the Platteville radar, and interferometers.)

5. MAC/EPSILON

- a. Two kinds of instruments were deployed. They were; (a) the IR Field Widened Interferometer Fourier spectrometer, and (b) two imagers. The predicted overcast inhibited the more ambitious plan of more spectrometers, etc.
- b. Reports based on IRFWI and imager information have been published on this data; but the unexpected, unplanned achievement was a correlated observation of auroral images with micropulsations at the same time.

6. ALOHA 90

- a. This campaign was designed to examine the difference between OH structures in a mountainous continental location and a midocean location. (There was much less difference than anticipated when the comparisons were made.)
- b. Results were published in a special issue of GRL. As will be seen from the text, all the goals have been achieved with the exception of; (a) stereo OH imaging, and (b) the slant vs zenith effects. The stereo imaging was defeated in part by the diffuse character of the images, whereas goal (b) remains on hold until priority and funds permit future work.

2.1 The Sacramento Peak Campaign (contributed by M. Taylor)

This campaign, the earliest in the MAPSTAR sequence, consisted of simultaneous imaging (University of Southampton) and Michelson interferometer (Utah State University)

measurements of the OH emission at mid-latitudes. The data obtained during this campaign were novel and results have strongly influenced the emphasis and direction of the MAPSTAR measurements.

The experimental instruments consisted of a low-light television camera (field-of-view 15° horizontal by 11° vertical) filtered to observe structure in the near infrared OH nightglow emission, co-aligned with a narrow field (0.8° circular), IR Michelson interferometer. The interferometer measured several OH Meinel bands rapidly at a given point within the TV image, allowing the intensity and the thermal signatures of the short-period gravity wave patterns to be uniquely determined. The television camera was mounted directly onto the interferometer telescope, and the location of the interferometer sample volume within the TV field was recorded by observing the positions of several known stars. Observations were made from Sacramento Peak NM (32.8° N, 105.8° W, 2820 m above sea level) during the new-moon period in June 1983. The measurements were made primarily at low elevation angles (typically 15° at field center) to facilitate the detection of wave structure.

The data have been analyzed to determine the spatial and temporal behavior of a well-formed short period (13.7 ± 1.2 min) wave pattern that was observed during the "bright night" display of 14/15 June. Coherent wave forms were observed for nearly 3 hours and detailed measurements were obtained. The temperature variations were relatively small (< 10 K), and in most cases the intensity wave preceded the temperature wave, but only by a small amount. We found the ratio of the relative amplitude of the intensity wave to the temperature wave (the Krassovsky η parameter) to be $\eta = 8$. This was considerably higher than predicted using the (then) existing models. Much in-house MAPSTAR effort has since been focused on modelling the response of the OH emission to gravity waves.

Spatial analysis of the pattern indicated an average horizontal wave length of 23 ± 1 km moving with a uniform velocity of 28 ± 2 m/s towards the north. Two large, bright bands were also visible to the unaided eye during this display. Their location, shape and orientation were similar to those imaged at near-IR wavelengths, but they appeared much broader. These forms probably arose from nightglow emissions at visible wavelengths perturbed by the same wave motion. Indeed, similar wave structure was also imaged in the OI (557.7 nm) line emission. Measurements using a 391.4 nm photometer confirmed that there was no local auroral precipitation during this display. The results of this investigation have been presented at several scientific meetings in Europe and the USA and have recently been published in the journal *Planetary and Space Science*. (Taylor et al³, 1991).

³Taylor, M.J., Espy, P.J., Baker, D.J., Sica, R.J., Neal, P.C., and Pendleton, W.R., Jr. (1991) Simultaneous intensity, temperature, and imaging measurements of short period wave structure in the OH nightglow emission, *Planet. Space Sci.*, 39:1171.

2.2 Campaign at Boot Lake, Colorado - June, 1984 (written by Wm. Pendleton)

The Boot Lake Campaign took place in Colorado, the primary site being Boot Lake, at 40° N latitude, during the June 1984 new-moon period (18-30 June). It has been termed a proof-of-principle campaign of the MAPSTAR Program⁴ (Ratkowski, 1985). Two things needed to be proven: (a) that the coordinated measurements would be of use, and (b) that the imaging Doppler interferometer radar would actually perform as anticipated. A fairly impressive array of optical, radar, and imaging instrumentation was assembled for the campaign, as summarized in Table 1. The radar was a prototype of the MAPSTAR Imaging Doppler Interferometer (IDI) operating at 2.66 MHz and making use of the Boot Lake ionosonde array. (See Section 7.1). The "observational windows" at the Boot Lake site are given in Table 1. An interesting data set resulted from this abbreviated campaign. However, during the following fiscal year, the available program funds were used for instrumentation development, and the coordinated analyses required to properly compare and interpret the various measurements were put on hold.

During the campaign, a strong correlation was noted between the occurrence of OH Meinel emission structures (as evidenced by both imaging observations and photometric observations of airglow activity) and 2.66 MHz radar returns from near the mesopause. However, the correlation was merely qualitative since criteria were not established to perform a detailed correlation analysis. Because the cause of the reflections from the 2.66 MHz radar is still not known precisely, attempts to develop a more complete understanding of the correlation between airglow structure and radar returns continue to be of interest.

The Boot Lake measurements and similar observations from Capilla and Sacramento Peaks in New Mexico during June 1983 (see Section 2.1) suggested a relatively high degree of airglow brightness variability near summer solstice at both sites. The frequently occurring thunderstorms in the region during the periods of interest are deemed probable sources of the wave activity inferred in the mesopause region from observations of airglow variability and structuring. The thunderstorms are famous for their ability to generate gravity waves.

The Boot Lake Campaign provided the basis for a significant contribution (six papers) at the AGU Spring 1985 special session entitled: "Wavelike Propagation in the Mesosphere and Thermosphere I" (R.L. Walterscheid, presider). These papers introduced the MAPSTAR Program to the scientific community. The abstracts of MAPSTAR papers presented at that session are included below.

The MAPSTAR Program: Scientific Goals and Overview

A. J. Ratkowski (Air Force Geophysics Laboratory, Hanscom AFB, MA 01731)

MAPSTAR (Middle Atmosphere Periodic-Structure-Associated Radiance)
is a new, mobile, multi-instrumented, multi-disciplinary, multi-organizational,

⁴Ratkowski, A. (1985) The MAPSTAR Program: Scientific Goals and Overview, EOS, 66:324.

TABLE 1 BOOT LAKE CAMPAIGN
INSTRUMENTATION/LOCATION

PRINCIPAL INVESTIGATOR	LOC	INSTRUMENT	SPECIES	SPATIAL RESOLUTION	TEMPORAL RESOLUTION
ADAMS	R	MAPSTAR IDI RADAR	DENSITY GRADIENT		
BAKER/PENDLETON/ ESPY	R	INTERFEROMETER	OH VT	1°	30 SEC
	R	(2) SCANNING PHOTOMETER A. 6300/5577/7400 N-S B. 6300/5577/7400 E-W	OH I	1°	15 SEC
	R	2-CH. RADIOMETER	OH(1.5)/O ₂ (1.27)		
HERNANDEZ	F	FABRY-PEROT	OI VT		5 MINS
	F	1/2 METER	OH 8-3		20 MINS
MENDILLO	M	ALL-SKY IMAGING	OI/OH		
MERIWETHER	R	2-BEAM PHOTOMETER	OH VT	10°	5/10 MINS
PETERSON	J	INT. CAMERA/TV	OH, OI	ALL-SKY	2-5SEC
	J	(2) PHOTOMETER	OH, OI	15°	20 SEC
	J	INT. TELESCOPE	OH, OI	VARIABLE	VARIABLE
	C	ALL-SKY CAMERA	FILTERED		
	R	ALL-SKY CAMERA	FILTERED		

KEY: C - CAPILLA PEAK M - MILLSTONE HILL
 F - FRITZ PEAK R - RADAR SITE (BOOT LAKE)
 J - WYOMING (JELM) I/T - INTENSITY/TEMPERATURE

ground-based program to examine sources of oscillatory variations in atmospheric hydroxyl radiance over the next four years under a number of geophysical conditions. Measurements of such radiance variations were recently performed during a proof-of-principle campaign in June 1984 with filtered TVs and cameras, radiometers, photometers, interferometers, an imaging radar, and an ionosonde. Examples from each and the goals of the individual studies will be presented. In addition, the issues that the MAPSTAR Program is attempting to address (source(s)/characteristics of oscillatory radiance, relation to geophysical indices, development of a predictive model,...) will be discussed.

This work is supported by the U.S. Air Force Office of Scientific Research (AFOSR).

*Mesospheric/Lower-Thermospheric Airglow Variability Near
Summer Solstice at Midlatitudes*

W.R. Pendleton, Jr., P. J. Espy, D. J. Baker, and P. B. Mace (All at Utah State University, Logan, UT 84322)

Photometric, radiometric, and interferometric measurements of mesospheric and lower thermospheric airglow emissions were carried out near summer solstice from Sacramento Peak, NM ($\approx 33^\circ$ N) in 1983 and from Boot Lake, CO ($\approx 40^\circ$ N) in 1984. While limited in scope, both sets of measurements are generally characterized by a high degree of variability in the airglow emission levels [$(\Delta I/I) < 0.3$] with a much smaller variability in the rotational temperature of OH ($X^2\pi_1$) [$(|\Delta T|/\bar{T}) < 0.06$]. In addition, the relatively slow (\approx hrs) large amplitude fluctuations in the OH Meinel emissions were frequently accompanied by well-defined, rapid fluctuations with quasi-periods in the range ≈ 4 -12 min. These more rapid fluctuations were characterized by peak-to-peak amplitudes ≈ 0.1 those of the major fluctuations with which they were associated. OH Meinel-filtered low-light-level video recordings, on the occasions of high airglow activity, clearly revealed near-IR airglow structures which were sometimes quasi-spatially periodic over a major section of the sky. Observations will be presented in this paper, and analyses of these and other complementary measurements will be discussed in a companion paper.

Analysis of Simultaneous Photometric Observations of 6900 Å, 7300 Å, and 7900 Å OH Bands and 5577 OI together with Radiometric Observations

A. W. Peterson (E. 520 Silver Pines, Colbert, WA 99005)

W. Pendleton (Utah State University, UMC 41, Logan, UT 84311)

J. J. Lin and T. F. Tuan (Both at Physics Department,
University of Cincinnati, Cincinnati, OH 45221)

Simultaneous observations of 6900, 7300, 7900 Å OH bands and 5577 OI emissions have been made at Boot Lake, Colorado, Jelm, Wyoming, and the Capilla Peak in New Mexico from May 20 (1984) to July 3 (1984).

Radiometric data from Boot Lake covering the same time period have also been taken.

Power spectrum analyses based on (1) Maximum Entropy, (2) Blackman & Tukey, (3) Modified Periodogram, (4) Maximum Entropy with M-step Difference Filter have been made for all the above results. Two particular days, one typically active (June 23) while the other very active (June 29), will be discussed in some detail. Correlation between the different observations made at the same time as well as appearance of short-period (5-12 minutes) peaks for highly disturbed conditions will also be considered.

Imaging Radar and Ionosonde Measurements of Mesospheric Structures

G. W. Adams, Physics Department and Center for Atmospheric and Space Sciences, Utah State University, Logan, UT 84322, J. W. Brosnahan, Tycho Technology PO Box 1716, Boulder, Colorado 80306

Measurements were made at the Boot Lake field site during the MAPSTAR-1 Campaign uslng a 2.66 MHz radar operated as an imaging Doppler interferometer. The NOAA/NSF HF Radar was also operated as an ionosonde. A strong correlation is observed between the occurrence of OH emission structures in the near infrared and radar scattering from near the mesosphere. Here we show ionograms and 2.66 MHz returns for selected periods during the campaign.

Modeling the Effects of Adiabatic Oscillations on Photochemical Systems

S. F. Nerney, Physics Department, Naval Postgraduate School, Monterey, CA 93943, G. W. Adams, Physics Department and Center for Atmospheric and Space Sciences, Utah State University, Logan, UT 84322, and R. A. Armstrong, Mission Research Corp. Nashua, NH

Acoustic-gravity waves in the atmosphere impose temperature and density variations on the photochemical species in the earth's atmosphere. Apparent effects due to such waves are observed in infrared emissions and radar scattering. Here we model the effects of an adiabatic sinusoidal oscillation in temperature and density on a simple two-reaction set.

Optical Observations of the Mesospheric Thermal Structure

G.E Johnson and J.W. Meriwether, Jr., (Space Physics Research Laboratory, Department of Atmospheric and Oceanic Science, The University of Michigan, Ann Arbor, MI 48109-2143)

L. L. Cogger and I. M. Murty (Physics Department, University of Calgary, Calgary, Alberta, T2N 1N4, Canada)

Optical observations of the horizontal thermal structure in the mesosphere were obtained with good precision (1-3 degrees) in the Colorado MAPSTAR Campaign, June, 1983, and with the optical observatory in Calgary. The technique derives the rotational temperature of the OH Meinel emissions from the ratio of P₁ (2) and the P₁ (5) OH line intensities of the 8-3 band near 730.0 nm measured with a tilting filter photometer programmed by a mini-computer to sample only the line and background positions in a tilt scan.

Our mapping strategy in the MAPSTAR Campaign included five directions, the cardinal positions and zenith, with a zenith angle of 25 degrees for the off-zenith points; the total cycle time of sampling was five minutes. The Calgary measurements have included more points distributed along the meridian with slightly higher error bars and about the same cycle time. The MAPSTAR results indicate that the major difference between quiet and active periods appears to be the presence of a thermal maximum near midnight with a spatial extent of a few hundred km.

2.3 MAPSTAR/MISTI Campaign at Poker Flat, Alaska

(contributed by R. Lowe and M. Taylor)

During July and August 1986, a noctilucent cloud campaign took place at Poker Flat, Alaska, combining rocket, MST radar and optical measurements. During the early part of the campaign, optical measurements were impossible since the sun was barely getting below the horizon. By the time that optical measurements were feasible (solar depression > 6°), the rocket and radar components of the campaign had been completed. The optical measurements continued from Aug 3 to Aug 20.

The basic optical spectral instrumentation for the campaign consisted of two Fourier transform spectrometers, the IRFWI (Infrared Field-Widened Interferometer) of Utah State University and the UWOMI-I (University of Western Ontario Michelson Interferometer I) mounted side-by-side at the Poker Flat Optical Observatory (65.13°N, 147.48°W). Each instrument measured the zenith airglow spectrum in the range 1000 to 1700 nm with similar temporal and spectral resolution, but the field-of-view of the IRFWI was considerably smaller (0.8° full angle) than that of the UWOMI-I (30°).

The purpose of the optical measurements was to observe any correlation between hydroxyl airglow behavior, either radiance or temperature, and the occurrence of noctilucent clouds. Because the OH and noctilucent clouds exist in close proximity in altitude to each other, it may be expected that measurements of the OH temperature during the noctilucent cloud season should reflect the conditions under which noctilucent clouds nucleate and grow. Current theories indicate nucleation at the mesopause at the very low temperatures, around

120-130 K, existing there. However, neither of the two previous studies to date (Shefov⁵, 1968; Harrison⁶, 1973) found any correlation between OH rotational temperature measurements and the occurrence of noctilucent clouds. Our data, obtained using sensitive, high-resolution instruments complemented by good observing geometry, may have at last found evidence for such a relationship.

To provide confirmation that any report of noctilucent cloud occurrence was valid, an imaging station was set up at Gulkana airport (62.2°N, 145.5°W), approximately 320 km south of the Poker Flat observing site. The instruments included a low-light-level television (LLLTV) system with several 35-mm SLR cameras (University of Southampton and Utah State University). Any noctilucent cloud over the interferometer site would appear at an elevation of ~ 12° and an azimuth of 322° in images from Gulkana.

During the campaign there were six nights during which weather conditions were suitable for observations at both Poker Flat and Gulkana. On three of these, there were confirmed noctilucent clouds overhead at Poker Flat; on the other three, there were none. There was no significant correlation between the observed radiance of the hydroxyl emission and the occurrence of noctilucent cloud. However, the rotational temperature obtained from the (3,1) band did show a correlation. On the three nights without noctilucent cloud, virtually all spectra (>97 percent) indicated a rotational temperature greater than 154 K whereas on the each of the three nights with noctilucent cloud a significant fraction of the rotational temperatures measured (between 15 and 50 percent) were lower than 154 K. This result is consistent with models of noctilucent cloud particle growth which require temperatures well below 150 K for particle growth and in which particles evaporate rapidly for temperatures greater than 150 K.

On four other nights during the campaign, apparent noctilucent clouds were observed from Poker Flat, but photographic evidence was not available to confirm the identification or to show whether they were in the field-of-view of the interferometers. On the last night of the campaign, what was apparently a noctilucent cloud was photographed from Poker Flat, the Gulkana site having been closed. During that night the rotational temperature was the highest observed during the campaign, dropping from 175 K when the apparent noctilucent clouds were photographed to 163 K at the end of the night. This result conflicts with the behavior on the three nights with confirmed noctilucent clouds, but the absence of confirming evidence from a remote site puts the identification as noctilucent clouds in some doubt. The early results of this study have been presented at several conferences and have been published in the proceedings of the International Workshop on Noctilucent Clouds, Tallinn, Estonia, (1989). A recent in-depth analysis of the data showing that there is a tendency for the OH temperature to be lower during times when noctilucent cloud were confirmed in the field-of-view of the interferometers, is in final preparation for publication.

⁵Shefov, N.N. (1968) The behaviour of upper atmosphere emissions during high meteoric activity, *Planet. Space Sci.*, **40**:235-242.

⁶Harrison, A.W., (1973) Spectrophotometric measurements of noctilucent clouds, *Can. J. Phys.*, **51**:373-377.

The campaign was one of the first ever to study the hydroxyl airglow during high latitude summer and provided a number of interesting results apart from those related to noctilucent clouds. The variation of average temperature during the campaign followed closely that in the CIRA-86 model atmosphere. Wave activity was observed on a number of occasions. On 11 Aug., UWOMI-I observed what appeared to be a nearly monochromatic wave with an η of 6.5 and a temperature amplitude of less than 2 K, one of the smallest amplitude waves ever detected. There was some evidence of harmonic generation in that a wave of small amplitude (<1 percent) with three times the frequency of the main wave was detected. During the same event, small (<2 min) phase differences of the wave in different vibrational levels were also observed in OH.

Papers and Presentations from MISTI Campaign

Lowe, R. P., K. L. Gilbert and D. N. Turnbull. *High latitude summer observations of the hydroxyl airglow*, *Planet Space Sci.* 39, 1263-1270, 1991.

Taylor, M. J., R. P. Lowe and J. Ulwick. *Coordinated measurements of noctilucent clouds and the hydroxyl nightglow emission* *EOS* 71, 572, 1990.

Lowe, R. P., K. L. Gilbert and D. N. Turnbull. *Hydroxyl airglow observations at high latitude under summer conditions*, *EOS* 70, 1245, 1990.

Lowe, R. P., K. L. Gilbert and D. N. Turnbull. *High latitude summer observation of intensity and rotational temperature of the hydroxyl airglow*, Joint Symposium Atmosphere Science IAGA/IAMAP, Exeter (UK) July 1988.

Lowe, R. P. and M. J. Taylor. *The implications of high hydroxyl rotational temperatures during noctilucent cloud displays* Noctilucent Cloud Symposium IAMAP, Reading (UK) August 1988.

Taylor, M. J., R. P. Lowe, D. J. Baker and J. Ulwick. *On the association of the OH nightglow emission with noctilucent clouds*, International Noctilucent Cloud Workshop, Tallinn, Estonia. July 1989.

Steed, A., J. Ulwick, R. P. Lowe, D. N. Turnbull and J. J. Taylor. *The association of noctilucent clouds with the OH airglow emission*, *EOS* 67, 1123, 1986.

2.4 MAC/EPSILON Campaign (written by M. Taylor and P. Espy)

This campaign was a multinational project undertaken as part of MAC (Middle Atmosphere Cooperation) to investigate turbulence and related phenomena at high latitudes. Measurements were made from northern Scandinavia during October 1987 using many ground-based and rocket-borne instruments.⁷ MAPSTAR participation consisted of a Michelson interferometer [Utah State University (USU)] located at Andoya Rocket Range, Norway, and TV measurements of OH and aurora (University of Southampton) from Finland.

⁷Thrane, E.V., (1990) Preface to "Middle Atmosphere Dynamics at High Latitudes," *J. Atmos. Terr. Phys.*, **52**:813-827.

Our TV cameras were located at two sites in northern Finland (Pittiovaara and Tankavaara) in an attempt to image gravity wave structure over the interferometer site at Andoya. Unfortunately, the weather during this campaign was particularly inclement and we were not able to image the faint nightglow emissions against the diffuse glow caused by aurora under low visibility conditions. However, we regularly recorded local auroral activity and on one occasion obtained data on an unusual auroral pulsation event. (See Section 2.1)

This data has been analyzed and compared with coincident magnetometer data (University of York, UK) which subsequently revealed that the auroral patches were the signature of a rare giant magnetic pulsation event (Pg). The results of this fortuitous research have been presented at scientific meetings and have so far led to two publications^{8,9}. The data have also been used by G. Chisham as part of his Ph. D thesis (University of York).

The main part of the MAC/EPSILON campaign was carried out during October and November, 1987, from Andenes, Norway (69°N, 16°E), and was planned as a case study of turbulence in the middle atmosphere. In MAC/EPSILON, sounding and meteorological rocket salvos were employed to provide a detailed study of specific events where strongly developed turbulence was occurring. The ground-based instrumentation not only provided information during these events, but also mapped the general behavior of the middle atmosphere under autumn and early winter conditions.

Utah State University contributed to the MAC/EPSILON campaign with both ground-based and rocketborne instrumentation. The ground-based equipment, which was supported by the MAPSTAR Program, consisted of a dual-channel radiometer and the USU Scanning Field-Widened Michelson Interferometer (SWAMI). This instrument is also called IRFWI when employed in a non-scanning mode as it has been in many MAPSTAR campaigns. The radiometer had a channel at 1530 nm, centered on the OH Meinel (3,1) band, and at 1270 nm, where the O₂ IR-Atmospheric (0,0) band occurs. The SWAMI operated over the wavelength range from 840 to 1600 nm and provided spectrally resolved measurements (resolution ~ 2.5 cm⁻¹, apodized) of the OH Meinel (3,1), (4,2), (8,5), (7,4), (6,3), and (5,2) bands with a temporal resolution of 20s. In addition, the SWAMI observed the O₂ IR-Atmospheric (0,0) and (0,1) bands, as well as aurorally produced emissions from N₂, atomic oxygen and helium.

The USU data during MAC/EPSILON consists of eight nights of radiometric and SWAMI data and corresponds to ~ 6,700 SWAMI scans. There were coincident Na-lidar and OH Meinel (8,3) band observations on five nights and nearly continuous EISCAT, SOUSY, MF radar and ionosonde measurements. All of these systems were operational on the night of the rocket salvos which provided *in-situ* measurements of the turbulent energy dissipation rate ϵ (after which the campaign is named) and the eddy diffusion coefficients. Additionally, there were

⁸Taylor, M.J., Chisham, G., and Orr, D. (1989) Pulsating auroral forms and their association with geomagnetic giant pulsations. *Planet. Space Sci.*, **37**:1477.

⁹Chisham, D., Orr D., Taylor, M., and Luhr, H. (1990) The Magnetic and optical signature of a Pg pulsation. *Planet. Space Sci.*, **38**:1443.

measurements of mesospheric winds and wind corners, electrical conductivities, and the ion and neutral composition (particularly atomic oxygen) from the rockets.

All of the USU data have been reduced and presented at several MAC/EPSILON data meetings. Additionally, the data have been published in a special issue of the *Journal of Atmospheric and Terrestrial Physics* entitled "Middle Atmosphere Dynamics at High Latitudes" (1990). Currently, we are comparing the SWAMI hydroxyl rotational temperatures with the Nalidar temperature measurements of the University of Bonn. A preliminary analysis of the hydroxyl layer height from this comparison was presented at the first Structured Optical Atmospheric Radiance (SOAR) Workshop held at Phillips Laboratory/Geophysics Directorate. Additional joint studies with both the radar and rocket measurements are anticipated.

2.5 MAPSTAR Colorado Campaign (contributed by M. Taylor and E. Dewan)

This campaign was the most intensive undertaken during the MAPSTAR Program. Measurements were made during three consecutive months, May, June, and July 1988, using several MAPSTAR instruments from three sites: a primary mountain site at the University of Colorado's INSTAAR (Institute for Alpine and Arctic Research) Mountain Research Station on Niwot Ridge near Ward, a secondary mountain site at Mary's Lake near Estes Park, and a plains site at Colorado State University's ECARC (Eastern Colorado Agricultural Research Center) near Sterling. Our TV observations were centered at INSTAAR, high above the Colorado plains. Observations from this site were made in conjunction with Michelson interferometer measurements (Utah State University) and were restricted mainly to observing a common volume of sky over the Sterling plains site. During June and July a second TV camera was operated from Mary's Lake to provide triangulation data on the OH structure. In addition, ground data were available from the University of Colorado's MEDAC system used in conjunction with the Platteville ST (stratosphere-troposphere) radar.

A large amount of image data was obtained during this campaign. To date, the data have been used to investigate the occurrence frequency of wave structure over a mountain site as well as the waves' properties. Theoretical studies indicate that the mountains themselves may be an important source for the waves. However, we have yet to identify such a wave in our data. The measurements have also been compared with the MEDAC meteor radar data from Platteville (University of Colorado) to investigate the effect of background winds on the wave motions and with tropospheric radar summary maps to investigate the possibility that local thunderstorms may have been a source of the waves imaged during this period.

On at least one occasion the meteor radar data have indicated that the mean background wind together with the 12- and 24-hour tidal wind components apparently exceeded the observed phase speed of an isolated wave pattern. Under these "critical conditions" the wave motion would be expected to be absorbed into the background flow or dissipated by various mechanisms, yet the image and interferometer data show that it existed for at least 1-2 hours after the critical condition was apparently reached. A report discussing

these measurements was presented at the 1989 Fall AGU Meeting and is currently in preparation for publication.

We also obtained all-sky video data for the first time during this campaign and have used it in a novel way to investigate wave filtering in the middle atmosphere by background winds. (See Section 4.1). By comparing the azimuths and speeds of over 20 wave displays imaged during this 3-month period with those expected, and assuming the video data result from tropospheric wave sources subjected to wind filtering in the middle atmosphere, any asymmetry in the data can be investigated. The data were compared with a model developed by T. F. Tuan and E. H. Ryan, University of Cincinnati, using climatological data. Remarkably, our nightglow data are fully consistent with the model predictions which suggest that wind filtering can play a significant role in governing the flow of wave energy through the atmosphere and that the troposphere is indeed a major source of gravity waves seen at mid-latitudes. A paper describing these results has been accepted for publication in the *Journal of Geophysical Research*.

The imaging systems used in this campaign were very sensitive to contamination by both natural and man-made light sources and, for this reason, they had to be located as far as possible from cities and operated only when the sun was at least 18° below the horizon and the entire moon was below the horizon as well. Figure 5 shows a map of the geographic area with indications of the instruments used at each location. All sites were within the borders of Colorado. At the site designated INSTAAR (altitude approximately 10,000 ft or 3050 m) we located the IRFWI instrument. The function of this instrument in our campaign was primarily to measure the temperature of the OH airglow. Its field of view (FOV) was approximately 1° . This instrument also provided measurements of the absolute brightness of the hydroxyl airglow. These latter were supplemented with measurements from photometers aligned with IRFWI. In addition, an imaging system was fixed to the IRFWI instrument so that when (and if) OH emission structure went through the FOV of the imager, one spot on the image would be measured in terms of absolute brightness and temperature. The wave activity was thus recorded in three ways simultaneously and the results were consistent.

In addition to the INSTAAR site, there was a second imaging site (also at about 10,000 ft or 3050 m altitude) at Mary's Lake. Both of these sites had imagers with fixed FOV's which overlapped the third site at ECARC. (See Figure 4). The locations of these imaging sites were chosen so that it would be possible to obtain stereoscopic images of the hydroxyl emissions from an area situated directly over ECARC at about 150 km horizontal distance from INSTAAR and Mary's Lake. This distance was chosen so that the elevation of the common volume over ECARC as seen from the mountain sites was low enough to take advantage of the Van Rhijn effect to enhance the contrast in the image. The mechanism for this contrast enhancement is explained in Tarrago and Chanin.¹⁰

¹⁰Tarrago, A., and Chanin, M.-L. (1982) Interpretation in terms of gravity waves of structures observed at the mesopause level by photography and lidar. *Planet. Space Sci.*, **30**:611-626.

MAPSTAR CAMPAIGN SUMMARY 1988

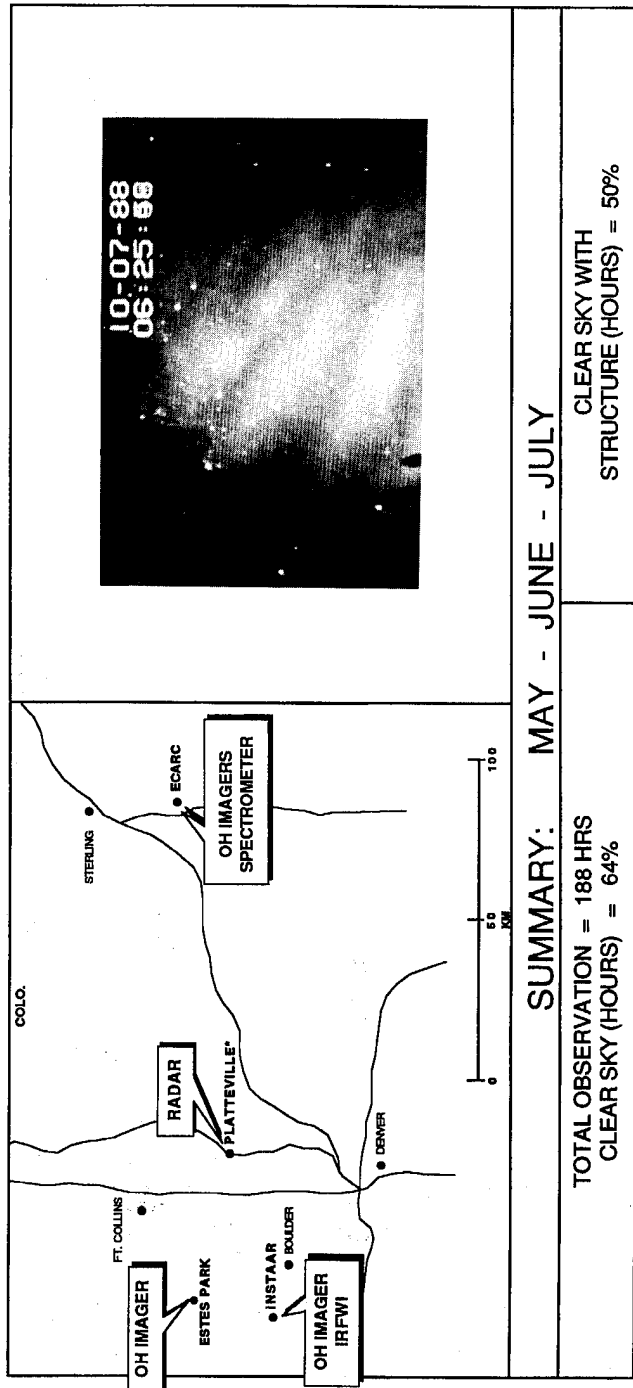


Figure 4. Map of Campaign Instrument Location and an Example of OH Imager Results (Taylor).

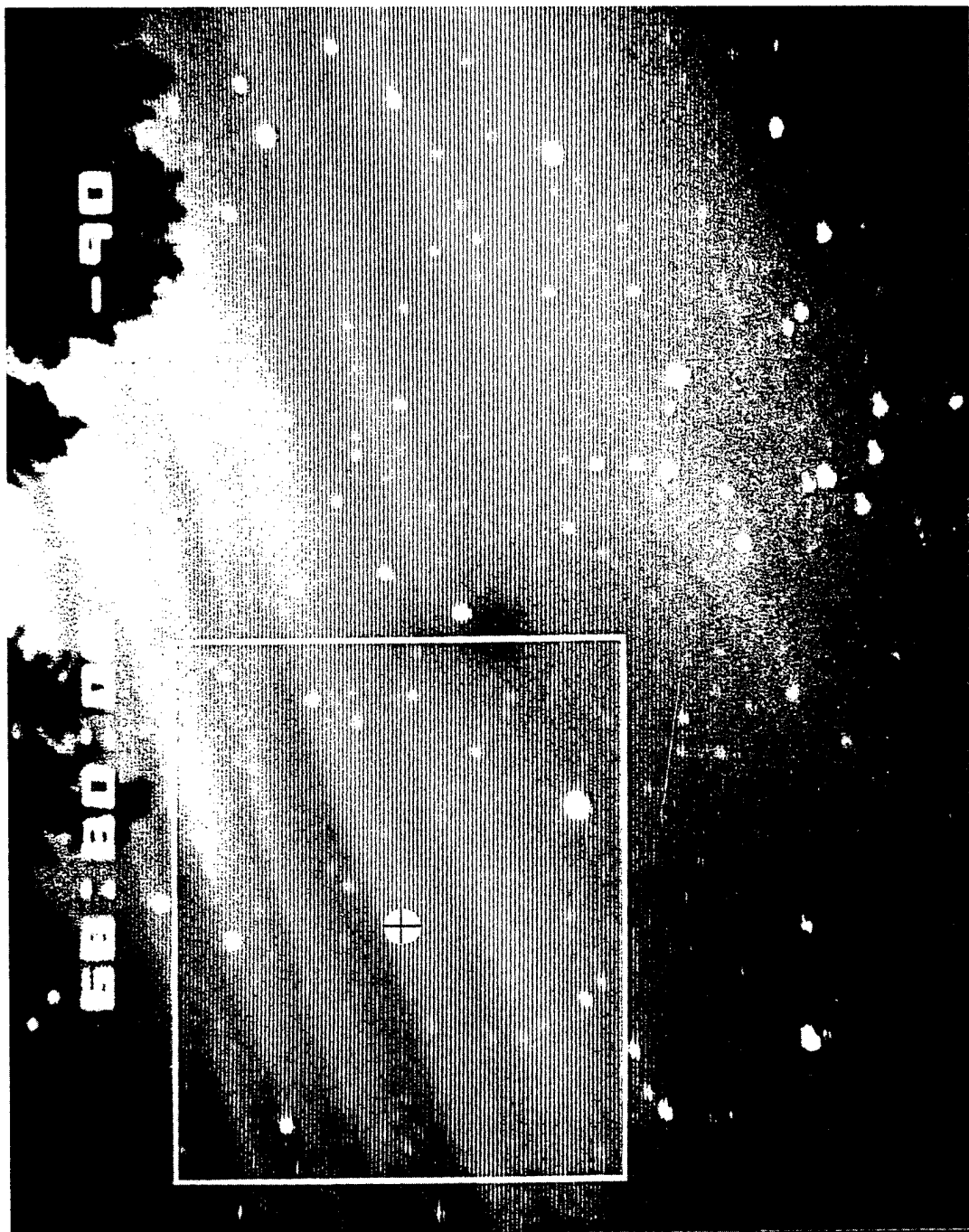


Figure 5. OH TV Image with Crossed Circle Marking the Position of Co-Aligned Interferometer Field of View (Taylor). The dark region at the center is due to a defect in the camera tube.

The instruments located at ECARC were all directed toward the zenith and thus there were two entirely different views of the same hydroxyl layer, one looking from the mountain stations at elevation 23° and the other from ECARC looking straight up. As indicated in Figure 5 the MAPSTAR interferometer was located at ECARC for measuring OH rotational temperature and absolute brightness. It was aimed at the zenith but also had the capability of flipping from one position to another and it was programmed to jump sequentially from the zenith position to two other off-zenith positions that formed a fixed equilateral triangle in the sky with legs of 10 km at altitude 85 km. These distances were designed to allow us to monitor gravity wave modulation without aliasing. That is, we sampled every wave at least at two points. Other instruments located at ECARC included all-sky and narrow-angle imagers and a zenith pointing OH photometer. The latter was employed to make absolute intensity measurements there for comparison with the interferometer readings.

Table 2 gives the dates and times when the various instruments obtained data. Note that all-sky images were obtained at both ECARC and INSTAAR. Film and video images were obtained during the campaign, and both narrow-field and all-sky images were recorded. The images were sometimes taken out of their usual operating mode to record structures occurring elsewhere in the sky.

In addition to the imagers, spectrometers, and photometers, we also had access to Colorado radar data, thanks to the efforts of Richard Strauch and Susan Avery (University of Colorado). The data consisted of horizontal winds in the troposphere and (sometimes) the stratosphere. They were deemed useful for (a) seeing if there were potential "critical layers" that might block or absorb gravity waves generated by tropospheric sources and thus prevent them from reaching the mesosphere from certain directions; and (b) obtaining estimates of wind velocities over the mountains to analyze orographically fixed patterns, potentially due to mountain waves. The Platteville ST radar (Figure 5) was outfitted with a MEDAC (Meteor Echo Detection and Collection system. This device, described by Wang et al¹¹, makes use of meteor trails to detect mesospheric winds when attached to an ST radar. It provides winds in an altitude range that includes the 80 to 100 km region of interest to us (due to the fact that the OH and OI emissions are centered at about 85 to 95 km, respectively). Such wind information is essential because the apparent motions of, for example, OH emissions, arise from two distinct causes, (1) wave propagation effects and (2) mean fluid motions or winds. The estimates of the latter from the MEDAC allow us to separate these two influences. [(See Taylor et al. *Planet Space Sci.* Vol 35 p. 413 (1987) and Taylor and Hapgood, *Planet Space* Vol 36, p. 975 (1988)].^{12,13}

¹¹Wang, S.T., Tetenbaum, D., Balsley, B., Obert, R., and Avery, S. (1987) A meteor echo detection and collection system for use on VHF radars, *Radio Science*.

¹²Taylor, M.J., Hapgood, M.A., and Rothwell, P. (1987) Observations of gravity wave propagation in the OI (557.7 nm), Na (589.2), and the near infrared OH nightglow emissions, *Planet. Space Sci.*, **35**:413.

¹³Taylor, M.J., and Hapgood, M.A. (1988) Identification of a thunderstorm as a source of short period gravity waves in the upper atmosphere nightglow emissions, *Planet Space Sci.*, **36**:975.

Table 2. Boot Lake Campaign: Observing Windows

A SUMMARY OF U.S.U. AIRGLOW OBSERVATION "WINDOWS" AT BOOT LAKE, CO. JUNE, 1984	
DATE (UT DAY)	PERIOD OF OBSERVATION (UNIVERSAL TIME)
18 (170)	1 2 3 4 5 6 7 8 9 10 11 12 MIDNIGHT (Mountain Daylight Time)
19 (171)	1 2 3 4 5 6 7 8 9 10 11 12
20 (172)	1 2 3 4 5 6 7 8 9 10 11 12
21 (173)	1 2 3 4 5 6 7 8 9 10 11 12
22 (174) (CLO/PCLO until 06:30) ²	1 2 3 4 5 6 7 8 9 10 11 12 → (CLEAR, SOME LIGHTNING)
23 (175)	1 2 3 4 5 6 7 8 9 10 11 12 (CLOUDY)
24 (176)	1 2 3 4 5 6 7 8 9 10 11 12 (CLEAR)
25 (177)	1 2 3 4 5 6 7 8 9 10 11 12 (CLEAR)
26 (178) (PCLO/CLEARING)	1 2 3 4 5 6 7 8 9 10 11 12 (CLEAR)
27 (179)	1 2 3 4 5 6 7 8 9 10 11 12 (PARTLY CLOUDY) [NO IRFWI DATA]
28 (180)	1 2 3 4 5 6 7 8 9 10 11 12 (CLEAR) [PCLO] → (CLEAR)
29 (181)	1 2 3 4 5 6 7 8 9 10 11 12 (CLEAR) [NO IRFWI DATA]
30 (182)	1 2 3 4 5 6 7 8 9 10 11 12 (CLEAR) *

² Selected for emphasis in initial data reduction analysis

* Selected for emphasis in initial data analysis

A SUMMARY OF U.S.U. RADAR OBSERVATIONS AT BOOT LAKE, CO. JUNE, 1984	
DATE (UT DAY)	UNIVERSAL TIME
18 (170)	2 3 4 5 6 7 8 9 10 Active 85 km Lightning Rain
19 (171)	2 3 4 5 6 7 8 9 10 Active E Blow Line Driver
20 (172)	2 3 4 5 6 7 8 9 10 Synthesizer fixed Very Quiet
21 (173)	2 3 4 5 6 7 8 9 10 Power Outage Very Quiet
22 (174)	2 3 4 5 6 7 8 9 10 Sporadic E Present
23 (175)	2 3 4 5 6 7 8 9 10 Quiet
24 (176)	2 3 4 5 6 7 8 9 10 Very Active
25 (177)	2 3 4 5 6 7 8 9 10 Moderately Active
26 (178)	2 3 4 5 6 7 8 9 10 Slight Activity
27 (179)	2 3 4 5 6 7 8 9 10 Quiet Power Surge-off the Air
28 (180)	2 3 4 5 6 7 8 9 10 Very Active
29 (181)	2 3 4 5 6 7 8 9 10 Extremely Active
30 (182)	2 3 4 5 6 7 8 9 10 *

² Selected for emphasis in initial data reduction analysis

Many of the findings during this campaign will be described below, but a major finding was that during only about 50 percent of the clear viewing time was there significant structure.

2.6 AIDA Campaign (contributed by E. Dewan)

The MAPSTAR participants in this NSF-sponsored campaign in Spring 1989 at Arecibo, Puerto Rico, were Gene Adams (Utah State University) and John Brosnahan (Tycho Technology) using the MAPSTAR Imaging Doppler Interferometer (IDI) radar instrument. Only the receiver of this device had been completed and therefore the Arecibo heater was used as a transmitter. It should be noted that this was the first time the receiver was used and initial field checks were made immediately prior to the campaign. This instrument was central to the main goal of the AIDA Campaign, which was to compare several different radar techniques to measure wind profiles in the middle atmosphere. There was already a strong suspicion that there were inconsistencies among the winds reported by various techniques, and AIDA was conceived to settle the problem by comparing the various methods simultaneously at the same location. The final result was that wind measurements were consistent up to 80 km, above which they diverged. The reason was that at high altitudes "glints" reflected by surfaces distorted by waves are measured by some radars as "winds" rather than wave velocities. Details were published in 1993.¹⁴

2.7 The ALOHA-90 Campaign (contributed by M. Taylor)

MAPSTAR measurements were made in conjunction with an airborne lidar program (C. Gardner, University of Illinois), which considerably enhanced the scope of this investigation into the study of gravity waves over a low-latitude oceanic site. Ground-based observations were made from Haleakala Crater, Maui, using a Michelson interferometer (University of Western Ontario) and four TV cameras (Southampton University) operating at visible and near IR wavelengths. Image measurements were obtained during two new-moon periods in March and April 1990, providing new and interesting data on gravity-wave occurrence and properties at low latitudes. For example, an initial analysis of the image data suggests that there are not significant differences between the waves seen over mountains (using the MAPSTAR Colorado 1988 data) and oceans, at least during the spring. A summary of these results was presented at the ALOHA-90 session of the Fall AGU Meeting (1990), and three papers detailing this research have been published in *Geophysical Research Letters*^{15,16,17}. Some of the results

¹⁴Brosnahan, J.W., and Adams, G.W. (1993) The MAPSTAR Imaging Doppler Interferometer (IDI) Radar: description and first results, *J. Atmos. Terr. Phys.*, **55**:203-208.

¹⁵Taylor, M.J., and Hill, M.J. (1991) Near infrared imaging of hydroxyl wave structure over an ocean site at low latitudes, *Geophys. Res. Lett.*, **18**:1333-1336.

are described in Section 6. Other analyses indicate that some of the short-period (5-10 min) wave sources may have been *in-situ* rather than tropospheric in origin.

2.8 Other MAPSTAR Related Campaigns (contributed by M. Taylor)

In addition to the nightglow measurements made during the MAPSTAR supported campaigns, we made near IR image observations from within the polar cap (Spitzbergen, 78°N) during January and February 1986 and 1987¹⁸. NLC measurements were also made in conjunction with EISCAT radar observations from northern Scandinavia¹⁹. Although the measurements were not part of the MAPSTAR program, analysis of these data has been supported in part by MAPSTAR. Results are described in reference 19.

3. IMAGING OF OH AIRGLOW WAVE STRUCTURE

3.1 Circular Waves in Airglow

Two papers published under MAPSTAR deal with the sources of dramatic circular-wave events in the airglow: Taylor et al.¹³ and Taylor and Hapgood²⁰. These papers present identification of a gravity-wave source for a known airglow pattern. These papers not only proved that the circular pattern in Figure 1 was due to gravity waves but in addition they showed that the waves were caused by a specific, documented thunderstorm that had occurred 6 hours prior to their observations. In Taylor et al.¹³ three airglow layers were used, namely OH near 85 km, OI near 90 km, and Na near 95 km. The circular patterns in the three images corresponding to these layers were displaced with respect to each other. The latter observation enabled the authors to estimate the geometry of the gravity wave phase fronts (recall Figures 2 and 3). Knowing this information as well as the wave period (from observation) they were then able to locate the source of the disturbance by ray tracing. The source position was also estimated by the locations of the centers of the circular patterns, and the results were entirely consistent. The time-of-flight of the wave energy was estimated from the vertical group velocity of the wave, which could be ascertained from the measured period and wavelength. There seems to be no room for reasonable doubt that the thunderstorm in question (which was

¹⁶Taylor, M.J., and Edwards, R. (1991) Observations of short period mesospheric wave patterns: In situ or tropospheric wave generation?, *Geophys. Res. Lett.*, **18**:1337-1340.

¹⁷Taylor, M.J., Turnbull, D.N., and Lowe, R.P. (1991) Coincident imaging and spectrometric observations of zenith OH nightglow structure. *Geophys. Res. Lett.*, **18**:1349-1352.

¹⁸Taylor, M.J., and Henriksen, K. (1989) Gravity wave studies at polar latitudes, in *Electromagnetic Coupling in the Polar Clefts and Caps*, Kluwer Academic Publishers, pp 421-434.

¹⁹Taylor, M.J., van Eyken, A.P., Rishbeth, H., Witt, G., Witt, N., and Clilverd, M.A. (1989) Simultaneous observations of noctilucent clouds and polar mesospheric radar echoes: evidence of non-correlation, *Planet. Space Sci.*, **37**:1013-1020.

²⁰Taylor, M.J., Hapgood, M.A., and Rothwell, P. (1987) Observations of gravity wave propagation in the OI (557.7nm), Na (589.2 nm), and the near infrared OH nightglow emissions, *Planet space sci.*, **35**:413-417.

documented in a satellite image) was the cause of the circular patterns.

The waves' group velocity pointed upwards at an elevation angle of 15°, the horizontal wavelength was 26 km, the horizontal phase velocity was 38 m/s (a little faster than highway traffic) and the wave period was around 20 min. This of course brings up the question of how thunderstorms actually generate sinusoidal waves. Taylor and Hapgood²⁰, cited experimental observations which support the idea that the thunderstorms act like sine-wave generators. Most scientists would have guessed that the sinusoidal patterns are caused by dispersion. At a NATO workshop in Loen, Norway, May, 1992, J. Holton showed a numerical model of gravity wave generation by a thunderstorm. It suggested that more than one sinusoidal gravity wave is generated, and (as is usual for gravity waves) the direction of propagation is determined by the frequency. Work by Stobie²¹ (Master's Thesis, Colorado State University, "Gravity Shear Waves Atop the Cirrus Layer of Intense Convective Storms"), presents several reasonable hypotheses to explain how the thunderstorm generates gravity waves. One of these uses an analogy between the ripples caused by a pebble penetrating the surface of a pond and the rapid penetration of the thunderstorm dome through the tropopause. Another possibility is that the periodic collapse and regrowth of the dome generates the waves.

Another member of the MAPSTAR team, A. Peterson. (1989, 1990, 1991)^{22,23,24} observed circular patterns in the airglow and also found thunderstorms at the epicenters at the appropriate time, thus lending further confirmation to the above findings.

3.2 Direct Comparison Between OH Wave Structures in Sky Images and in Interferometer Measurements

One of the original goals of the MAPSTAR project was to compare the OH Meinel brightness variations as seen, for example, on a Low Light Level Television (LLLTV) imager with the simultaneously measured OH rotational temperatures and absolute brightnesses obtained from a co-aligned interferometer. The location of the region measured by the interferometer was indicated on the TV image of Figure 5. In the earlier of two sets of measurements using IRFWI this region was quite small, corresponding to an FOV of a bit less than one degree. As shown by Neal²⁵ and Taylor et al.³ the difference in OH temperature between a bright and a dark band is typically less than 10 K. On the other hand, the brightness variations are quite large by comparison (up to 30 percent). In other words, the amplitude of the fractional

²¹Stobie, J. (1975) *Gravity Shear Waves Atop the Cirrus Layer of Intense Convective Storms*, Master's Thesis, Colorado State University.

²²Peterson, A. (1989) Analysis of an extensive, long wavelength OH wave packet generated by a thunderstorm, *EOS*, **70**:1244 (AGU Fall Meeting).

²³Peterson, A. (1990) Color photographs of active OI (5577) and OH airglow with comparisons to video and fisheye pictures. AGU Spring Meeting, *EOS*, **71**:571.

²⁴Peterson, A. (1990) Analysis of an OH wave packet generated by a thunderstorm.

²⁵Neal, P.C. (1985) *High Resolution Measurements of OH Infrared v Infrared Airglow Structure*, Ph.D. Thesis, Utah State University, Dept. of Engineering, MAPSTAR Data Report No. 2.

intensity variation was about 8 times larger than the associated fractional temperature variations. In the second set of measurements Taylor et al³ used a CCD camera in conjunction with the UWOMI instrument. In this case, the interferometer had a 30° FOV. When this FOV was taken into account, it was found that the image and interferometric brightness variations matched very well. One other finding was of interest, namely that in the CCD images there were fine-scale motions with periods *too short* to be gravity waves. This may imply, for the first time, that acoustic vibrations can cause small-scale IR structure. This is an extremely important finding from the systems applications point of view. (Compare Section 11.6). In this connection it should be mentioned that an experiment involving a supersonic jet aircraft showed that acoustic waves can cause measurable effects upon the ionosphere according to Thrane (private conversation).

3.3 Structure Sky Cover and the Kink in the Radiometer Power Spectra - Relation to Bright Nights

OH structure is not present in the sky at all times. (See, for example, the Colorado 1988 Campaign discussion above). In addition, sometimes the structure fills the entire sky, and sometimes it fills only a fraction of the sky. It was present to some noticeable degree for about 50 percent of the clear nights in the Colorado 1988 Campaign. In the ALOHA-90 Campaign there was very little structure in the first moon-down viewing period, whereas in the next moon-down period there was a large amount of structure. We realized that it would be beneficial to quantify the amount of structure in the sky at any given time. The percent of sky cover by clouds is a parameter long used by meteorologists and, by analogy, we define the *structure sky-cover* parameter. This was used in Taylor²⁶ and Espy and Taylor²⁷, to characterize the all sky observations in the Colorado Campaign. Espy and Taylor²⁷ made a very important discovery. They found an extremely strong (and statistically significant) correlation between (a) the percent structure sky cover and (b) a kink, or change of slope, of the power spectrum of the output from an OH Meinel-band radiometer pointed at the zenith. The radiometer measured the brightness as a function of time at one spot in the sky. This was done for many nights. One power spectrum was obtained for each full night of observation. Figure 5 shows an example of one such spectrum and, as indicated, there is a break or kink in the curve. The particular frequency at which the kink occurred changed from night to night. It was compared to the structure sky-cover parameter for each night, and Figure 6 shows how these are correlated. The correlation, as can be seen from Figure 7, is very high. Espy has explored this problem further, and he has found that the break occurs when the power-law

²⁶Taylor, M.J. (1989) *Comparison of Southampton Image Data and Thunderstorm Maps for the Colorado MAPSTAR Campaign, 1988*, MAPSTAR report, June 1989.

²⁷Espy, P., and Taylor, M.J. (1991) Radiometric measurements and PSD's vs Taylor All-Sky-Structure-Cover-Percent-Parameter, MAPSTAR Workshop, April 22-23, 1991, Hanscom AFB, MA.

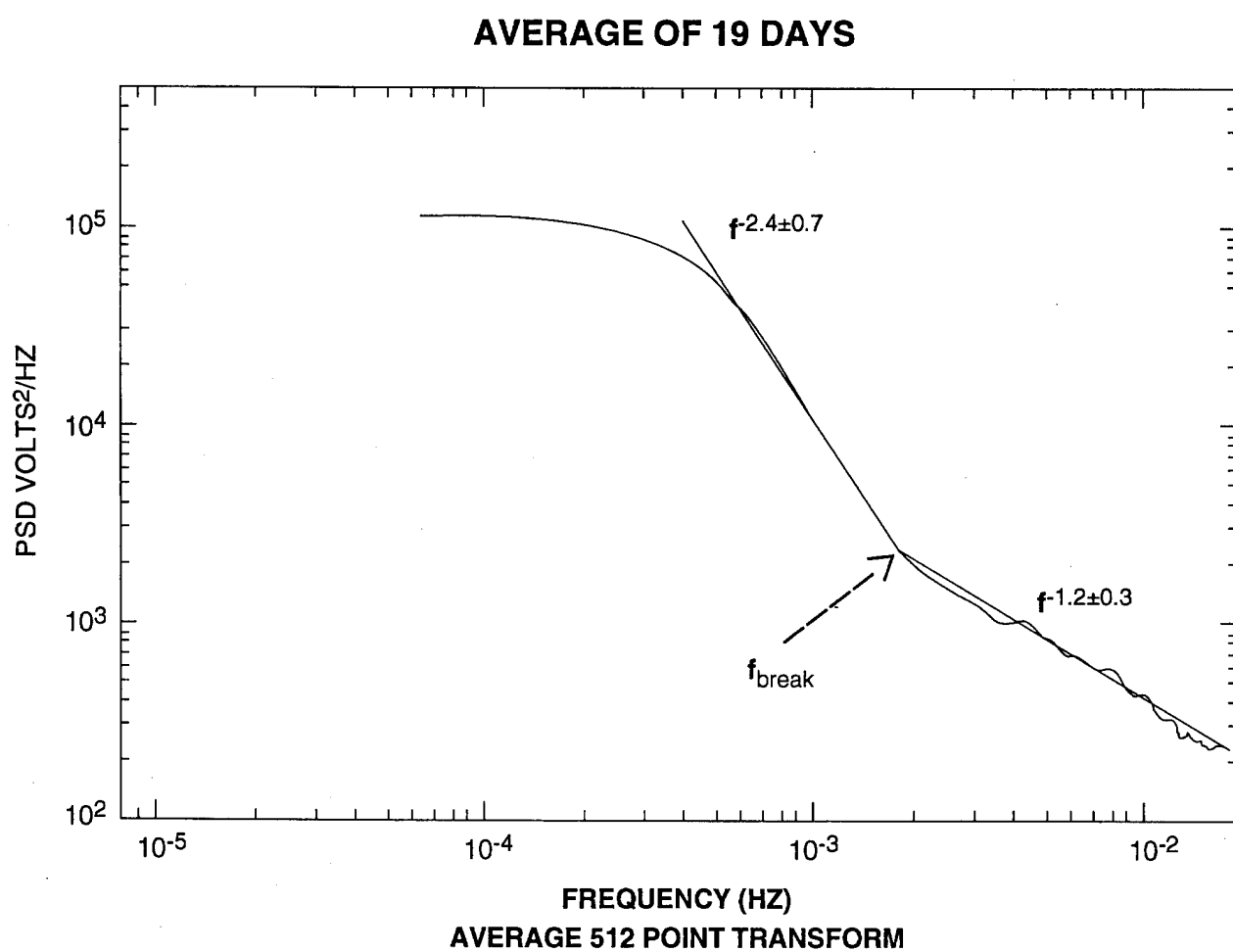


Figure 6. Example of PSD of Brightness Variation of OH Layer Viewed at Zenith by Means of a Photometer (Espy).

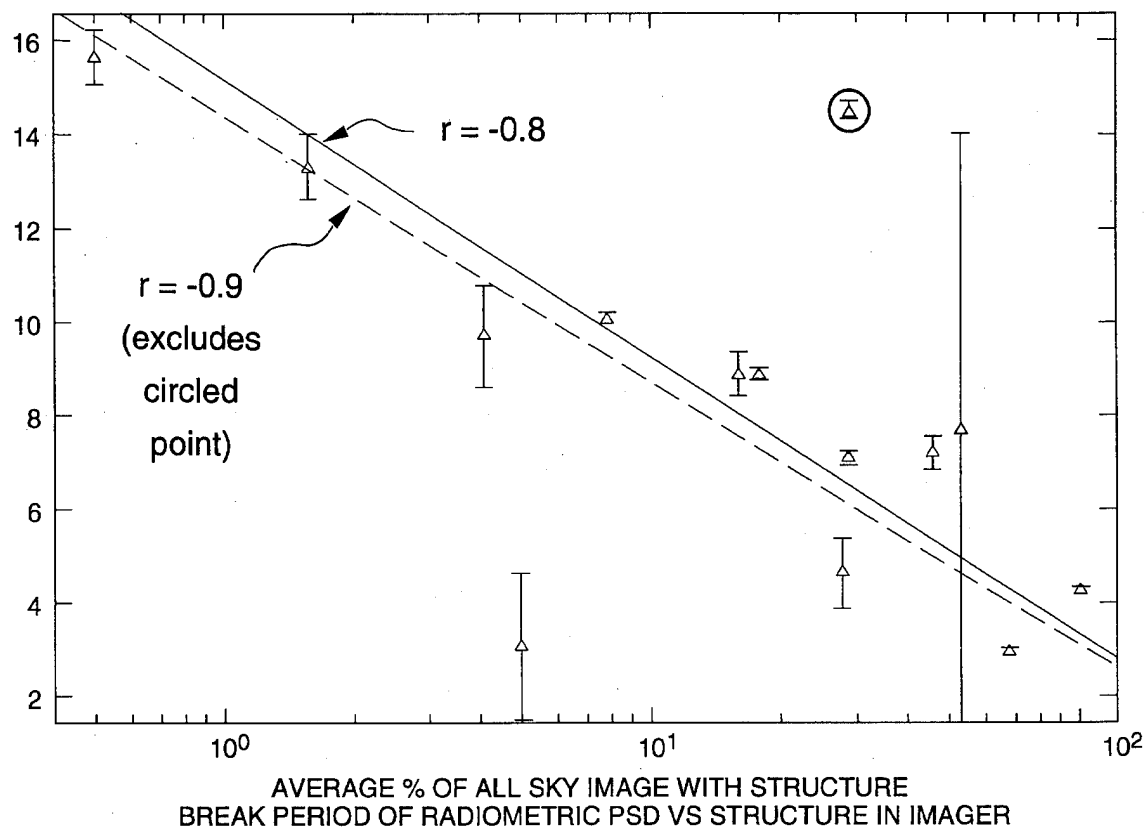


Figure 7. Correlation Between the Frequency Position of the PSD "Break" (see Figure 6) and the Percent of Sky Covered with "Structure" (Espy).

slope of the PSD hits the "noise floor" of the instrument. The kink movement reflects the general power of the brightness fluctuations, which are observed to change in direct proportion to the amount of sky cover. At this time the details of this finding remain to be explained. The finding is very useful because the measurements at one spot in the sky tell you about the structure present over the entire sky.

3.4 The Question of Bright Nights

One of the scientific issues in the 1988 Colorado Campaign regards the occurrence of "bright nights". A "bright night", as the term will be used in this report, is a night where there is structure visible to the naked eye. (Another use of this term refers to the occasions when the airglow background level is much brighter than usual.)²⁸ During the Colorado Campaign there were four bright nights (days 192, 194, 197 and 199) in July, one in May (137) and none in June. Bright nights, however, are regarded as very rare events and for this reason four within one month came as a large surprise. Could the large number of thunderstorms in this area during July explain this finding? Taylor studied this problem by comparing the radar summary charts several hours prior to both the bright nights and a number of control nights. If, in fact, the greater presence of thunderstorms were responsible for bright nights then this association would show up. At the conclusion of the MAPSTAR Program (September 1991) no association had been found,²⁹ apparently leaving the question of bright nights a mystery. After MAPSTAR, under the SOAR Program, Tuan found that wind profile blocking by means of critical-layer interactions would prevent thunderstorms in certain locations from launching waves that can influence the region of airglow under observation. The question will have to be addressed again, with the effects of the wave blocking accounted for.

How do critical layers block the upward propagation of waves? The critical layer is that altitude where the wave velocity is equal to the mean wind. In a frame of reference moving with the atmosphere at that altitude, the wave has an infinite period. Such a wave cannot propagate. Instead, it breaks, and the energy goes into the mean flow.

3.5 Ripple Waves and Their Origins

Historically Peterson was the first person to point out the frequent occurrence of "ripples" in the OH airglow. These consisted of localized patches of wave groups of short horizontal wavelengths. See his paper with Adams.³⁰ Peterson found what he considered to be a statistical correlation between the Kp geomagnetic index and ripples. He also noted a

²⁸Hoffmeister, (1952) Investigations on Bright Night Sky and Luminous Bands, *Brit Astronom. Assn.*, **62**:288.

²⁹Taylor, M.J., Ryan, E.H., Tuan, T.-F., and Edwards, R. (1993) Evidence of preferential directions for gravity wave propagation due to wind filtering in the middle atmosphere, *J. Geophys. Res.*, **98**:6047-6057.

³⁰Adams, G.W., Peterson, A.W., Brosnan, J.W., and Neuschafer, J.W. (1988) Radar and optical observations of mesospheric wave activity during the lunar eclipse of 6 July 1982, *J. Atmos. Terr. Phys.*, **50**:11-20.

statistical relation between ripples and lunar position, ripples occurring more frequently when the moon was at the nadir (or at lower lunar transit). Subsequently Taylor and Hapgood³¹ called such correlations into question, and a debate with Peterson is now occurring. It is fair to say that, at present, the cause of ripple events is unknown. This question has scientific significance, but it has also practical implications as well because the smallest structures in IR clutter have the most impact on the Air Force's surveillance systems (as is also the case for the acoustic type waves mentioned above). This is therefore an area which merits more research in the future. Finally it should be mentioned that Tuan et al³² have described how "ripple" might be the result of an instability of large scale waves.

3.6 Horizon To Horizon Sinusoidal Waves

Figure 8 shows an all-sky image, recorded by Peterson at ECARC during the 1988 Colorado Campaign, where a sinusoidal variation in brightness extends from horizon to horizon. This represents an area of 1000 km X 1000 km with approximately twenty cycles across the sky. This observation raises a number of questions. What is the source of these waves? Are they trapped waves? Why is the image not in the form of a *wave packet* since there exists an instability (Benjamin Feir)³³ that causes sine waves to break up into wave packets. Do such airglow sine waves turn into packets somewhere? When Peterson observed such a display it was considered to be rare. Subsequently, with the advent of more sensitive CCD cameras it has been found that they are not so rare. Taylor and others have also observed such images, but the many questions about their origin and behavior still remain.

To answer each question the following procedures would be needed. The source of gravity waves can be ascertained by locating likely sources such as thunderstorms or jet streams and then using ray tracing techniques such as those used by Taylor, Tuan, and Hines. The question of trapped waves can be investigated theoretically if one has information on the profiles of buoyancy frequency and wind. When the gravity wave's local frequency is equal to the buoyancy frequency (for example, because of Doppler shifting) it will be reflected and it can be thus trapped between two altitudes. (See Section 4.4). The questions regarding the Benjamin Feir instability are contingent upon a theoretical proof that it applies to internal waves. I am not aware of such a proof.

³¹Taylor, M.J., and Hapgood, M.A. (1990) On the origin of ripple-type wave structure in the OH nightglow emission. *Planet. Space Sci.*, **38**:1421.

³²Tuan, T.-F., Hedinger, R., Silverman, S., and Okuda, M (1979) On gravity wave induced Brunt-Vaisala oscillations. *J. Geophys. Res.*, **84**:393-398.

³³Infeld, E., and Rowlands, G. (1990) *Nonlinear Waves, Solitons, and Chaos*, Cambridge Press.

A. PETERSON

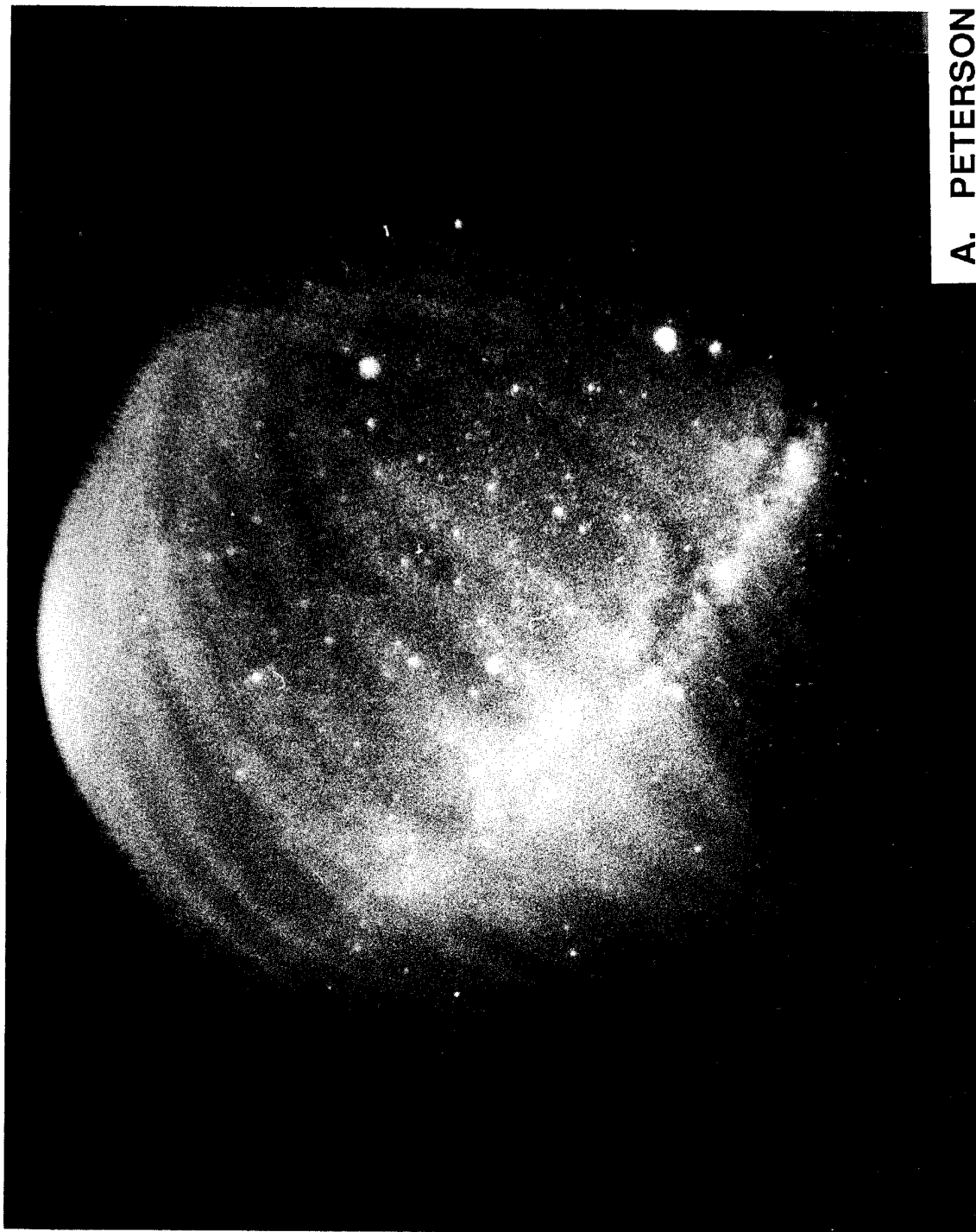


Figure 8. Example of All-Sky Image of OH Brightness Showing a Train of Sine Waves Propagating from Horizon to Horizon (Peterson).

3.7 Simultaneous Color Imaging of OH, OI, and Na Airglow

As was previously mentioned, there are three important airglow layers in the 80 to 100 km region. They are the OH layer at 85 km (Meinel band in the visible and near infrared), the OI green line (557.7 nm) at 90 km, and the yellow Na D lines (589.2 nm) at 95 km. The frontispiece (p. ii) shows one of many color photographic time exposures obtained by Peterson³⁴ (note star-streaks due to earth rotation) which show displaced wave structures in the three colors. At present there are neither simultaneous spectral measurements nor absolute brightness measurements, which would be essential to give scientific evidence that the red, green, and yellow patterns are coming from the airglow layers. On the other hand, there is no obvious alternative explanation for the image. Such photographs suggest that it would be useful to obtain more quantitative measurements in the future. This could be combined with the "ray tracing by phase front" technique pioneered by Taylor et al^{19,20} to determine the vertical progression of the waves.

4. WAVE PROPAGATION, CRITICAL LAYERS, AND AIR PARCEL TRAJECTORIES

A number of predominantly theoretical efforts during the MAPSTAR program studied (a) the blocking of waves traveling from the troposphere to the mesosphere, (b) the trapping of such waves, and (c) the shapes of the trajectories of air parcel motion caused by waves.

4.1 Wind-Profile Blockage of Upwelling Gravity Waves

When waves propagate upwards from their tropospheric sources, it is possible that, at some point, they will encounter winds moving at the same speed and direction as their phase velocity. When this occurs the wave frequency is Doppler-shifted to zero. This is described by saying that the wave has encountered a "critical level". When this happens, the wave usually gives up its energy to the mean flow and does not propagate higher. Of course, the situation is more complicated than this simplified account would suggest. As has been pointed out, for example by Hines³⁵, waves do not reach the critical level without first becoming unstable. McIntyre³⁶ has likened a critical layer to a beach at the edge of the water, which the waves never reach. They break and dissipate their energy before reaching the beach. Our main interest in these critical levels is in the fact that they can block the upward propagation of waves so that they never reach the OH layer. This implies that, for example, a thunderstorm at

³⁴Peterson, A. (1989) 1. Horizon to horizon monochromatic sine-wave in OH airglow - All Sky film camera image., and 2. Color photograph of OH, Na, and O airglows. (Private data submission to MAPSTAR Project).

³⁵Hines, C.O. (1974) Some Consequences of Gravity-Wave Critical Layers in the Upper Atmosphere in Motion, AGU Meeting 1974.

³⁶McIntyre, M. (1992) Comment made at NATO Advanced Research Workshop, Loen, Norway (See also Holton, J.R., and Durann, D. (1993) convectively generated stratospheric gravity waves: The role of mean wind shear, in *Coupling Processes in the Lower and Middle Atmosphere*, Ed. by E.V. Thrane, T.A. Blix, and D.C. Fritts, NATO ASI Series, Kluwer Pub. Co.

a given location cannot, by means of the waves it launches, influence the structure of airglow over certain regions of the sky even if the waves initially propagate in the proper direction. The wind blocking regions are determined jointly by (a) the wave properties and (b) the wind profile between the source and the airglow layer. In Taylor et al, Tuan produced "blocking diagrams" based on climatological winds and tidal models²⁹ and these were compared to Taylor's images during the Colorado Campaign. The authors concluded that "Comparison of the predicted (that is, the least restricted) and the observed directions of the wave motion show almost complete agreement with theory suggesting that middle atmospheric winds may play an important role in governing the flux and azimuthal distribution of short period waves reaching the upper atmosphere." As was mentioned in Section 3, this type of analysis also has been applied to the question of correlation between "bright nights" in the MAPSTAR Colorado data and thunderstorms.

4.2 Gravity-Wave Ducting

Gravity waves can be trapped between two altitudes in the atmosphere or between a certain altitude and the ground. There are at least two mechanisms that can cause this.^{37,38} One is called Doppler ducting. Reflection occurs when a wave reaches an altitude where its frequency is shifted (by the Doppler effect, due to wind change with altitude) to the buoyancy, or Brunt-Vaisala, frequency. Rather than proceeding to a region where the wave would have a frequency higher than the buoyancy frequency, the wave is reflected, for there is a forbidden region in the frequency spectrum of acoustic-gravity waves above the buoyancy frequency above which waves in the gravity-wave branch cannot propagate. The second mechanism leading to ducting is Brunt ducting. Gravity-wave reflections leading to ducting can occur even in a constant wind field if the Brunt, or buoyancy, frequency changes with altitude, due to changes in the atmospheric temperature and composition. Once again, when the frequency of the wave reaches local buoyancy frequency the wave must be reflected. This happens preferentially for high-frequency (short-period) waves. Wang and Tuan³⁸ have described the influence of the combined Brunt-Doppler ducting on short-period gravity waves and discussed how the ducting is modified by viscosity, instability, and nonlinearity.

³⁷Chimonas, G., and Hines, C. (1986) Doppler ducting of atmospheric gravity waves, *J. Geophys. Res.*, **91**:1219.

³⁸Wang, D.Y., and Tuan, T.F. (1988) Brunt-doppler ducting of small-period gravity waves, *J. Geophys. Res.*, **93**:(A9)9916-9926.

4.3 Gravity-Wave Air Parcel Trajectories

The waves responsible for the airglow structures involve fluid motions of the atmosphere which, for any given parcel of air, form closed loops. These, in general, have the shape of an ellipse. The question arises: What shape are the trajectories for the waves that cause the patterns seen in the airglow? Are they very "circular" or, at the other extreme, are they very linear in shape?^{20, 21} Using the information regarding wave frequency and horizontal wavelength reported by Taylor, Tuan et al,²⁹ were able to show that typical trajectories have the form shown in Figure 9. As can be seen the orbits are surprisingly linear in their shape and the waves can be regarded as plane waves, that is, the parcels oscillate in a straight line. The next question is then: What is the shape of the bright regions of airglow?" This is an unanswered question because it has not been examined in detail by experts. In follow-on work Tuan et al³⁹ studied the implications of these findings for direct optical observation of the moving air parcels, using Fabry Perot interferometers.

4.4 Effects of Wave Orientation Upon Ground-Based Measurements of Airglow Temperature and Brightness Fluctuations

It has been known for a long time^{40,41,42} that brightness in airglow is larger when viewed at a low elevation angle from the observer. It could be several times more discernable at low elevation than at zenith. This is because the emitting layer is finite in thickness (of order 7 km) and, as it is viewed from lower angles, the line-of-sight through the emitting volume is increased. Also it is known that large zenith angles enhance brightness contrasts in wave structures¹⁰ Yoshimoto's PhD thesis at USU under MAPSTAR sponsorship studied the effect of gravity-wave orientation upon the phase between temperature and brightness variations caused by these waves in OH.⁴³ These calculations were used in the design of the Colorado Campaign. The design called for both a zenith-looking interferometer at ECARC and another at INSTAAR looking into the same volume of airglow. Yoshimoto also pointed out that gravity waves, due to dispersion, should "chirp", that is change frequency with time, and that source distance can be estimated from this. While this possibility was already implied in former work

³⁹Tuan, T.-F., Lowe, R.P., Isler, J., Picard, R., and Bhattacharyya, A., Analysis of air parcel motion in the presence of gravity waves and winds, Submitted to *Can. J. Phys.* 1995.

⁴⁰van Rhijn, P.J. (1925) *Publ. Ast. Lab. Groningen*, **43**.

⁴¹van Rhijn, P.J. (1919) On the brightness of the sky at night and the total amount of starlight, *Pub. Ast. Lab. Groningen*, **43**.

⁴²van Rhijn, P.J. (1919) On the brightness of the sky at night and the total amount of starlight, *Ap. J.*, **31**.

⁴³Yoshimoto, H (1990) *Study on Dynamics of the Waves in the Mesospheric Hydroxyl Layer*, Ph.D. Thesis, Utah State University, Dept. of Electrical Engineering, Scientific Report by Space Dynamics Laboratory.

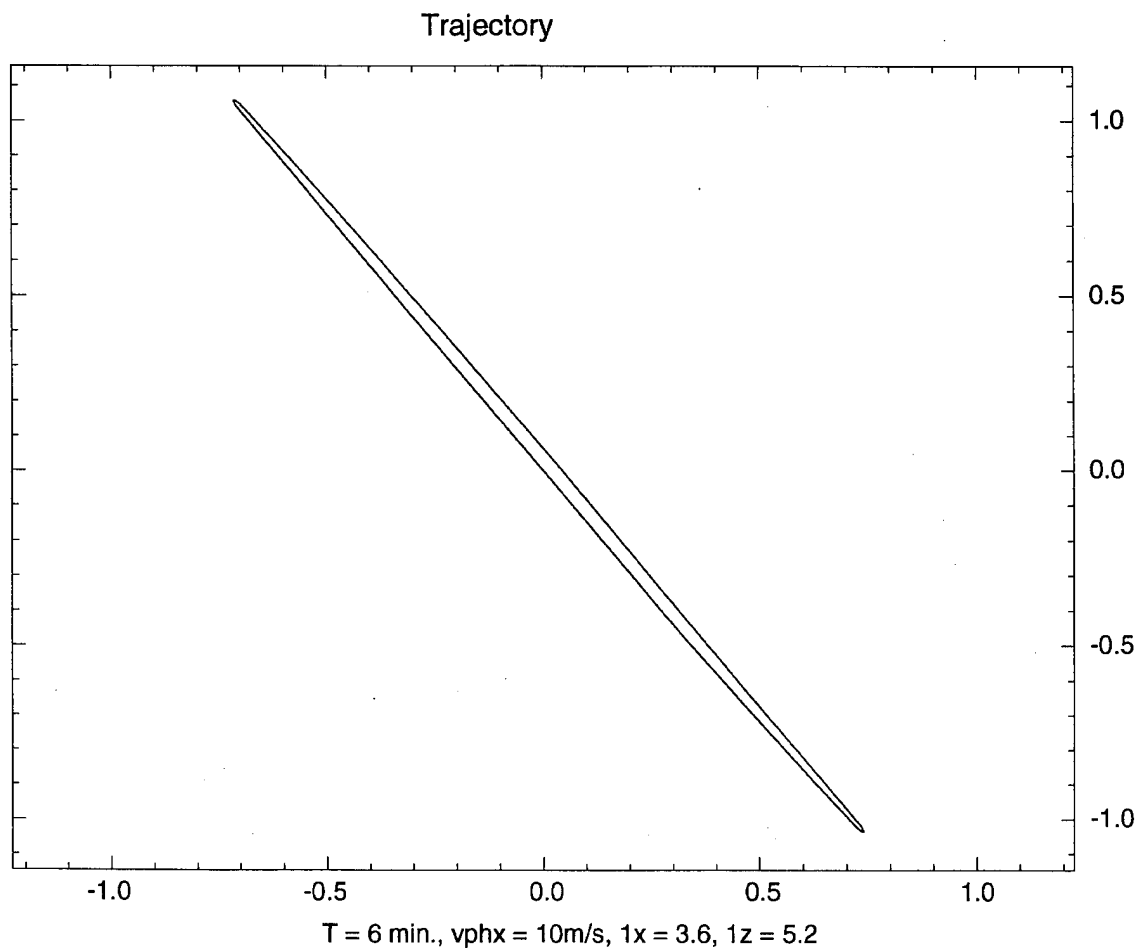


Figure 9. Simulated Orbit of an Air Parcel of Motion Due to a 6 Minute Period Gravity Wave.
Longer periods would have more linear trajectories (Tuan).

by Hines³⁵ and by Francis⁴⁴ this procedure has never been applied to airglow patterns. In oceanography this procedure is quite standard and the distance of a storm is estimated from the rate of change of ocean-wave periods.

5. THE POWER SPECTRAL DENSITIES (PSDS) OF GRAVITY WAVES - THEORY AND EXPERIMENT

5.1 History of Gravity-Wave Saturation Studies

The first model for the spectra of internal gravity waves was created by Garrett and Munk in 1972. This was in the context of the waves within the ocean. Their model was a purely empirical one but it did rely in part on known wave theory in the form of dispersion and polarization relations. The most striking feature of the waves that was included in the model was that these wave spectra have a surprising degree of universality, contradicting the expectation that under very different climatic and geographic conditions the wave spectra would also be very different. This "universality" means that the spectral amplitudes remained within about a factor of 2 or 3 of a universal mean value, regardless of location and environmental conditions. The spectral slopes were also always between -2 and -3. In 1979, I pointed out that the Garrett-Munk model might apply to the atmosphere, and VanZandt subsequently proved that this was indeed true,⁴⁵ giving an explicit version of the Garrett-Munk model for the atmosphere. Then a paper was published by Dewan, Grossbard, Quesada, and Good,⁴⁶ that showed a very dramatic example of spectral universality for stratospheric winds (See Figure 10). Subsequently, Dewan and Good⁴⁷, gave a possible physical explanation for this universality based on the concept of saturation. Their explanation was a very simple one. Atmospheric gravity waves are known to grow as they ascend in altitude, due to the exponential decrease of density with height. However, they can grow only a limited amount before their amplitude becomes too large for stability and they break either from the convective or the shear-induced instability mechanism. This suggests that there may be an analogy between these waves and the saturated surface ocean waves that form whitecaps when they reach a certain amplitude where the downward accelerating crest approaches the

⁴⁴Francis S.H. (1975) Global propagation of atmospheric gravity waves: A review, *J. Atmos. Terr. Phys.*, **37**:1011-1054.

⁴⁵VanZandt, T.E. (1982) A universal spectrum of buoyancy waves in the atmosphere, *Geophys. Res. Lett.*, **9**:575-578.

⁴⁶Dewan, E.M., Grossbard, N., Quesada, A., and Good, R.E. (1984) Spectral analysis of 10 m resolution scalar velocity profiles in the stratosphere, *Geophys. Res. Lett.*, **11**:624.

⁴⁷Dewan, E.M., and Good, R.E. (1986) Saturation and the universal spectrum for vertical profiles of horizontal scalar winds in the atmosphere, *J. Geophys. Res.*, **91**(D2):2,742-2,748.

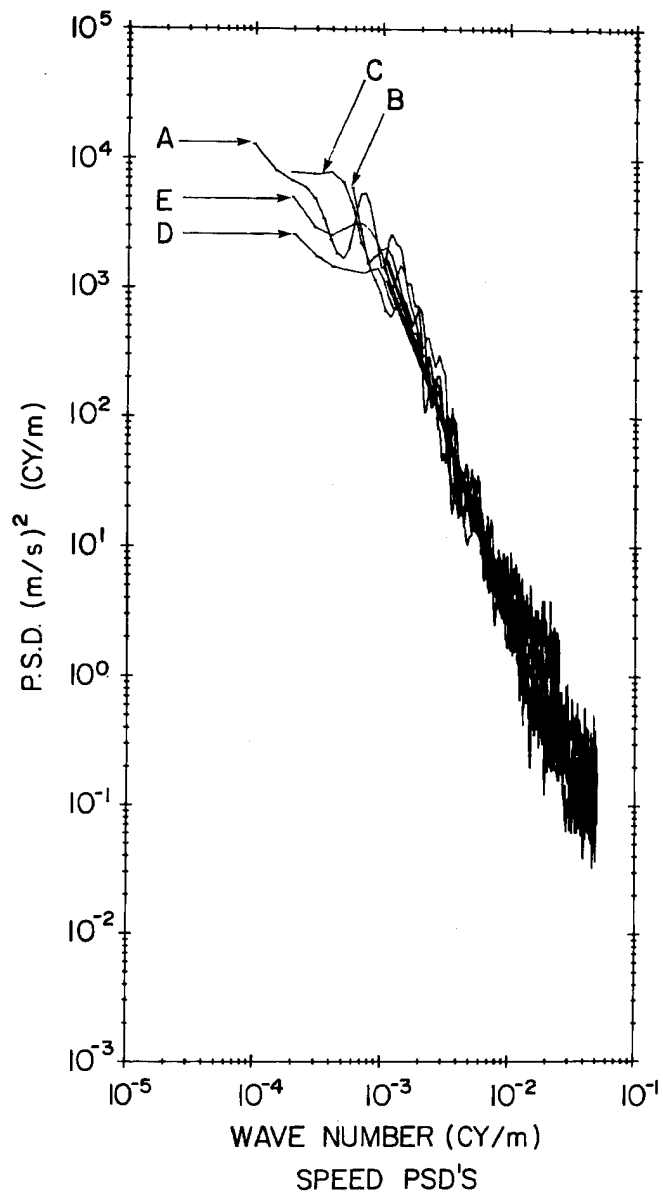


Figure 10. Well Known Example of Universal PSD (vertical wave number, horizontal speeds) of Gravity Waves in the Lower Stratosphere (Dewan, Good, Grossbard et al).

acceleration of gravity. Due to the linear instability, their amplitude cannot grow any higher because turbulence drains their energy. As was shown in Dewan and Good⁴⁷, it is possible to deduce on dimensional grounds alone (similarity theory) that the particular spectra at issue (vertical wave number, horizontal wind fluctuations) would depend on the vertical wave number, k_z , as k_z^3 , and would have amplitudes directly proportional to the squares of the buoyancy frequency N . They also showed that this set of predictions was in very good agreement with the experiment. They compared the stratospheric and tropospheric spectra and found that the latter were, as predicted, about a factor of 3 lower in amplitude. Smith, Fritts, and VanZandt⁴⁸, subsequently extended this work, and these two papers have been, and continue to be, cited extensively in the literature. (over 87 citations as of July 1995). Recently, competing theories by Hines, Weinstock, and others have been advanced and gravity-wave saturation has become an area of very active research. Weinstock's theory says that the saturation is due to wave mode interactions that limit amplitudes by draining them when they are larger than a certain amount. Hines' theory, which also involves wave-wave interactions, involves the Doppler spreading of small waves by the large waves. Ultimately the small waves are annihilated by background winds when their periods are Doppler shifted to infinity (critical level).

5.2 Gravity-Wave Frequency Spectra

The universal spectral theories described above address only the form of the vertical wave-number spectrum and do not explain either the frequency spectra or horizontal wavenumber spectra of the waves. For this reason, further work was carried out under MAPSTAR. The physical model finally obtained depends on the notion that the waves can interact with each other and that the wave energy can cascade from larger to smaller scales to the point where it can dissipate through either a turbulent or viscous mechanism. This happens because large waves have smaller waves that feed on their shears, and smaller waves have still smaller waves that repeat this process in a self-similar manner down the scales.⁴⁹ The theory is analogous in some ways to the theory for turbulence energy spectra due to Kolmogorov. In the latter theory large eddies break into smaller eddies, and smaller eddies break into still smaller eddies, and so on. This wave theory was published by Dewan^{50,51} and it has numerous experimental ramifications. One of the most important of these is that the frequency spectra of horizontal velocity, and also of temperature fluctuations, are proportional to the turbulent energy-dissipation rate, ϵ , and to the inverse of the frequency

⁴⁷Smith, S.A., Fritts, D.C., and VanZandt, T.E. (1987) Evidence for a saturated spectrum of atmospheric gravity waves, *J. Atmos. Sci.*, **44**:1404-1410.

⁴⁸Dewan, E.M. (1979) Stratospheric wave spectra resembling turbulence, *Science*, **204**:832-835.

⁴⁹Dewan, E.M. (1990) *Power Spectra of Internal Gravity Waves*, Geophysics Laboratory, GL-TR-90-0233, NTIS number ADA 231596.

⁵⁰Dewan, E.M. (1991) Similitude modeling of internal gravity wave spectra, *Geophys. Res. Lett.*, **18**:1473-1476.

squared (ω^2). In Section 6, the first test of this prediction will be described. To date the wave cascade theory predictions are consistent with experimental observations.

5.3 Gravity-Wave-Induced Temperature Fluctuations

The theory of atmospheric acoustic-gravity waves⁵², as published by Hines in 1960, predicts that these waves cause fluctuations in temperature. This happens by means of two separate physical mechanisms. The first mechanism involves the adiabatic compression and expansion of air parcels as the wave alternatively raises and lowers them. These oscillating changes in pressure cause the temperature to oscillate. The second physical mechanism also changes the temperature through pressure changes; however, it does so without altitude changes. It resembles acoustic compression and expansion in this limited sense. Makhlof et al⁵³ showed that the two mechanisms contribute to the total fractional temperature change through separate additive terms and also showed that the latter acoustic-type of change is insignificant as long as the wave's horizontal speed is small compared to the speed of sound. This condition is met by most of the waves seen in the airglow images of Taylor and Peterson. From this we can conclude that, for sufficiently small phase speeds, *measurements of temperature fluctuations of air parcels correspond to measurements of height fluctuations*, and, a 1°K change in temperature corresponds to about a 100 m change in height. This fact is used in Section 6 below to connect Dewan's spectral theory with MAPSTAR observations.

5.4 Potential Applications

At this time, the N^2 amplitude dependence of the saturated wave vertical wavenumber spectrum as well as its k^3 dependence have been thoroughly tested in the radar and lidar literature. In contrast, the ϵ dependence predicted by Dewan's theory for the frequency spectrum has yet to be *directly* tested in an experiment where both ϵ and the spectrum are measured at the same time. If the scaling of the power spectrum with ϵ proves valid and experiments agree with prediction, then it will become possible to measure the important parameter ϵ directly from spectra of lidar temperature time series.

Another application of the spectral models that is closer to the direct Air Force systems needs is the ability to predict the dominant scales of the waves as a function of altitude (Figure 11). Such waves would lead to clutter in Air Force surveillance systems. The main wave scales

⁵²Hines, C.O. (1960) Internal atmospheric gravity waves at ionospheric heights, *Can. J. Phys.*, **38**:1441-1481, and Correction. (1964) *Can. J. Phys.*, **42**:1425-1427.

⁵³Makhlof, U., Dewan, E.M., Isler, J.R., and Tuan, T.-F. (1990) On the importance of the purely gravitationally induced density, pressure, and temperature variations in gravity waves: their application to airglow observations, *J. Geophys. Res.*, **95**:4103-4111, also, Makhlof, U., Picard, R.H., and Winick, J.R. (1990) Modulation of the hydroxyl emission by a monochromatic gravity wave in a realistic, non-isothermal atmosphere, *EOS*, **71**:1496.

TURBULENCE AND WAVE SCALE ESTIMATES

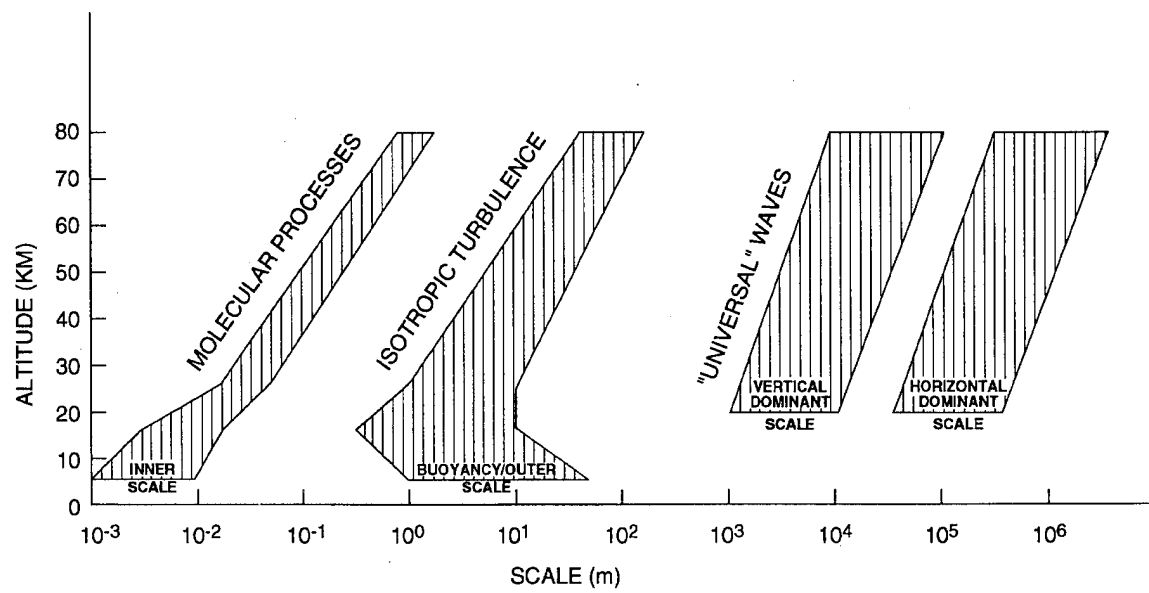


Figure 11. Scales of Turbulent Inner and Outer Scales as Well as Wave "Outer" Scales Estimated by Dewan.

move from short wavelengths to long wavelengths as the altitude increases. Also shown are the relevant scales for turbulent velocity fluctuations.

6. MAPSTAR OH AIRGLOW TEMPERATURE AND BRIGHTNESS FLUCTUATIONS

6.1 Temperature Power Spectra: Model Compared to Data

The temperature of the OH airglow layer was measured on 23 nights by means of the ground-based IRFWI Fourier spectrometer during the MAPSTAR 1988 Colorado Campaign. These data were spectrally analyzed and the temperature spectra were compared to the predictions of Dewan's model^{50,51}. (See Section 5.2). It was found that the experimental spectra had both the shape and the amplitude that were theoretically predicted. Agreement of slope was within experimental error while agreement of amplitude was consistent with bounds of the observations. The results were published in Dewan, Pendleton, Grossbard, and Espy⁵⁴. Figure 12 shows the comparison between theory and experiment. This paper is unusual in that both the physical theory and its first (and successful) experimental test were carried out by the same group during the same program.

6.2 Processing of Data Having Gaps or Intervals of Missing Information

During the course of this work it was found necessary to cope with sizeable data gaps caused by the necessity to realign the interferometer several times during a night. Grossbard and Dewan found two techniques to do this and presented them to an IEEE/ASSP signal processing meeting.⁵⁵

6.3 OH Airglow Brightness Power Spectra

During the same campaign Peterson measured OH brightness at the ECARC site by means of a zenith-pointing photometer. These data were subjected to time series analysis and Figure 13 shows an example. These spectra suggest that the slopes of the frequency PSDs of brightness are a bit steeper than frequency PSDs of temperature. This implies that the Krassovsky ratio is relatively constant with respect to frequency, which is both surprising and not yet understood. The OH brightness spectra will be combined with the temperature spectra from IRFWI and from UWOMI-1 in a future publication under the SOAR Program.

⁵⁴Dewan, E.M., Pendleton, W., Grossbard, N., and Espy, P., (1992) *Geophys. Res. Lett.*, **19**:597-600.

⁵⁵Grossbard, N., and Dewan, E.M. (1991) Methods for estimating the autocorrelation and power spectral density function when there are many missing data values, ASSP Workshop on Spectral Estimation and Modeling, Oct. 10-12, 1991.

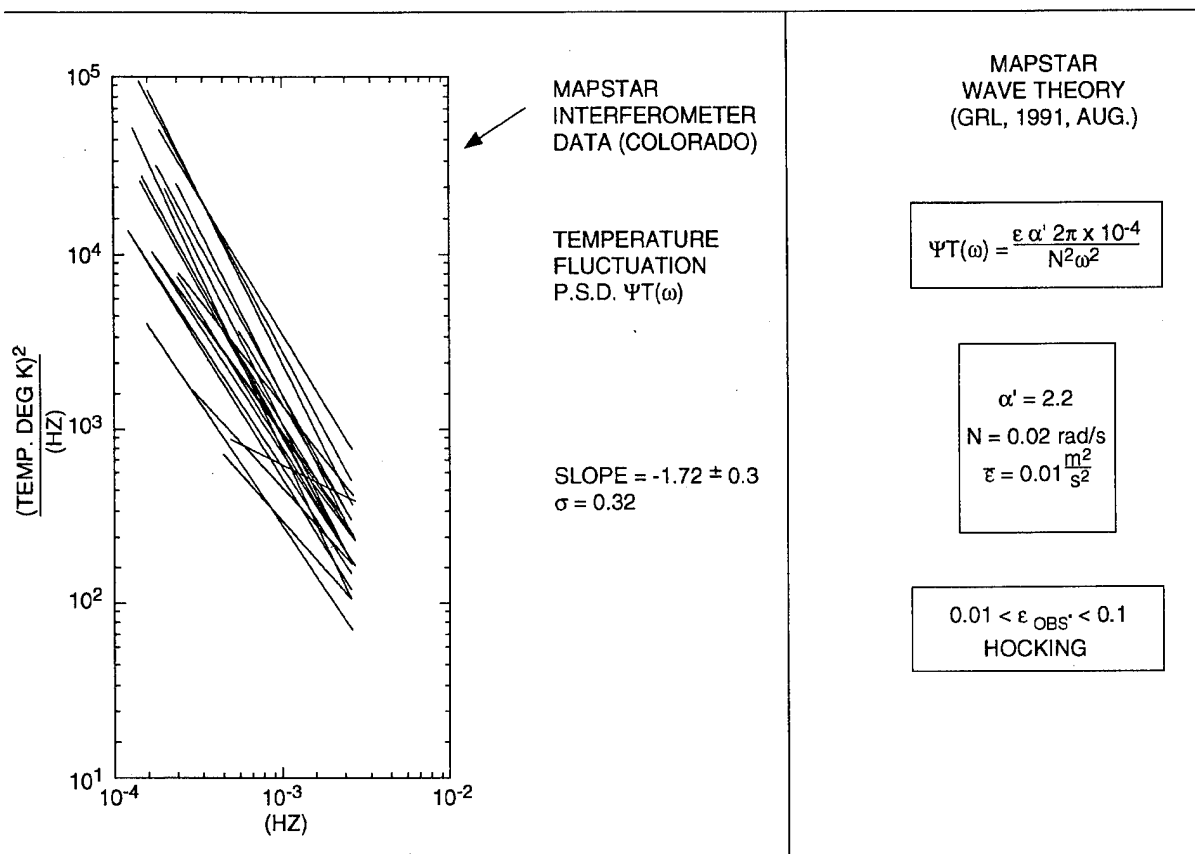


Figure 12. Temperature Spectra (fitted line) Showing $\omega^{-5/3}$ Slopes (temporal frequency) and Amplitude in Agreement with Observed ϵ Values as Predicted by Cascade Scaling (Dewan, Pendleton, Espy, and Grossbard).

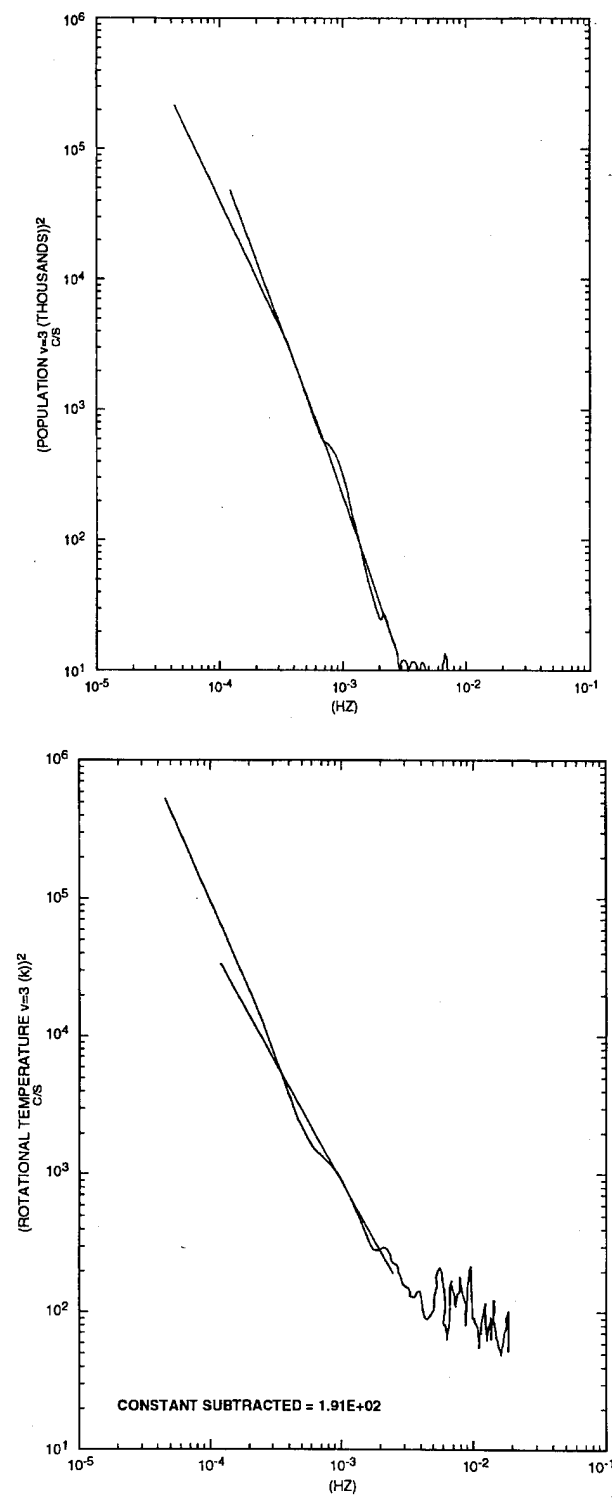


Figure 13. (a) PSD of Brightness Variation in OH (Lowe et al), (b) PSD of Temperature Variation OH (Lowe et al). These were obtained from Mt. Haleakela, Hawaii during the 1990 ALOHA Campaign.

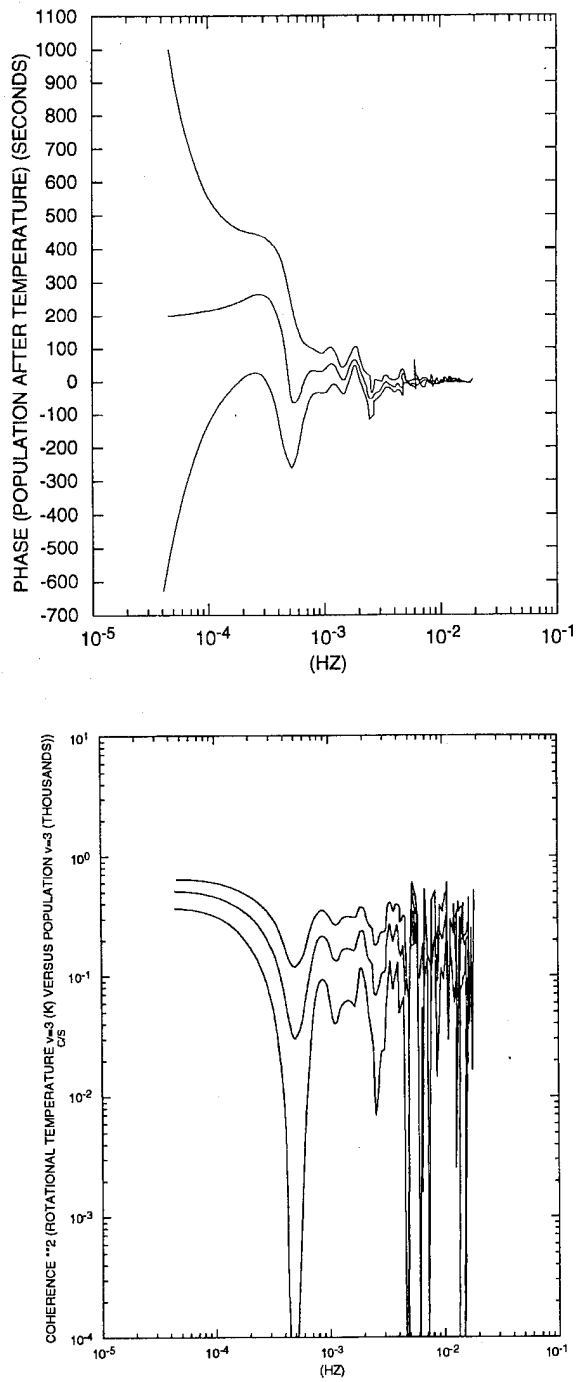


Figure 14. Results of a Cross-Spectral Analysis of the Signals (temperature and brightness) Shown in Figure 13. (a) Shows phase and (b) the coherence between the signals. The upper and lower curves were intended to represent "error bars" relating to plus or minus one standard deviation. The main conclusion is that the main frequencies of interest (10^{-3} Hz to 5.5×10^{-4} Hz) or 5 min. (buoyancy period to 1/2 hour) there is a coherence around 0.1 and the phase is around 0°

6.4 OH Temperature-Brightness Cross-Spectra

In other work the cross-spectral analysis of simultaneously measured intensities and temperatures from the IRFWI and UWOMI measurements is currently underway. The resulting coherence, or normalized cross-spectral density, versus frequency, for the UWOMI data from the ALOHA Campaign is shown in Figure 14. The cross spectrum is defined as the frequency transform of the cross-correlation⁵⁶ They show a nearly zero phase difference between the two signals, which shows that the intensity and temperature signals are nearly in phase. This is consistent with the conclusions of Lowe et al.⁵⁷ The theoretical implication is that the waves are trapped.⁵⁸ (This according to C. Hines, Private Communication.)

6.6 Source of Brightness Fluctuations and Photochemical/Dynamical Models

As mentioned above, the main sources of fluctuations in wind velocity and density in the mesosphere and lower thermosphere are acoustic-gravity waves. The density fluctuations induce temperature fluctuations (see Section 5) as well as fluctuations in the concentrations of every minor species, of every reactive metastable species, and of every excited state. Thus the rates of dynamical processes such as advection, as well as the rates of collisional and photochemical production and loss processes for states that radiate light, all fluctuate due to the presence of the gravity wave. The response of emissions, such as the OH Meinel-band airglow, to gravity-wave modulation has been developed under the MAPSTAR Program. The novelty of the model is that it is able to include effects not included in prior models, such as quenching, wave-induced advection, and a realistic non-isothermal atmosphere. This model is being prepared for publication under the SOAR Program. It is also being further developed by adding a background wind model and by including the Doppler-shifting of the gravity waves by the background wind. Comparisons between the model predictions and the MAPSTAR data sets are also underway.

7. NEW INSTRUMENTATION

7.1 The MAPSTAR Radar and the IDI (Imaging Doppler Interferometer) Method of Adams and Brosnahan

MAPSTAR sponsored the design and construction of a revolutionary new atmospheric wind measuring radar based on the IDI (Imaging Doppler Interferometer) method. The IDI

⁵⁶Blackman, R., and Tukey, J. (1958) *The Measurement of Power Spectra*, Dover, New York.

⁵⁷Lowe, R.P., Gilbert, K.L., and Turnbull, D.N., (1991) High latitude summer observations of hydroxyl airglow, *Planet, Space Sci.*, **39**:1263-1270.

⁵⁸Hines, C.O., Private Communication

method involves three techniques used simultaneously. These are (a) the usual radio ranging technique, which gives distance of a scatterer (or reflector) by means of the signal round-trip time, or time delay between the transmitted and received signals, (b) the Doppler technique that measures the radial velocity of the scattering or reflecting volume by means of a frequency shift, and (c) an interferometric technique that yields the direction of the received signal by means of phase measurements over two mutually perpendicular receiving antenna arrays. When more than one scattering volume returns a signal in one range gate they are distinguished from each other by means of their individual Doppler-shifted frequencies, so that the IDI can "look" in several directions simultaneously. The transmitter was operated at around 2 MHz, which is a low frequency that ordinarily would entail the use of a large (= 100 in.) diameter antenna. The use of interferometry allows one to eliminate this costly requirement and therefore to use a small, inexpensive antenna that is easy to transport. This causes the instrument's antenna pattern to have a very large main lobe but, due to interferometry, the latter is now an advantage, making it possible to receive from many directions simultaneously. In this way the IDI obtains a three-dimensional picture of positions and velocities of "scatterers". For more of the details of this technique the reader may consult Brosnahan and Adams,¹⁴ and Adams et al.^{59,60}

Demonstrations of the IDI concept by means of a prototype instrument at Boot Lake,^{61,62} Colorado and analyses of the resulting data are given in Adams et al,^{61,62} Turek,⁶³ Coble⁶⁴, and Halderman.⁶⁵ See also Section 2.2 where the Boot Lake Campaign is described. One of the studies, for example, consisted of imaging a TID (Traveling Ionospheric Disturbance) in time and space⁶¹. Another investigation examined the aspect sensitivity of the backscattering of the radar signal as a function of altitude⁶². Indeed, a large altitude dependence was found. Presumably the scatterers are related to turbulence, but their nature remains, by and large, a mystery. They are the subject of much scientific interest at present. The IDI, therefore, has a second role in addition to measuring winds. This role consists of

⁵⁹Adams, G.W., Edwards, D.P., and Brosnahan, J.W. (1985) The imaging doppler interferometer: data analysis, *Radio Science*, **20**:1481-1492

⁶⁰Adams, G.W., Brosnahan, J.W., Walden, D.C., and Nerney, S.F. (1986) Mesospheric observations using a 2.66 MHz radar as an imaging doppler interferometer: description and first results, *J. Geophys. Res.*, **91**:1671-1683.

⁶¹Adams, G.W., Brosnahan, J.W., and Haldermen, T.D. (1988) Direct radar observations of TID's in the D and E Regions, *J. Atmos. Terr. Phys.*, **50**:931-935.

⁶²Adams, G.W., Brosnahan, J.W., and Johnson, R. (1989) Aspect sensitivity of 2.66 MHz radar returns from the mesosphere, *Radio Science*, **24**:127-132.

⁶³Turek, R.S. (1986) *An Analysis of Upper Atmospheric Parameters Derived From the Observation of Meteor Echoes by a 2.66 MHz Radar*, Master's Degree Thesis, Utah State University in Dept. of Soil Science and Biometeorology (Aeronomy), CASS Report GR-06, Center for Atmospheric and Space Science.

⁶⁴Coble, B.B. (1987) *Middle Atmospheric Wind Measurement Using a Medium Frequency Radar*, Master's Degree Thesis, Utah State University, in Dept. of Soil Science and Biometeorology, CASS Report GR-07, Center for Atmospheric and Space Sciences.

⁶⁵Halderman, T.D. (1987) *An Analysis of Apparent-Motion Vectors in, and the Structure of, a Mid-Latitude Sporadic E Layer Using a 2.66 MHz Radar*, Master's Degree Thesis, Utah State University, in Dept. of Soil Science and Biometeorology, (Aeronomy), CASS Report GR-08, Center for Atmospheric and Space Sciences.

probing the atmosphere to learn more about its turbulence.

In one of the IDI prototype studies, Coble, showed radar returns⁶⁴ coming back from the altitude region of 50 - 70 km. There seems currently to be no proven theory to explain these returns (unless the IDI technique is far more sensitive than previous techniques). This circumstance caused some members of the radar community to express skepticism and blame the result on an artifact due to a return received in a side-lobe of the main beam. It is clear that more work must be done to validate this interesting result.

Some of the scientific findings resulting from the IDI radar by Adams and co-workers will be discussed in Section 9. As was already mentioned, the construction of the instrument was not completed under MAPSTAR due to increases in cost and a funding cut. Adams et al had to make up for the lack of a transmitter by using the Arecibo heater as a transmitter during the AIDA Campaign. Construction of the receiver was completed, but the transmitter was incomplete. In addition, they had to rely on off-line data processing since their on-line software was not yet completed. Nevertheless, AIDA Campaign participation allowed direct comparison to be made between the IDI and other more established methods of wind measurements for the first time. (See Section 9.2 for results).

Gene Adam's untimely death did not allow him to see publication of his successful participation with the IDI in the AIDA Campaign (two papers in JATP, 1992). His goal of building a completed on-line-data-processing IDI will be carried out by his surviving colleagues.

7.2 Infra-Red Field Widened Interferometer (IRFWI)

Early in the MAPSTAR Program there was an important modification of USU's venerable IRFWI instrument to enable it to have a high light flux throughput, but, at the same time, to have a small FOV. The description of this modification together with a description of the observations in the Sac Peak Campaign are described by P. Neal²⁵. The technique subsequently used to extract temperatures from the OH IR spectra was described in other MAPSTAR publications by Chao⁶⁶, and Hammond.⁶⁷ The IRFWI instrument played a major role in the MAPSTAR Program, including the 1988 Colorado Campaign, and was responsible, for example, for the data used in Dewan et al⁵⁴.

7.3 The Infrared MAPSTAR Interferometer/Spectrometer

A second infrared instrument, the MAPSTAR interferometer, was designed and built during the MAPSTAR Program⁶⁸. It was deployed during two campaigns, MISTI and Colorado

⁶⁶Chao, S.C. (1987) Signal Processing of Hydroxyl Airglow Interferometric Data, in *MAPSTAR Data Report No. 3*.

⁶⁷Hammond, M.R. (1992) *A Study of Temperature Derived from the OH Meinel (3.1) and (7.4) Bands in the Night Airglow*, Master's Degree Thesis, Utah State University, Department of Physics.

⁶⁸Ware, G., and Goode, D. (1988) *MAPSTAR Interferometer Piece Part Drawings*, MAPSTAR Data Report No. 9.

1988. The objective in the design of this instrument was to have it carry out real time data processing and actually give temperature versus time in the field. In addition, it was designed to point sequentially in three directions in the sky forming an equilateral triangle, making it a most primitive (to be sure) "imager" for brightness and temperature of the OH airglow layer. In this way, OH structure and its motion could be inferred in a manner analogous to that used in the commonly used spaced-antenna drift (SAD) method of inferring atmospheric motions by radar. Stacey⁶⁹, shows how this could be achieved. Methods of data analysis to get temperatures that were optimally smoothed and filtered by means of a Kalman filter were developed and tested by Stirling, Pike, and Ware⁷⁰, and a despiked spectral catalogue was produced of day 138 of the Colorado 1988 Campaign. A paper by Ware based on this campaign was presented to the AGU. The final completion of this instrument was prevented by funding limitations. (See Ware and Baker.⁷¹)

8. EXPERIMENTAL FINDINGS OF MAPSTAR

8.1 Gravity-Wave-Driven OH Airglow Findings

8.1.1. OROGRAPHIC EFFECTS ON OH STRUCTURE

One of the original goals of the MAPSTAR Program was to measure OH structure from several different geographical locations that had markedly different orographic conditions, for example, mountains vs mid-ocean. Originally it was believed that, since wind flowing over mountains is a well documented source of atmospheric gravity waves, one could expect to find a significant difference in the OH structure over mountains as compared to over oceans or flat lands. In the reports by Taylor and others from Hawaii during ALOHA¹⁵ and from Colorado during the 1988 Mapstar Campaign⁷², in addition to Taylor and Henriksen¹⁸ it was found that there was *no evidence for a difference in OH structure* despite differences in latitude and orography. The authors interpreted this, at first surprising, finding as evidence that the sources of the waves responsible for the observed structure were airborne rather than orographic. Further evidence that this interpretation is valid is the fact that none of the observed structure showed any behavior that would indicate that it was "locked" to orography in the manner of mountain waves. In other words, none of the structure remained nearly stationary or reversed direction in response to changes of low-altitude winds. Mountain-wave

⁶⁹Stacey, N. (1987) Finding the direction, speed, and Wavelength of OH airglow waves from three observation points, in MAPSTAR Data Report No. 8.

⁷⁰Stirling W., Pike, J., and Ware, G. (1987) Temperature Estimation from OH Radiation, in MAPSTAR Data Report No. 8.

⁷¹Ware, G., and Baker, D. (1990) Spatially separated observations of OH intensity and rotational temperature waves, EOS, **71**:573.

⁷²Taylor, M.J. (1991) MAPSTAR Final Report, subcontract 387-003 and C802640 (period covered, October 1987 to 30 June 1991) between Utah State University and Southampton University, U.K., presented at the Final MAPSTAR Workshop, University of Western Ontario, London, Ontario, September 1991

type structures have never been clearly documented in the mesospheric and thermospheric emissions to my knowledge, except perhaps in some unpublished observations by A. Peterson.

Why are orographic wave patterns so rare in airglow? The answer seems to be that such waves can be filtered out on their way to the mesosphere from the troposphere. In the 1988 Colorado Campaign, it was predicted by D. Fritts during a MAPSTAR workshop, prior to the campaign, that mountain waves would not reach the mesosphere at that time of year in Colorado. The reason cited was critical-layer blockage.

8.1.2 IN-SITU GRAVITY WAVE GENERATION

During the ALOHA Campaign there were two observations of fields of coherent short-period waves seen in conjunction with long-period waves. These are described in Taylor and Edwards¹⁶, who made the case that the short-period waves, or billows, were generated *in-situ* by the long-period waves. The process they considered to be responsible was related to the Kevin-Helmholtz instability³².

8.1.3 SIMULTANEOUS RADAR AND IMAGER OBSERVATIONS

As was mentioned above, radar measurements of mean winds at the OH altitudes were obtained over Platteville during the 1988 Colorado Campaign. Taylor, Conner, Avery, and Pendleton⁷³, reported a wave in the airglow with phase velocity equalling the mean wind velocity at the airglow altitude of 85 km. When this condition occurs one has, as discussed in Section 4.1, a critical layer for that wave. The authors have not completed their final interpretations of this rather strange observation. It may have been a growing "Kelvin Helmholtz billow"; but to prove that the wind shear at 85 km is sufficiently great to cause this effect would have required a resolution greater than was available to them.

8.1.4 CO-VARIATION OF THE TEMPERATURE AND INTENSITY OF OH AIRGLOW

During the ALOHA Campaign, Turnbull and Lowe⁷⁴ measured, by means of a Michelson interferometer, both the absolute brightness (I) and temperature (T) of the OH airglow. They noted that I and T changed synchronously and that there was no phase lag between them. Current work in progress by Dewan and Grossbard involves the use of cross-spectral analysis on this data. They have confirmed that that phase differences between the two fluctuations are essentially zero for frequencies of interest.

⁷³Taylor, M.J., Connor, L., Avery, S.K., and Pendleton, W., Jr. (1992) Evidence of preferential directions for gravity wave propagation due to wind filtering in the middle atmosphere, *J. Geophys. Res.*,

⁷⁴Turnbull, D.N., and Lowe, R.P. (1991) Temporal variations in the hydroxyl nightglow observed during ALOHA-90, *Geophys. Res. Lett.*, **18**:1345-1348.

8.1.5 SIMULTANEOUS GROUND MEASUREMENTS OF OH TEMPERATURE BY LIDAR AND INTERFEROMETER/SPECTROMETER

A campaign was conducted at Wright Patterson AFB by R. Lowe and J. Meriwether involving simultaneous operation of a Fourier spectrometer and a lidar. The lidar employed a large astronomical telescope to obtain the largest power-aperture product for lidar to date, making possible reliable measurements in the 80 km region. In this manner it was possible for both instruments to observe the temperature in the OH layer at the same time. This was done to test a possible solution to a long-standing problem. At present, typical Rayleigh lidars cannot measure absolute temperature but can only infer temperature changes with altitude from density changes. Thus the temperatures must be "anchored" to a known value at some altitude to know the absolute temperatures at all the other altitudes. The usual procedure is to assign to the highest altitude a standard temperature from a climatological model appropriate to the location and time of year. In this experiment the possibility of using the interferometer to obtain the "anchor temperature" was tested. Preliminary results suggest that some problems still remain to be ironed out. Gravity waves tend to keep temperatures changing and this may have introduced the problems that Lowe and Meriwether encountered. It may be necessary to include special averaging procedures before consistency is achieved. However, a very important and long-standing problem may soon be solved by this technique.

8.2 Findings on Wind Measurements

8.2.1 PSDs OF STRATOSPHERIC WIND COMPONENTS

Vertical profiles of horizontal winds were obtained in the stratosphere by means of rocket laid smoke trails photographed in time-lapse fashion from locations on the ground under the CIAP Program. Subsequently Dewan et al⁷⁵, published PSDs for five zonal and five meridional wind profiles. All of the profiles exhibited the universal slope of -3. However, there was a statistically significant difference between the amplitudes of the fluctuations in the two directions. The zonal fluctuations were on average about 25 percent larger than meridional.

8.2.2 DEFINITIVE MESOSPHERIC RADAR WIND PROFILE MEASUREMENT COMPARISON

There are several radar techniques to measure wind profiles. These include, for example, meteor radar, incoherent scatter radar, partial reflection, spaced-antenna drift (SAD), Doppler radar, and the previously mentioned MAPSTAR IDI radar. It has been observed that sometimes these radars give mutually inconsistent results which are far beyond what can be attributed to experimental error. The only possible explanation is that they are not all

⁷⁵Dewan, E.M., Grossbard, N., Good, R.E., and Brown, J. (1988) Power Spectral Densities of Zonal and Meridional Winds in the Stratosphere, *Physica Scripta*, **37**:154-157.

measuring fluid motions, but are measuring different phenomena sometimes. C. Hines has suggested, for example, that some radars (for some altitudes) might be measuring a "glint" from a surface which is distorted by a wave. In this case, what may show up on the radar as fluid motion (a so-called wind) may instead be wave phase motion.

To try to resolve this conflict, Hines organized the AIDA 89 campaign under NSF sponsorship in Arecibo, Puerto Rico. Wind measurements by several side-by-side radars were compared. Two of these were incoherent scatter radars and the MAPSTAR IDI radar, even though the latter instrument lacked a transmitter. The Arecibo heater transmitter was used for that purpose, and the MAPSTAR IDI receiver array was operated for the first time. The results are definitive and it has been established that the IDI (and by implication the SAD) and incoherent scatter radars give the same results (within error) up to 80 km altitude. Up to 80 km, in other words, the winds retrieved are consistent. Above 80 km they are not consistent and the radars, therefore, must be measuring different atmospheric parameters.

The results have been published by Brosnahan and Adams¹⁴, and Hines, Adams et al⁵⁹, in a special issue of Journal of Atmospheric Physics (JATP) devoted to the AIDA Campaign. This issue was dedicated posthumously to Gene Adams.

8.2.3 IDI TIDAL MEASUREMENTS

An additional and important finding made in the AIDA Campaign was also reported in the JATP special issue. This was the discovery that, although consistent wind measurement results could not be obtained above 80 km, it was nevertheless possible to measure tides consistently. The inconsistency of the results is removed and one can find the tides by means of long time averages. This presumably filters out any short-term wave phase velocity effects and recovers tidal fluid motions.

These dramatic results would have been impossible to obtain during the AIDA campaign without the participation of the MAPSTAR interferometer. The fundamental question "what are the electromagnetic scatterers" for the IDI is a problem still not solved.

9. OH MOLECULAR SPECTROSCOPY AND MESOPAUSE-REGION TEMPERATURE MEASUREMENTS (contributed by R.H. Picard)

The method used to measure temperature from OH Meinel-band emission observations on the ground makes use of a high-resolution spectrometer, such as a long-path-difference Fourier (Michelson) interferometer/spectrometer or a Fabry-Perot interferometer. The technique uses the relative amplitudes of two lines in the same band of the IR rovibrational spectrum of the OH molecule. The concept of temperature is, in general, based on thermodynamic equilibrium, and the lower atmosphere is generally characterized by a state known as *local thermodynamic equilibrium* (LTE). Under such a condition, the ratio of the populations in any two energy levels is given by a Boltzmann distribution. However, there are

insufficient collisions to maintain OH vibrational levels in thermodynamic equilibrium in the mesosphere region, where the Meinel emissions originate, and the OH Meinel emissions are non-LTE emissions, as are most other emissions from the mesosphere and thermosphere. Under non-LTE conditions, one can still determine the temperature from the ratio of populations of two *rotational* levels in the same vibrational state, which still follow a Boltzmann distribution, although the populations of different vibrational states are no longer Boltzmann distributed or related to the temperature. The individual rotational levels result in fine structure on the overall molecular vibrational transition, which can be observed and used to infer temperature.

The strengths of the lines in the Meinel band depend not only on the temperature, but on intrinsic factors arising out of quantum radiation theory. To determine the temperature, one must know the radiative transition probability, or the transition probability per unit time, also known as the Einstein A-coefficient. The transition rate depends, in turn, on the transition (induced) electric-dipole moment of the molecule as a function of internuclear separation. Under MAPSTAR sponsorship, Turnbull and Lowe^{76,77} determined the electric-dipole moment of OH from airglow measurements and used these values to publish up-to-date values of Einstein A-coefficients for OH rovibrational transitions (Turnbull and Lowe, 1988). The A-coefficients were fully consistent with airglow measurements and represented a significant improvement in the current state-of-the art.

In recent years there has been considerable activity in identifying sources of rotational nonequilibrium, or non-LTE rotation, effects at mesospheric and lower-thermospheric altitudes. Such effects have been studied intensively in OH under MAPSTAR auspices by Pendleton, Espy, and Hammond⁷⁸, (1993). Such rotational non-LTE effects usually involve a small fraction of the total OH vibrational-level population and are most obvious in high-lying rotational states. Even in the presence of non-LTE rotation, the bulk of the population in a vibrational state is in rotational equilibrium, and can be fit to a Boltzmann distribution from which the temperature can be found.

What happens when OH temperatures determined by using the rotational distribution in high-vibrational-level (high-v) states are compared to OH temperatures determined similarly from low-v states? The answer seems to be that the temperature can be somewhat different, and such high-v/low-v differences are observed quite commonly in the MAPSTAR database and elsewhere. Lowe, Gilbert, and Turnbull⁵⁷, gave some evidence for why this might occur. Based upon reasonable estimates they argued that the high-v radiation came from an altitude 300 m higher than the low-v radiation. They found this by making use of gravity waves observed in

⁷⁶Turnbull, D.N., and Lowe, R.P., (1988) An empirical determination of the dipole moment function of OH ($X^2\Pi$), *J. Chem. Phys.*, **89**:2763-2767.

⁷⁷Turnbull, D.N., and Lowe, R.P. (1989) New hydroxyl transition probabilities and their importance in airglow studies, *Planet Space Sci.*, **37**:723-738.

⁷⁸Pendleton, W.R., Espy, P.J., and Hammond, M.R. (1993) Evidence for Non-LTE Rotation in the OH Meinel Nightglow, *J. Geophys. Res.* **93**:11,567-11,579.

both the high-v and low-v temperatures and measuring their relative phases. The difference in temperature then can be ascribed to a difference in altitude. The interested reader will find the details in their paper. Similar conclusions are also seen in current research by Pendleton et al.

10. RESPONSE OF AIRGLOW BRIGHTNESS TO WAVES

One of the current areas of airglow research is gravity-wave driven airglow. This research attempts to theoretically model the physics (and sometimes the chemistry) of the effects of waves upon, for example, the OH emission. Two papers published in this area under MAPSTAR are Isler, Tuan, Picard, and Makhlof⁷⁹ and Isler, Tuan, He and Picard⁸⁰. These theoretical papers have as their main conclusion that: for certain parametric values, the response of the airglow to a wave can be significantly nonlinear even though the gravity wave itself is in the linear wave regime. This means that a sinusoidal gravity-wave input can cause a significantly non-sinusoidal brightness variation of airglow. The nonlinearity in the airglow response to waves has, to lowest order, a power-law response function (with a positive exponent). Thus the effect on the response amplitude is to sharpen the wave crests and flatten the troughs; this effect is seen in the simulations. A spectral analysis shows that higher harmonics of the basic sinusoidal input frequency are present. The above theoretical formulation and simulations assumed that the photochemical species reacting to produce the excited radiating states, for example, H and O₃ in the case of the Meinel airglow, are themselves passive tracers carried along by the bulk atmospheric wave motion. Thus no chemistry was included.

In general, the airglow response will be altered for chemically reacting species. This is true for both the linear response and the nonlinear response. Incorporating photochemistry into the gravity-wave response models is a prime goal of the SOAR Program. However, this work was already begun under MAPSTAR. See, for example, Makhlof et al⁵³.

At this point it is appropriate to say that one of the significant findings of the MAPSTAR Program was that small fractional temperature variations can cause larger (by about one order of magnitude) fractional airglow brightness variations. There theoretically might be a phase difference between the temperature and brightness waves which is a function of frequency. The standard way to relate brightness variation to temperature variation is through the so-called Krassovsky ratio η , which is defined as the ratio of the fractional brightness variation ($\Delta I/I$) to fractional temperature variation ($\Delta T/T$). For the dominant wave periods commonly seen, the MAPSTAR experiment teams (for example, Lowe et al, 1991) frequently found $\eta = 8$. MAPSTAR modelers find that such values are possible under a range of conditions. However,

⁷⁹Isler, J.R., Tuan, T.-F., Picard, R.H., and Makhlof, U. (1991) On the response of Airglow to Linear Gravity Waves, *Geophys. Pes.*, **96**:14, 141-14,152.

⁸⁰Isler, J.R., Tuan, T.-F., He, R., and Picard, R.H. (1995) Perturbation treatment of the nonlinear response of minor atmospheric species to linear gravity waves, submitted to *J Geophys. Res.*

many observations in the literature report $\eta = 1$. We are now investigating possible reasons for this difference, including errors in data handling, as well as Doppler and photochemical effects.

11. RESULTS ON NOCTILUCENT CLOUDS, AURORAS, SOLAR INFLUENCE, AND 'BRIGHT NIGHTS'

11.1 Pulsating Auroras

During the MAC/EPSILON Campaign (Section 2.4), Taylor and his co-workers set up two OH LLLTV camera sites for stereo imaging in Finland. Unfortunately, due to inclement weather and interference from auroral emissions, no OH imaging was obtained. However, one day after the campaign had ended, and the sites were being dismantled, one imager was able to record an unusual pulsating aurora. The magnetic micropulsations were being recorded at the same time as Taylor's observations and as a result of this piece of serendipity, a scientific discovery was made. Figure 15 shows a sample of the schematic of an auroral image showing the areas that pulsated *simultaneously* with the magnetic variations. These results were published by Chisham, Orr and Taylor⁹. The magnetic and auroral luminosity pulsations had previously been associated, but Taylor et al, (1989) showed explicitly that the magnetic pulsations with a period of 77 s were synchronized and in one-to-one correspondence with the auroral luminosity variations. The authors mentioned that their observations could be understood in terms of the theory of high-altitude hydromagnetic waves.

11.2 Nightglow and Noctilucent Clouds

Gravity waves are commonly seen in ordinary tropospheric clouds. Looking down from an airplane window one can observe periodic gravity-wave structures in these clouds, often multiple overlapping structures from differing directions. When they are seen in noctilucent clouds the effect is far more dramatic (recall that both wave amplitude and characteristic wave-length grow with altitude). Noctilucent clouds occur at about 82 km altitude.

A widely held theory is that noctilucent clouds are found near the summer polar mesopause where the coldest temperatures on earth cause the small amount of ambient water vapor to condense on available dust nuclei and grow into small ice particles. Now it turns out that the height of noctilucent clouds is comparable to that of the OH layer (~ 83 km), and this raises an interesting question. Since one can measure OH rotational temperatures (and since the altitudes are close), can one correlate the occurrence of noctilucent clouds with the OH temperature, such that low OH temperatures are associated with an increased probability of observing noctilucent clouds? As plausible as this hypothesis might be, Taylor, Lowe, Baker, and Ulwick, (1989) found no evidence in the data for an association of noctilucent cloud

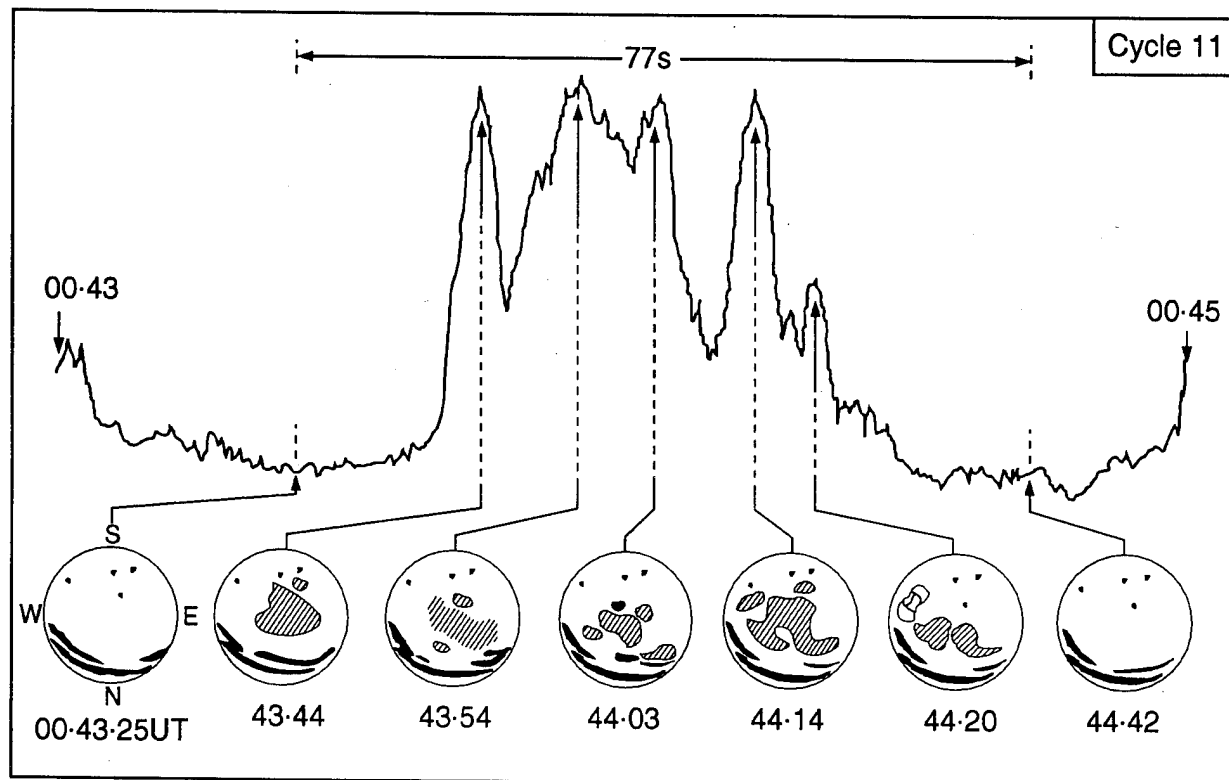


Figure 15. Plot of Zenith Intensity for Cycle 11 as Determined from the Video Records. The sketches show the all-sky auroral activity at several instances during this cycle. The hatched areas show the pulsating patches and the shaded areas the bright arcs to the North.

occurrence and OH temperature. Nevertheless, this does not necessarily cast doubt on the plausible microphysical theory of noctilucent cloud formation. We note that OH temperatures reflect the mean temperature across the OH layer. If there is a gravity wave present, the minimum

temperature could be quite a bit lower and hence still allow noctilucent clouds to form.

11.3 Bright Nights and Thunderstorms

As previously mentioned, there were several so-called bright nights observed during the MAPSTAR Colorado 1988 Campaign. Again, the term "bright night" is intended to signify the presence of visual structure (to the naked, dark-adapted eye). What caused bright nights to occur? The most obvious possibility was that there were stronger gravity-wave sources prior to the bright night occurrence, and these could well have been thunderstorms. This idea is consistent with the fact that most of the bright nights occurred in July when most of the thunderstorm activity was present. Stronger thunderstorms imply larger amplitude waves which imply larger height variations in the OH layer, causing larger adiabatic density and temperature changes. These changes, finally, would cause larger intensity fluctuations which would show up as higher contrast structures.

This possibility was carefully examined by Taylor⁸¹. His conclusion was that the comparison between radar summary charts [showing thunderstorm cloudtop heights (or "intensity"), locations and times] and OH images did not show evidence of an association between thunderstorms and bright nights. In other words non-bright nights in July had the same kind of thunderstorm activity. We are thus left with a scientific mystery; however, it was subsequently realized that during the campaign the wind conditions would have prevented many of the thunderstorms from affecting the OH region under observation through blocking by critical layer formation. This issue will be revisited in future research with the blocking diagrams discussed in Section 4 taken into account.

11.4 Noctilucent Clouds and Polar Mesospheric Summer Echoes (PMSEs)

Polar mesospheric summer radar echoes (PMSEs) are from altitudes close to those for the noctilucent clouds. They also occur during the same season and in the same location as noctilucent clouds and, naturally, the question comes up as to whether or not they are parts of the same overall physical phenomenon viewed by different means. This possibility was explored by Taylor et al¹⁹, and their results indicate no evidence for a correlation between the occurrence of noctilucent clouds and PMSEs.

⁸¹Taylor, M.J. (1989) *First Results from the MAPSTAR Colorado Campaign*, MAPSTAR Interim Report No. 4, Submitted to Utah State University February 1989.

11.5 Sunspot - Weather Correlations: Are They Real?

In a recent series of papers by Labitzke and Van Loon⁸² it was announced that, at long last, there was definitive scientific evidence that the temperature of the northern hemisphere was controlled by the solar sunspot cycle. This result received international public media attention. Because structure depends on gravity waves and the latter are caused, for the most part, by weather conditions, it was deemed appropriate to check these findings on solar-weather relations. It should be mentioned that in order to "see" the sunspot effect, Labitzke and Van Loon had to observe temperature only during a certain phase of the quasi-biennial oscillation (QBO). The QBO refers to mean winds near the equator which reverse once every year or so in a quasiperiodic manner.

Dewan and Shapiro⁸³ found that the assignment of statistical significance by Labitzke and Van Loon⁸², was due to an error that they made concerning the number of statistical degrees of freedom in the problem. They thought that there were about twice as many as were there in reality. Thus, while it cannot be proven that there is *no* sunspot-weather relation, what was observed is also consistent with chance alone. Dewan and Shapiro mentioned other sources of artifacts in the analysis due to aliasing, which had been published previously by Teitelbaum and Bauer⁸⁴. In short, there is no evidence *for* the solar effect and the more likely explanation is an aliasing effect due to under-sampling a two-plus year cycle (the QBO) at an exactly-spaced interval of 2 years. A stroboscopic effect leads to the illusion of a cycle indistinguishably close to 11 years. This generic artifact is well advertised in books on time-series analysis, but in practice one is usually concerned with aliasing at much higher frequencies than one-half cycle per year. This may explain why the possible artifact was initially overlooked by Labitzke and Van Loon.

11.6 Sound Waves in Airglow Structure?

Up to this point all of the MAPSTAR theoretical and empirical studies taken together formed a coherent picture of how gravity waves in the atmosphere formed the structures that are seen in the OH airglow. In the final MAPSTAR workshop, in London, Ontario, R. Lowe presented scanning photometer data from the UWOSCR instrument (University of Western Ontario Scanning Radiometer) which showed in a 3-D animation display how the spatial pattern of OH brightness varies in time. Some of the features seen seemed to move at the sound velocity and resembled solitons. These observations at the end of the program served to

⁸²Labitzke, K., and van Loon, H. (1988) Association between the 11-year solar cycle, the QBO and the atmosphere. Part I: the troposphere and stratosphere in the northern hemisphere in winter, *J. Atmos. Terr. Phys.*, **50**:197.

⁸³Dewan, E.M., and Shapiro, R. (1991) Are sunspot-weather correlations real? *J. Atmos. Terr. Phys.*, **53**:171-174.

⁸⁴Teitelbaum, H., and Bauer, P. (1990) *Ann. Geophys.*, **8**:239.

remind us that by no means do we have all the answers and that a great deal more work remains to be done.

12. RESEARCH QUESTIONS RAISED BY MAPSTAR ON WAVE-DRIVEN AIRGLOW AND ASSOCIATED TOPICS

The mere acquisition of experimental data does not, in itself, usually constitute a scientific result worth publishing. The latter often requires that specific questions of a sort relating to some conceptual model, theory, or hypothesis be answered by the data. Only then would the data have a context and also satisfy a scientific need. For this reason, a list of questions that are in some way "important" (that is, leading to better understanding) can be very useful in stimulating and guiding future work. In the field of mathematics, Hilbert's list of such questions was so useful that it had a great impact on that field. The following list does not have any such pretension, but we consider it worth publishing as a MAPSTAR product because, at the very least, it will guide our research in the SOAR Program and might serve to recruit other scientists in the community to join with our efforts.

1. The theory described above for gravity wave horizontal wave number and frequency power spectra predicts an ϵ (dissipation rate) dependence. See details in Dewan^{50,51}. In particular $\Psi_V(k_x) \sim \epsilon^{2/3} k_x^{-5/3}$ and $\Psi_{v_h} \sim \Psi_T(\omega) \sim \epsilon \omega^2$. Are these consistent with experiments where ϵ is actually measured concurrently with velocity or temperature spectra?

The parameter ϵ can be measured by balloonborne thermosondes to mid-stratospheric altitudes, and by Doppler radar or rockets at higher altitudes. Also, temperatures can be measured by balloonborne instruments at lower altitudes and rockets at higher altitudes. Lidars and high-resolution optical spectrometers can measure temperature PSDs and, of course, radar can provide velocity PSDs over a wide range of altitudes. Many experimental possibilities exist for testing this theory.

2. What causes a bright night to occur? By bright nights here we mean visible structure of airglow to the naked eye.

Could it be caused by larger amplitude gravity waves? Could it require higher concentrations of odd oxygen near the OH layer? Would both of these factors have to be present in order to have a bright night (in the structure sense)?

3. How do thunderstorms physically generate gravity waves?

Do they act as sine-wave (or multi-sine-wave) generators or do they generate impulses which are then subsequently Fourier decomposed by atmospheric dispersion of the waves?

4. Can mountain waves appear in airglow structure?

Their presence would be indicated by the fact that their position would be controlled by lower level winds. To test this definitively one would need to have a radar wind profiler. However, if a wave in the airglow near a mountain maintains an approximately constant

position in the sky randomly moving slowly forward, and then backward, then it could possibly be a mountain wave.

5. What causes the waves, seen in both airglow and NLCs which are called "ripples". If they are due to the Kelvin-Helmholtz instability, a measurement of the wind profile through the layer could show that the shear satisfied the Richardson number condition for instability.

6. What is the physics behind the horizon-to-horizon sine waves in the airglow as seen in the all-sky-imagers? Are they trapped waves?

The latter could be tested by means of wind profilers to see if Doppler ducting conditions prevail. The frequencies of the waves would determine their phase planes and these could indicate the possibility of trapping. How are these sine waves generated in the first place? Can one find horizon-to-horizon trains of wave packets?

8. What is the shape of airglow brightness power spectra for OH and other radiators as a function of gravity wave excitation conditions? What is the nonlinear response of airglow to gravity waves when chemistry cannot be neglected?

9. It is possible to detect the "chirp" effect in airglow, as suggested by Yoshimoto in his MAPSTAR sponsored Ph.D. thesis? Can it be used to identify the source of the waves in question?

10. What do the two dimensional PSDs of OH brightness and temperatures show? Are their slopes consistent with the theory given here?^{50,51}

11. Is it possible to document tidal modulations in OH airglow temperatures and intensities? If so, could this be useful in understanding middle atmosphere dynamics?

12. Are there sound-wave modulations in the airglow structure? This could be very important in systems applications, especially if they are associated with small horizontal scales.

13. What are the so-called "scatterers" that the IDI radar detects? Why exactly do different radar techniques measure different "winds" above 80 km?

14. Can the altitude variations in NLC's be correlated with the simultaneously measured interferometric temperatures in OH in the same location? What is the phase relation between NLC height variations and temperature variations if they are correlated?

References

1. Taylor, M.J. (1985) *Observation and Analysis of Wave-like Structures in the Lower Thermospheric Nightglow Emissions*, Ph.D. Thesis, Southampton University, U.K.
2. Gossard, E., and Hooke, W. (1975) *Waves in the Atmosphere*, Amsterdam, Elsevier
3. Taylor, M.J., Espy, P.J., Baker, D.J., Sica, R.J., Neal, P.C., and Pendleton, W.R., Jr. (1991) Simultaneous intensity, temperature, and imaging measurements of short period wave structure in the OH nightglow emission, *Planet Space Sci.*, **39**:1171
4. Ratkowski, A. (1985) The MAPSTAR Program: Scientific Goals and Overview, *EOS*, **66**:324
5. Shefov, N.N. (1968) The behaviour of upper atmosphere emissions during high meteoric activity, *Planet. Space Sci.*, **40**:235-242
6. Harrison, A.W., (1973) Spectrophotometric measurements of noctilucent clouds, *Can. J. Phys.*, **51**:373-377
7. Thrane, E.V., (1990) Preface to "Middle Atmosphere Dynamics at High Latitudes," *J. Atmos. Terr. Phys.*, **52**:813-827
8. Taylor, M.J., Chisham, G., and Orr, D. (1989) Pulsating auroral forms and their association with geomagnetic giant pulsations, *Planet. Space Sci.*, **37**:1477
9. Chisham, D., Orr, D., Taylor, M., and Luhr, H. (1990) The Magnetic and optical signature of a Pg pulsation, *Planet. Space Sci.*, **38**:1443
10. Tarrago, A., and Chanin, M.-L. (1982) Interpretation in terms of gravity waves of structures observed at the mesopause level by photography and lidar, *Planet. Space Sci.*, **30**:611-626
11. Wang, S.T., Tetenbaum, D., Balsley, B., Obert, R., and Avery, S. (1987) A meteor echo detection and collection system for use on VHF radars, *Radio Science*
12. Taylor,, M.J., Hapgood, M.A., and Rothwell, P. (1987) Observations of gravity wave propagation in the OI (557.7 nm), Na (589.2), and the near infrared OH nightglow emissions, *Planet. Space Sci.*, **35**:413

13. Taylor, M.J., and Hapgood, M.A. (1988) Identification of a thunderstorm as a source of short period gravity waves in the upper atmosphere nightglow emissions, *Planet. Space Sci.*, **36**:975
14. Brosnahan, J.W., and Adams, G.W. (1993) The MAPSTAR Imaging Doppler Interferometer (IDI) Radar: description and first results, *J. Atmos. Terr. Phys.*, **55**:203-208.
15. Taylor, M.J., and Hill, M.J. (1991) Near infrared imaging of hydroxyl wave structure over an ocean site at low latitudes, *Geophys. Res. Lett.*, **18**:1333-1336
16. Taylor, M.J., and Edwards, R. (1991) observations of short period mesospheric wave patterns: In situ or tropospheric wave generation?, *Geophys. Res. Lett.*, **18**:1337-1340
17. Taylor, M.J., Turnbull, D.N., and Lowe, R.P. (1991) Coincident imaging and spectrometric observations of zenith OH nightglow structure, *Geophys. Res. Lett.*, **18**:1349-1352
18. Taylor, M.J., and Henriksen, K (1989) Gravity wave studies at polar latitudes, in *Electromagnetic Coupling in the Polar Clefts and Caps*, Kluwer Academic Publishers, pp 421-434
19. Taylor, M.J., van Eyken, A.P., Rishbeth, H., Witt, G., Witt, N., and Clilverd, M.A. (1989) Simultaneous observations of noctilucent clouds and polar mesospheric radar echoes: evidence of non-correlation, *Planet. Space Sci.*, **37**:1013-1020
20. Taylor, M.J., Hapgood, M.A., and Rothwell, P. (1987) Observations of gravity wave propagation in the OI (557.7 nm), Na (589.2 nm), and the near infrared OH nightglow emissions, *Planet. Space Sci.*, **35**:413-417
21. Stobie, J. (1975) *Gravity Shear Waves Atop the Cirrus Layer of Intense Convective Storms*, Master's Thesis, Colorado State University
22. Peterson, A. (1989) Analysis of an extensive, long wavelength OH wave packet generated by a thunderstorm, *EOS*, **70**:1244 (AGU Fall Meeting)
23. Peterson, A. (1990) Color photographs of active OI (5577) and OH airglow with comparisons to video and fisheye pictures, AGU Spring Meeting, *EOS*, **71**:571
24. Peterson, A. (1990) Analysis of an OH wave packet generated by a thunderstorm.
25. Neal, P.C. (1985) *High Resolution Measurements of OH Infrared Airglow Structure*, Ph.D. Thesis, Utah State University, Dept. of Engineering, MAPSTAR Data Report No. 2
26. Taylor, M.J. (1989) Comparison of Southampton Image Data and *Thunderstorm Maps for the Colorado MAPSTAR Campaign, 1988*, MAPSTAR report, June 1989
27. Espy, P., and Taylor, M.J. (1991) Radiometric measurements and PSD's vs Taylor All-Sky-Structure-Cover-Percent-Parameter, MAPSTAR Workshop, April 22-23, 1991, Hanscom AFB, MA.
28. Hoffmeister, (1952) Investigations on Bright Night Sky and Luminous Bands, *J. Brit Astronom. Assn.*, **62**:288
29. Taylor, M.J., Ryan, E.H., Tuan, T.-F., and Edwards, R. (1993) Evidence of preferential directions for gravity wave propagation due to wind filtering in the middle atmosphere, *J. Geophys. Res.*, **98**:6047-6057
30. Adams, G.W., Peterson, A.W., Brosnahan, J.W., and Neuschafer, J.W. (1988) Radar and optical observations of mesospheric wave activity during the lunar eclipse of 6 July 1982, *J. Atmos. Terr. Phys.*, **50**:11-20

31. Taylor, M.J., and Hapgood, M.A. (1990) on the origin of ripple-type wave structure in the OH nightglow emission, *Planet. Space Sci.*, **38**:1421
32. Tuan, T.-F., Hedinger, R., Silverman, S., and Okuda, M (1979) on gravity-wave induced Brunt-Vaisala oscillations, *J. Geophys. Res.*, **84**:393-398
33. Infeld, E., and Rowlands, G. (1990) Nonlinear Waves, *Solitons, and Chaos*, Cambridge Press
34. Peterson, A. (1989) 1. Horizon to horizon monochromatic sine-wave in OH airglow - All Sky film camera image., and 2. Color photograph of OH, Na, and O airglows. (Private data submission to MAPSTAR Project)
35. Hines, C.O. (1974) Some Consequences of Gravity-Wave Critical Layers in the Upper Atmosphere in Motion, AGU Meeting, 1974
36. McIntyre, M. (1992) Comment made at NATO Advanced Research Workshop, Loen, Norway (See also Holton, J.R., and Durann, D. (1993) convectively generated stratospheric gravity waves: The role of mean wind shear, in *Coupling Processes in the Lower and Middle Atmosphere*, Ed. by E.V. Thrane, T.A. Blix, and D.C. Fritts, NATO ASI Series, Kluwer Pub. Co.)
37. Chimonas, G., and Hines, C. (1986) Doppler ducting of atmospheric gravity waves, *J. Geophys. Res.*, **91**: 1219
38. Wang, D.Y., and Tuan, T.F. (1988) Brunt-doppler ducting of small-period gravity waves, *J. Geophys. Res.*, **93**:(A9)9916-9926
39. Tuan, T.-F., Lowe, R.P., Isler, J., Picard, R., and Bhattacharyya, A., Analysis of air parcel motion in the presence of gravity waves and winds, Submitted to *Can. J. Phys.* 1995
40. van Rhijn, P.J. (1925) *Publ. Ast. Lab. Groningen*, **43**
41. van Rhijn, P.J. (1921) on the brightness of the sky at night and the total amount of starlight, *Pub. Ast. Lab.*, Groningen, **31**
42. van Rhijn, P.J. (1919) on the brightness of the sky at night and the total amount of starlight, *Ap. J.*, **31**
43. Yoshimoto, H. (1990) *Study on Dynamics of the Waves in the Mesospheric Hydroxyl Layer*, Ph.D. Thesis, Utah State University, Dept. of Electrical Engineering. Scientific Report by Space Dynamics Laboratory
44. Francis S.H. (1975) Global propagation of atmospheric gravity waves: A review, *J. Atmos. Terr. Phys.*, **37**:1011-1054
45. VanZandt,T.E. (1982) A universal spectrum of buoyancy waves in the atmosphere, *Geophys. Res. Lett.*, **9**:575-578
46. Dewan, E.M., Grossbard, N., Quesada, A., and Good, R. E. (1984) Spectral analysis of 10 m resolution scalar velocity profiles in the stratosphere, *Geophys. Res. Lett.*, **11**:624
47. Dewan, E.M., and Good, R.E. (1986) Saturation and the universal spectrum for vertical profiles of horizontal scalar winds in the atmosphere, *J. Geophys. Res.*, **91**(D2):2,742-2,748
48. Smith, S.A., Fritts, D.C., and VanZandt, T.E. (1987) Evidence for a saturated spectrum of atmospheric gravity waves, *J. Atmos. Sci.*, **44**:1404-1410
49. Dewan, E.M. (1979) Stratospheric wave spectra resembling turbulence, *Science*, **204**:832-835
50. Dewan, E.M. (1990) *Power Spectra of Internal Gravity Waves*, Geophysics Laboratory, GL-TR-90-0233, NTIS number ADA 231596

51. Dewan, E.M. (1991) Similitude modeling of internal gravity wave spectra, *Geophys. Res. Lett.*, **18**:1473-1476
52. Hines, C.O. (1960) Internal atmospheric gravity waves at ionospheric heights, *Can. J. Phys.*, **38**:1441-1481, and Correction, (1964) *Can. J. Phys.*, **42**:1425-1427
53. Makhlof, U., Dewan, E.M., Isler, J.R., and Tuan, T.-F. (1990) on the importance of the purely gravitationally induced density, pressure, and temperature variations in gravity waves: their application to airglow observations, *J. Geophys. Res.*, **95**:4103-4111, also, Makhlof, U., Picard, R.H., and Winick, J.R. (1990) Modulation of the hydroxyl emission by a monochromatic gravity wave in a realistic, non-isothermal atmosphere, *EOS* **71**:1496
54. Dewan, E.M., Pendleton, W., Grossbard, N., and Espy, P., (1992) *Geophys. Res. Lett.*, **19**:597-600
55. Grossbard, N., and Dewan, E.M. (1991) Methods for estimating the autocorrelation and power spectral density function when there are many missing data values, ASSP Workshop on Spectral Estimation and Modeling, Oct 10-12, 1991.
56. Blackman, R., and Tukey, J. (1958) *The Measurement of Power Spectra*, Dover, New York
57. Lowe, R.P., Gilbert, K.L., and Turnbull, D.N., (1991) High latitude summer observations of the hydroxyl airglow, *Planet. Space Sci.*, **39**:1263-1270
58. Hines, C.O., Private Communication
59. Adams, G.W., Edwards, D.P., and Brosnahan, J.W. (1985) The imaging doppler interferometer: data analysis, *Radio Science*, **20**:1481-1492
60. Adams, G.W., Brosnahan, J.W., Walden, D.C., and Nerney, S.F. (1986) Mesospheric observations using a 2.66 MHz radar as an imaging doppler interferometer: description and first results, *J. Geophys. Res.*, **91**:1671-1683
61. Adams, G.W., Brosnahan, J.W., and Haldermen, T.D. (1988) Direct radar observations of TID's in the D and E Regions, *J. Atmos. Terr. Phys.*, **50**:931-935
62. Adams, G.W., Brosnahan, J.W., and Johnson, R. (1989) Aspect sensitivity of 2.66 MHz radar returns from the mesosphere, *Radio Science*, **24**:127-132
63. Turek, R.S. (1986) *An Analysis of Upper Atmospheric Parameters Derived From the Observation of Meteor Echoes by a 2.66 MHz Radar*, Master's Degree Thesis, Utah State University in Dept. of Soil Science and Biometeorology (Aeronomy), CASS Report GR-06, Center for Atmospheric and Space Science
64. Coble, B.B. (1987) *Middle Atmospheric Wind Measurements Using a Medium Frequency Radar*, Master's Degree Thesis, Utah State University, in Dept. of Soil Science and Biometeorology, CASS Report GR-07, Center for Atmospheric and Space Sciences
65. Halderman, T.D. (1987) *An Analysis of Apparent-Motion Vectors in, and the Structure of, a Mid-Latitude Sporadic E Layer Using a 2.66 MHz Radar*, Master's Degree Thesis, Utah State University, in Dept. of Soil Science and Biometeorology, (Aeronomy), CASS Report GR-08, Center for Atmospheric and Space Sciences
66. Chao, S.C. (1987) Signal Processing of Hydroxyl Airglow Interferometric Data, in *MAPSTAR Data Report No. 3*
67. Hammond, M.R. (1992) *A Study of Temperature Derived from the OH Meinel (3,1) and (7,4) Bands in the Night Airglow*, Master's Degree Thesis, Utah State University, Department of Physics

68. Ware, G., and Goode, D. (1988) *MAPSTAR Interferometer Piece Part Drawings*, MAPSTAR Data Report No. 9
69. Stacey, N. (1987) Finding the direction, speed, and Wavelength of OH airglow waves from three observation points, in MAPSTAR Data Report No. 7
70. Stirling, W., Pike, J., and Ware, G. (1987) Temperature Estimation from OH Radiation, in MAPSTAR Data Report No. 8
71. Ware, G., and Baker, D. (1990) Spatially separated observations of OH intensity and rotational temperature waves, *EOS*, **71**:573.
72. Taylor, M.J. (1991) MAPSTAR Final Report, subcontract 387-003 and C802640 (period covered, October 1987 to 30 June 1991) between Utah State University and Southampton University, U.K., presented at the Final MAPSTAR Workshop, University of Western Ontario, London, Ontario, September 1991
73. Taylor, M.J., Connor, L., Avery, S.K., and Pendleton, W., Jr. (1992) Evidence of preferential directions for gravity wave propagation due to wind filtering in the middle atmosphere, *J. Geophys. Res.*,
74. Turnbull, D.N., and Lowe, R.P. (1991) Temporal variations in the hydroxyl nightglow observed during ALOHA-90, *Geophys. Res. Lett.*, **18**:1345-1348
75. Dewan, E.M., Grossbard, N., Good, R.E., and Brown, J. (1988) Power spectral densities of zonal and meridional winds in the stratosphere, *Physica Scripta*, **37**:154-157
76. Turnbull, D.N., and Lowe, R.P., (1988) An empirical determination of the dipole moment function of OH ($X^2\Pi$), *J. Chem. Phys.*, **89**:2763-2767
77. Turnbull, D.N., and Lowe, R.P., (1989) New hydroxyl transition probabilities and their importance in airglow studies, *Planet. Space Sci.*, **37**:723-738
78. Pendleton, W.R., Espy, P.J., and Hammond, M.R. (1993) Evidence for Non-LTE Rotation in the OH Meinel Nightglow, *J. Geophys. Res.*, **98**:11,567-11,579
79. Isler, J.R., Tuan, T.-F., Picard, R.H., and Makhlouf, U. (1991 on the response of Airglow to Linear Gravity Waves, *J. Geophys. Res.*, **96**:14,141-14,152
80. Isler, J.R., Tuan, T.-F., He, R., and Picard, R.H. (1995) Perturbation treatment of the nonlinear response of minoratmospheric species to linear gravity waves, submitted to *J. Geophys. Res.*
81. Taylor, M.J . (1989) *First Results from the MAPSTAR Colorado Campaign*, MAPSTAR Interim Report No. 4, Submitted to Utah State University February 1989
82. Labitzke, K., and van Loon, H. (1988) Association between the 11-year solar cycle, the QBO and the atmosphere. Part I: the troposphere and stratosphere in the northern hemisphere in winter, *J. Atmos. Terr. Phys.*, **50**:197
83. Dewan, E.M., and Shapiro, R. (1991) Are sunspot-weather correlations real? *J. Atmos. Terr. Phys.*, **53**:171-174
84. Teitelbaum, H., and Bauer, P. (1990) *Ann. Geophys.*, **8**:239

Bibliography

B1 MAPSTAR PUBLICATIONS

The first part of this bibliography is arranged by type of publication. The second part, starting with section B5, shows publications and presentations by groups of authors.

Adams, G.W., Brosnahan, J.W., and Haldermen, T.D. (1988) Direct radar observations of TID's in the D and E Regions, *J. Atmos. Terr. Phys.*, **50**:11-20

Adams, G.W., Brosnahan, J.W., and Johnson, R. (1989) Aspect Sensitivity of 2.
66 MHz radar returns from the mesosphere, *Radio Sci.*, **24**:127-132

Adams, G.W., Brosnahan, J.W., Walden, D.C., and Nerney, S.F. (1986) Mesospheric Observations using a 2.66 MHz Radar as an Imaging Doppler Interferometer: Description and First Results, *J. Geophys. Res.*, **91**:1671-1683

Adams, G.W., Edwards, D.P., and Brosnahan, J.W. (1985) The Imaging Doppler Interferometer: Data Analysis, *Radio Science*, **20**:1481-1492

Adams, G.W., Peterson, A.W., Brosnahan, J.W., and Neuschaefer, J.W. (1988) Radar and optical observations of mesospheric wave activity during the lunar eclipse of 6 July 1982, *J. Atmos. Terr. Phys.*, **50**:11-20

Baker, D. (1988) Modeling of Mesospheric OH Airglow Fluctuations and Waves Using S-Domain Radiance Transference, in *Progress in Atmospheric Physics*, R. Rodrigo et al., eds, Kluwer Academic Publishers, 77-95

Brosnahan, J.W., and Adams, G.W. (1993) The MAPSTAR Imaging Doppler Interferometer (IDI) Radar: Description and First Results, *J. Atmos. Terr. Phys.*, **55**:203-208, AIDA Special Issue, March 1993

Chao, S.C. (1987) Signal Processing of Hydroxyl Airglow Interferometric Data, in *MAPSTAR Data Report No. 3*

Chisham, G. (1990) Ph.D. Thesis, Physics Department, University of York, U.K.

Chisham, G., Orr, D., Taylor, M.A., and Luhr, H. (1990) The magnetic and optical signature of a Pg pulsation, *Planet. Space Sci.*, **38**:1443

Coble, B.B. (1987) *Atmospheric Wind Measurements Using a Medium Frequency Radar*, Masters Degreee Thesis, Utah State University, in Dept. of Soil Science and Biometeorology, CASS Report GR - 07., Center for Atmospheric and Space Sciences.

Dewan, E. (1991) Similitude modeling of internal gravity wave spectra, *Geophys. Res. Lett.*, **18**: 1473-1476

Dewan, E. (1990) *Power Spectra of Internal Gravity Waves*, Geophysics Laboratory (AFSC), GL-TR-90-0233, Special Reports, No. 265, ADA 231596

Dewan, E., and Good, R.E., (1986) Saturation and the universal spectrum for vertical profiles of horizontal scalar winds in the atmosphere, *J. Geophys. Res.*, **91**,D2:2,742-2,748 (precursor to MAPSTAR, but relevant).

Dewan, E., Grossbard, N., Good, R.E., and Brown, J., (1988) Power spectral densities of zonal and meridional winds in the stratosphere, *Physica Scripta*, **37**:154-157 (precursor to MAPSTAR, but relevant).

Dewan, E., Pendleton, W., Grossbard, N., and Espy, P. (1992) Mesospheric OH airglow temperature fluctuations: A Spectral Analysis, *Geophys. Res. Lett.*, **19**:597-600

Dewan, E., and Shapiro, R., (1991) Are sunspot-weather correlations real?, *J. Atmos. Terr. Phys.*, **53**:171-174 (1991)

Gadsden, M., and Taylor, M.J. (1992) Anweisungen fur die photographischen aufnahmen der leuchtenden nachtwolken - 103 years on, *J. Atmos. Terr. Phys.*, **56**:447-459

Gardner, C.S., Kane, T.J., Yeo, J.H., Niciejewski, R.J., Hecht, J.H., Walterschied, R.L., Lowe, R.P., and Turnbull, D.N. (1991) Formation characteristics of sporadic Na layers observed simultaneously by LIDAR and airglow instruments during ALOHA-90, *Geophys. Res. Lett.*, **18**:1369-1372

Gilbert, K.L., and Lowe, R.P. (1990) The effect of quenching on the correlation of hydroxyl airglow intensities and rotational temperatures, *EOS*, **70**:1245

Gilbert, K.L., and Lowe, R.P. (1988) Does the hydroxyl rotational temperature vary with vibrational level?, *EOS*, **69**:13

Gilbert, K.L., and Lowe, R.P. (1987) A synthetic spectrum fitting technique for determining hydroxyl rotational temperature, *EOS* **68**:1389

Good, R.E., Beland R., Murphy, E., Brown, J., and Dewan, E. (1988) Atmospheric models of optical turbulence, *SPIE Reports*, Vol. 928, *Modeling of the Atmosphere*, L. Rothman, Ed., pp. 165-186

Goodrich, M.A. (1994) *Estimation of Mesospheric OH Radiance and Rotational Temperature Wave Velocities*, Master's Thesis, Brigham Young University, April 1994

Halderman, T.D. (1987) *An Analysis of Apparent-motion Vectors in, and the Structure Of, a Mid-Latitude Sporadic E Layer Using a 2.66 MHz Radar*, Master's Degree Thesis, Utah State University in Dept. of Soil Science and Biometeorology (Aeronomy), CASS Report GR-08 (Center for Atmospheric and Space Sciences)

Hammond, M.R. (1992) *A Study of Temperature Derived from the OH Meinel (3,1) and (7,4) Bands in The Night Airglow*, Master's Degree Thesis, Utah State University, Department of Physics

He, F., Tuan, T.-F., and Isler, J. (1990) Gravity wave scattering from critical-layer regions, *EOS*, **71**:573

He, F., Tuan, T.-F., Isler, J., and Picard, R. (1990) Optical model analysis of gravity wave reflections from critical layers, *EOS*, **71**:1496

He, F., Tuan, T.-F., and Picard, R. (1991) Modelling of optical model treatment of gravity wave-critical layer interaction, *EOS*, **72**:208

He, F., Tuan, T.-F., and Picard, R. (1991) Determination of optical model parameters for gravity wave-critical layer interaction and the physics for over reflection, *EOS*, **72**:375

Hines, C.O. (1993) Preface to, Arecibo Initiative in Dynamics of the Atmosphere, AIDA ACT'89, *J. Atmos. Terr. Phys.*, **55**:197-199

Hines, C.O., Adams, G.W., Brosnahan, J.W., Djuth, F.T., Salzer, M.P., Tepley, C.A., and Van Baelen, J.S. (1993) Multi-instrument observations of mesospheric motions over Arecibo:comparisons and interpretations, *J. Atmos. Terr. Phys.*, **55**:241-287

Isler, J.R., Tuan, T.-F., Picard, R.H., and Makhlof, U. (1991) On the nonlinear response of airglow to linear gravity waves, *J. Geophys. Res.*, **96A**:14,141-14,152

Isler, J.R., Tuan, T.-F., He, F., and Picard, R.H. (1994) Perturbation treatment of the nonlinear response of minor atmospheric species to linear gravity waves, *J. Geophys. Res.* (revision)

Li, Xuerong (1995) *Optical Model Analysis of Gravity-Wave Critical Layer Interactions in a Realistic Atmosphere*, Ph.D. Thesis, University of Cincinnati.

Lowe, R.P., Gilbert, K.L., and Turnbull, D.N. (1991) High latitude summer observations of the hydroxyl airglow, *Planet. Space Sci.*, **39**:1263-1270

Makhlof, U., Dewan, E., Isler, J.R., and Tuan, T.-F., (1990) On the importance of the purely gravitationally induced density, pressure, and temperature variations in gravity waves: Their application to airglow observations, *J. Geophys. Res.*, **95**:(A4)4103-4111 (1990)

Makhlof, U., Wang, D.Y., Lin, J.J., and Tuan, T.-F. (1987) Effects of different gravity-wave models and horizontal winds on the mesospheric emission, *EOS*, **68**:1394

Munasinghe, Gamini, Tuan, T.-F., and Bhattacharyya, Alok (1995) On the use of dilatation as a dependent variable for gravity wave propagation. *J. Geophys. Res.*, in publication

Neal, P.C. (1985) *High Resolution Measurements of OH Infrared v Infrared Airglow Structure*, Ph.D. Thesis, Utah State University, Dept. of Engineering, MAPSTAR Data Report No. 2

Pendleton, W.R., Espy, P.J., and Hammond, M.R. (1993) Evidence for Non-LTE Rotation in the OH Meinel Nightglow, *J. Geophys. Res.*, **98**:11,567-11,579

Roper, R.G., Adams, G.W., and Brosnahan, J.W. (1993) Tidal winds at mesopause altitudes over Arecibo (18° N, 67° W), April 5-11, 1989 (AIDA '89), *J. Atmos. Terr. Phys.*, AIDA Special Issue, **55**:289-312, March 1993

Simmons, D.A.R., Henriksen, K., Taylor, J.J., and Hermansen, D (1990) A remarkable outburst of solar activity and its geomagnetic effects, *J. Br. Astron. Assoc.*, **100**:280

Stacey, N. (1987) *Finding the Direction, Speed, and Wavelength of OH Airflow Waves from Three Observation Points*, in MAPSTAR Data Report No. 7

Stacey, N., Wille, R., and Transtrum, N. (1990) *Catalog Plots for Stirling, Colorado, 1988 Day 138*, MAPSTAR Report

Stirling, W., Pike, J., and Ware, G. (1987) *Temperature Estimation from OH Radiation*, in MAPSTAR Data Report No. 8

Stirling, W.C., Ware, G.A., and Pike, J. (1988) *Rotational Temperature and Intensity Estimates from Mesospheric OH Radiation*, MAPSTAR Workshop Report

Taylor, M.J. (1991) *MAPSTAR Final Report*, on sub contract 387-003 and C802640 [period covered, 1 October 1987 to 30 June 1991], between Utah State University and Southampton University, U.K. Presented at the final MAPSTAR workshop, University of Western Ontario, London, Ontario, September 1991

Taylor, M.J. (1991) Final Report, on subcontract between Southampton University and University of Cincinnati, issued as part of Air Force Contract F19628-87-K-0023 (covering 3 May 1990 to 4 April 1991), Submitted to University of Cincinnati, June 1991, contributed to PL-TR-91-2193; ADA 244504

Taylor, M.J. (1989) *Comparison of Southampton Image Data and Thunderstorm Maps for the Colorado MAPSTAR Campaign, 1988*, MAPSTAR Report, June 1988

Taylor, M.J. (1989) *First Results from the MAPSTAR Colorado Campaign*, MAPSTAR Interim Report No. 4, submitted to USU February, 1989

Taylor, M.J. (1986) TV observations of mesospheric wave structure, in: Collections of the Works of the International Workshop of Noctilucent Clouds, *Valgus*, 153

Taylor, M.J. (1985) MAPSTAR Final Report, on subcontract 85-049, [period covered, 1 October 1985 to 30 September 1987] between Utah State University and Southampton University, U.K., submitted to USU November 1987

Taylor, M.J. (1985) MAPSTAR Final Report, on subcontract 85-049, [period covered, 1 January 1985 to 30 September 1985] between Utah State University and Southampton University, U.K., submitted to USU November 1985

Taylor, M.J. (1985) *Observation and Analysis of Wave-like Structures in the Lower Thermospheric Nightglow Emissions*, Ph.D. Thesis, Southampton University, U.K.

Taylor, M.J., Chisham, G., and Orr, D. (1989) Pulsating auroral forms and their association with geomagnetic giant pulsations, *Planet. Space Sci.*, **37**:1477

Taylor, M.J., Connor, L., Avery, S.K., and Pendleton, Jr., W (1995) Simultaneous radar, imaging and interferometer measurements at mesospheric heights, *Submitted to J. Geophys Res.* (Presented at Winter AGU Meeting, San Francisco)

Taylor, M.J., and Edwards, R. (1991) Observations of short period mesospheric wave patterns; *in situ* or tropospheric wave generation? *Geophys. Res. Lett.*, **18**:1337

Taylor, M.J., Espy, P.J., Baker, D.J., Sica, R.J., Neal, P.C., and Pendleton, Jr., W. (1991) Simultaneous temperature, intensity and imaging measurements of short period wave structure in the OH nightglow emission, *Planet. Space Sci.*, **39**:1172

Taylor, M.J., and Hapgood, M.A. (1990) On the origin of ripple-type wave structure in the OH nightglow emission, *Planet Space Sci.*, **38**:1421

Taylor, M.J., and Hapgood, M.A. (1988) Identification of a thunderstorm as a source of short period gravity waves in the upper atmospheric nightglow emissions, *Planet. Space Sci.*, **36**:975

Taylor, M.J., Hapgood, M.A., and Rothwell, P. (1987) Observations of gravity wave propagation in the OI (577.7 nm) and the near infra-red OH nightglow emissions, *Planet. Space Sci.*, **35**:413

Taylor, M.J., and Henriksen, K. (1989) Gravity wave studies at polar latitudes, in *Electromagnetic Coupling In the Polar Clefts and Caps*, P.E. Sandholt and A. Egeland, eds., Kluwer Academic Publishers, pp. 421-4

Taylor, M.J., and Hill, M.J. (1991) Near infrared imaging of hydroxyl wave structure over an ocean site at low latitudes *Geophys. Res. Lett.*, **18**:1333-1336

Taylor, M.J., Lowe, R.P., and Baker, D.J. (1995) Hydroxyl temperature and intensity measurements during noctilucent cloud displays, *Annales Geophysicae*, in press, 1995

Taylor, M.J., Lowe, R.P., Baker, D.J., and Ulwick, J. (1989) On the association of the OH nightglow emission with noctilucent clouds, *Proceedings, International Noctilucent Cloud Workshop*, Tallinn, Estonia,

Taylor, M.J., Ryan, E.H., Tuan, T.-F., and Edwards, R. (1992) Evidence of preferential directions for gravity wave propagation due to wind filtering in the middle atmosphere, *J. Geophys. Res.*, **98**:6047-6057

Taylor, M.J., Turnbull, D.N., and Lowe, R.P. (1991) Coincident imaging and spectrometric observations of zenith OH nightglow structure, *Geophys. Res. Lett.*, **18**:19-1352

Taylor, M.J., van Eyken, A.P., Rishbeth, H., Witt, G., Witt, N., and Clilverd (1989) Simultaneous observations of noctilucent clouds and polar mesospheric radar echoes: evidence of non-correlation, *Planet. Space Sci.*, **37**:1013-1020

Tuan, T.-F. (1991) *An Investigation in Atmospheric Dynamics and Its Effects on Optical Emission*, PL-TR-91-2193, Phillips Laboratory, Hanscom AFB, MA, Final Report, Contract F19628-87-K-0023, University of Cincinnati, NTIS No. ADA 244504

Tuan, T.-F. (1989) Nonlinear airglow response III, *EOS*, **70**(Addendum 4)

Tuan, T.-F., Hedinger, R., Silverman, S., and Okuda, M. (1979) On gravity wave induced Brunt-Vaisala oscillations, *J. Geophys. Res.*, **84**:393-398

Tuan, T.-F., Isler, J., and Makhlof, U. (1988) Nonlinear airglow response to linear gravity waves, *EOS*, **69**:12

Tuan, T.-F., Lowe, R.P., Isler, J.R., Picard, R.H., and Bhattacharyya, A. (1995) Analysis of air parcel motions in the presence of gravity waves and winds; implications for direct optical wave observations, Submitted to *Can. J. Phys.*

Tuan, T.-F., and Wang, D.Y. (1984) Reply to Hines' 'Comments on "potential" treatment of atmospheric waves', *J. Geophys. Res.*, **89**:3965. N.B. This paper was written as part of the precursor to MAPSTAR.

Turek, R.S. (1986) *An Analysis of Upper Atmospheric Parameters Derived from the Observation of Meteor Echoes by a 2.66 MHz Radar*, Master's degree thesis, Utah State University in Dept of Soil Science and Biometeorology (Aeronomy), CASS Report GR-06, Center for Atmospheric and Space Science

Turnbull, D.N., and Lowe, R.P. (1991) Temporal Variations in the hydroxyl nightglow observed during ALOHA-90, *Geophys. Res. Lett.*, **18**:15-18

Turnbull, D.N., and Lowe, R.P. (1990) A summary of the results obtained by the UWO ground-based MI during ALOHA '90', *EOS*, **71**:1501 (invited paper) See Yoshimoto et al

Turnbull, D.N., and Lowe, R.P. (1989) A review of the evidence for vertical separation of the emission heights of the vibrational levels of the hydroxyl airglow, *EOS*, **70**:1245

Turnbull, D.N., and Lowe, R.P. (1989) New hydroxyl transition probabilities and their importance in airglow studies, *Planet. Space Sci.*, **37**:723-738

Turnbull, D.N., and Lowe, R.P. (1988) An empirical determination of the dipole moment function of OH ($X_2\text{II}$), *J. Chem. Phys.*, **89**:2763-2767

Turnbull, D.N., and Lowe, R.P. (1987) Effect of transition probabilities on the determination of rotational temperatures in OH, *EOS*, **68**:1389

Turnbull, D.N., and Lowe, R.P., (1986) A new dipole moment function for OH based on airglow and laboratory observations *EOS*, **67**:1124

Turnbull, D.N., Lowe, R.P., and Gilbert, K.L. (1988) The measurement and significance of hydroxyl vibrational level populations in the night airglow, *EOS*, **69**:13

Wang, D.Y., and Tuan, T.-F. (1988) Brunt-doppler ducting for small-period gravity waves, *J. Geophys. Res.*, **93**(A9):9916-9926

Wang, D.Y., and Tuan, T.-F. (1986) Effects of dissipation and instability on guided short-period gravity waves, *EOS*, **67**:319

Wang, D.Y., and Tuan, T.-F. (1986) Propagation of short-period gravity waves, *EOS*, **66**:987

Ware, G., and Baker, D. (1990) Spatially separated observations of OH intensity and rotational temperature waves, *EOS*, **71**:573

Ware, G., and Goode, D. (1988) *MAPSTAR Interferometer Piece-Part Drawings*, MAPSTAR Data Report No. 9

Yoshimoto, H. (1990) *Study on Dynamics of the Waves in the Mesospheric Hydroxyl Layer*, Ph.D. Thesis, Utah State University, Dept. of Electrical Engineering. Scientific Report by Space Dynamics Laboratory

B2 ADDITIONAL (NON-MAPSTAR) PUBLICATIONS

Baker, D.J., Lowe, R.P., Ware, G., and Yoshimoto, H. (1986) Wave modulation transferrance to IR fluctuations in the mesosphere, *EOS*, **67**:1124

Blackman, R., and Tukey, J. (1958) *The Measurement of Power Spectra*, New York, Dover

Brown, J., Dewan, E., Murphy, E., and Thomas, P. (1989) *Study of Possible Solar Heating Effects on Thermosonde Probes - Error Analysis*, Geophysics Laboratory (AFSC), GL-TR-89-0178 NTIS No. ADA 218116

Gossard, E., and Hooke, W. (1975) *Waves in the Atmosphere*, Amsterdam, Elsevier

infeld, E., and Rowlands, G. (1990) *Nonlinear Waves, Solitons, and Chaos*, Cambridge Press

Teitelbaum, H., and Bauer, P. (1990) *Ann. Geophys.*, **8**:239

B3 MAPSTAR PRESENTATIONS

Dewan, E. (1992) Mesospheric dynamics and OH airglow temperature measurements, Invited paper, CEDAR Workshop, June 21-26, 1992, Boulder, CO

Dewan, E. (1992) Physical models for atmospheric gravity wave spectra and vertical transport implications, NATO Advanced Workshop, May 23-29, 1992, Loen, Norway

Dewan, E. (1992) Mesospheric dynamics and OH airglow temperature measurements, AGU Spring Meeting, May 1992

Dewan, E. (1991) On the question of interpretation of atmospheric gravity wave spectra from lidar and balloon measurements, AGU Fall Meeting, Dec 1991

Dewan, E. (1991) Ground-based measurements of mesospheric OH airglow temperature fluctuations, their PSD's and quantitative interpretation in terms of a gravity wave model, AGU Spring Meeting, May 1991

Dewan, E. (1990) A physical basis for the spatial and temporal gravity wave 'universal' spectrum, AGU Fall Meeting, Dec 1990

Dewan, E. (1989) The MAPSTAR mesospheric hydroxyl airglow 1988 field campaign - an overview, AGU Fall Meeting, Dec 1989

Dewan, E. (1989) Why do atmospheric gravity waves have a 'universal power spectral density'? Invited presentation at SUNY, Albany, NY, Apr 24, 1989

Dewan, E.M. (1988) Statistical test for causal correlation between time series having large autocorrelation: are sunspot-weather correlations real?, CEDAR Workshop, Boulder CO, June 6-10 1988

Dewan, E.M. (1987) New results concerning the saturation explanation of the universal gravity wave spectral model , GRATMAP Meeting, Adelaide, Australia, May 18-23, 1987

Dewan, E.M. (1986) Waves & Turbulence, the physical difference, Scripps workshop, San Diego, 3-5 Dec 1986

Dewan, E.M., and Fougere, P., (1987) Gravity waves and the maximum entropy method of spectral analysis, GRATMAP Meeting, Adelaide, Australia, May 18-23, 1987

Dewan and Good, R.E., (1986) Explanations of the universal vertical wavenumber spectrum of gravity waves, Scripps Workshop, San Diego, 3-5 Dec 1986

Dewan, and Grossbard, N., (1987) Contrast between Fourier and Maximum Entropy spectral analysis applied to atmospheric wave data, AGU Fall Meeting, Dec 6-11, 1987

Dewan, E., Pendleton, W., Grossbard, N., and Espy, P., (1991) Gravity-wave spectra from ground-based OH mesospheric temperature measurements and interpretations via a cascade model, CEDAR Workshop, Boulder, CO, June 17-21, 1991

Dewan, E.M. and Tuan, T.-F. (1988) On hydrostatic and non-hydrostatic changes of pressure caused by atmospheric gravity waves, AGU Fall Meeting, Dec 5-9, 1988, EOS, **69**:12

Espy, P., and Taylor, M.J. (1991) Radiometric Measurements and PSD's vs. Taylor All-Sky-Structure-Cover-Percent-Parameter, MAPSTAR Workshop April 22-23, 1991, Hanscom AFB, MA

Grossbard, N., and Dewan, E., (1991) Methods for estimating the autocorrelation and power spectral density function when there are many missing data values, ASSP Workshop on Spectral Estimation and Modeling, Oct 10-12, 1991

Isler, J., Makhlof, U., Tuan, T.-F., and Picard, R.H. (1989) Lagrangian approach to airglow response, EOS, **70**:1242

Isler, J., Tuan, T-F., He, F., and Dewan, E., (1990) Trajectories of linear gravity wave fluid elements, their possible observation with interferometers, AGU Fall Meeting, Dec 1990, EOS, **71**:1495

Isler, J., Tuan, T.-F., Makhlof, U., and Picard, R.H. (1988) Perturbation treatment of nonlinear airglow response, EOS, **69**:1324

Lowe, R.P. (1991) Presentation to Final MAPSTAR Workshop, University of Western Ontario, 24 September 1991

Lowe, R.P., (1991) Simultaneous measurements of the horizontal structure and spectrum of the hydroxyl in the zenith, Eighteenth Annual European Meeting on Atmospheric Studies by Optical Methods, Tromso, Norway, June 1991

Lowe, R.P. (1990) Recent observations of gravity wave effects in the hydroxyl airglow, Seventeenth Annual European Meeting on Atmospheric Studies by Optical Methods, Abastumani, Georgia, September 1990

Lowe, R.P., Gilbert, K.L., and Turnbull, D.N. (1990) Hydroxyl airglow observations at high latitude under summer conditions, EOS, **70**:1245

Lowe, R.P., Gilbert, K.L., and Turnbull, D.N., (1988) High latitude summer observation of intensity and rotational temperature of the hydroxyl airglow, Joint Symposium on a Middle Atmosphere Science IAGA/IAMAP, Exeter (UK), July 1988

Lowe, R.P., and Taylor, M.J. (1988) The implications of high hydroxyl rotational temperatures during noctilucent cloud displays, Noctilucent Cloud Symposium IAMAP, Reading (UK) August 1988

Lowe, R.P., Turnbull, D.N., Meriwether, J.W., Dao, P.D., and McNutt, R.T. (1990) Simultaneous lidar and Fourier transform spectrometer observations of temperature fluctuations of the midlatitude mesopause region, *EOS*, **71**:573

Peterson, A (1989) 1. Horizon to Horizon Monochromatic Sine-Wave in OH Airglow - All Sky Film Camera Image., and 2. Color Photograph of OH, NA, and OI Airglows, Private Data Submissions to MAPSTAR Project

Peterson, A.W., Lin, J.J., and Tuan, T.-F. (1985) Analysis of simultaneous observation of 6300A, 7300A, 7900A OH bands and 5577 OI together with radiometric observations, *EOS*, **66**:324

Peterson, A.W., and Tuan, T.-F. (1983) Visual, photographic and photometric observations of OH (7300) and OI (5577) emissions during the bright night of June 14-15, 1983, *EOS* (Fall, 1983)

Rothwell, P., Taylor, M.J., Tagirov, V.R., and Chernous, S.A. (1990) On the auroral sources of internal gravity waves, 17th Annual Meeting on Atmospheric Studies by Optical Methods, Abastumani Astrophysical Observatory, Georgian SSR, USSR, September 1990

Ryan, E.H., and Tuan, T.F. (1991) Gravity waves blocking by critical layers, in paper presented at Middle Atmosphere Periodic Structure and Associated Radiance (MAPSTAR) Meeting, AFGL, 22-23 Apr., 1991

Steed, A., Ulwick, J., Lowe, R.P., Turnbull, D.N., and Taylor, M.J. (1986) The association of noctilucent clouds with the OH airglow emission, *EOS*, **67**:1123

Taylor, M.J. (1991) High Latitude noctilucent clouds and low latitude airglow studies, Invited talk, The Auroral Observatory, University of Tromso, Norway, May 1991

Taylor, M.J. (1990) Observations of mesospheric wave structure over an ocean site at low latitudes, Special session on the ALOHA-90 Campaign, American Geophysical Union, San Francisco, December 1990

Taylor, M.J. (1990) Noctilucent cloud studies at Southampton, invited talk, Department of Physics, University of Tartu, Estonian SSR, USSR, November 1990

Taylor, M.J., (1990) Measurements of Wave Motions in the near infrared OH nightglow emission, 17th Annual Meeting on Atmospheric studies by Optical Methods, Abastumani Astrophysical Observatory, Georgian SSR, USSR, September 1990

Taylor, M.J. (1989) Studies of middle atmosphere motions as revealed by the airglow emissions, Invited talk, Arrhenius Laboratory, University of Stockholm, Sweden, March 1989

Taylor, M.J. (1988) On the optical signature of a giant auroral pulsation event, Magnetospheric, Ionospheric, Solar Terrestrial (MISTI) Meeting, Sheffield, U.K., April 1988

Taylor, M.J. (1988) TV measurements of hydroxyl nightglow structures, invited talk, Physics Dept., University of Western Ontario, London, Ontario, Canada, February 1988

Taylor, M.J. (1988) Analysis techniques for airglow image data, Invited talk, Electrical Engineering Department, Brigham Young University, Provo, Utah, USA, January 1988

Taylor, M.J. (1987) Infra-red imaging of gravity waves in the nightglow emissions, Invited talk, Geophysical Institute, University of Alaska, Fairbanks, Alaska, USA, August 1987

Taylor, M.J. (1986) Low Light TV measurements of OH wave structure, Invited talk for Progress in MAP-Related projects symposium, Royal Astronomical Society, London, U.K., Spring 1986

Taylor, M.J. (1985) Breaking long period waves as a source of OH airglow structure, Invited talk, Air Force Geophysics Laboratory, Hanscom AFB, Bedford, MA, December 1985

Taylor, M.J. (1985) On the morphology of OH airglow structure, Invited talk, American Geophysical Union, San Francisco, USA, December 1985

Taylor, M.J., and Henriksen, K. (1988) Gravity Wave studies at polar latitudes, Invited talk, NATO Advanced Workshop on Electromagnetic Coupling in the Polar Clefts and Caps, Lillehammer, Norway, September 1988

Taylor, M.J., Lowe, R.P., Baker, D.J., and Ulwick, J. (1988) On the association of the OH nightglow emission with noctilucent clouds, International workshop on noctilucent Clouds Tallinn, Estonia, 27-31 July 1988

Taylor, M.J., Lowe, R.P., and Ulwick, J. (1990) Coordinated measurements of noctilucent clouds and the hydroxyl nightglow emission, American Geophysical Union Meeting, Baltimore, MD, Spring 1990, *EOS*, **71**:572

Taylor, M.J., Ryan, E.H., and Tuan, T.-F. (1991) Effects of wind filtering on OH airglow observations of gravity wave propagation, American Geophysical Union meeting, San Francisco, CA, December 1991, *EOS*, **72**:208

Turnbull, D.N., Lowe, R.P., and Gilbert, K.L. (1991) Temporal variations of the OH nightglow, IUGG General Assembly, Vienna, Austria, August 1991

Wang, D.Y., and Tuan, T.-F. (1987) Effects of the variation of Brunt period with height on gravity waves, International Union of Geodesy and Geophysics (IUGG), XIX General Assembly, **3**:789

Ware, G., Baker, D., and Taylor, M. (1993) High-altitude infrared emission "clouds:" structures and motions, Annual meeting of the Utah Academy of Sciences, Arts, and Letters, May 1993, (Submitted to *ENCYLIA*, Nov. 1993)

Yoshimoto, H., Lowe, R.P., and Turnbull, D.N. (1990) The detection and interpretation of internal gravity wave signatures in ground-based hydroxyl airglow data from ALOHA '90 and from the Delaware Observatory, *EOS*, **71**:1501

B4 NON-MAPSTAR PRESENTATIONS

Espy, P., and Taylor, M.J. (1992) Break period of radiometric PSD vs structure in imager, presented at SOAR Workshop No. 2, 1 Oct 1992

Lowe, R.P., Gilbert, K.L., Baker, K.J., and Steed, A. (1986) Cross calibration of hydroxyl airglow intensities and rotational temperatures, *EOS*, **68**:1396

Makhlof, U., Picard, R.H., and Winick, J.R. (1991) The hydroxyl airglow: Steady state and response to gravity wave forcing, General Assembly, International Union of Geodesy and Geophysics, Vienna, 11-24 Aug

Makhlof, U., Picard, R.H., and Winick, J.R. (1991) The effect of quenching on modulation of the hydroxyl emission layer by gravity waves, Spring Meeting, AGU, 28-31 May, (Abstract published in *EOS*, **72**:208, April 1991)

Makhlof, U., Picard, R.H., Winick, J.R., Tuan, T.-F., and Ryan, E. (1991) Hydroxyl airglow fluctuation due to gravity waves propagating in a realistic atmosphere in the presence of background wind, *EOS*, **72**:374

Makhlouf, U., Picard, R.H., and Winick, J.R. (1990) Modulation of the hydroxyl emission by a monochromatic gravity wave in a realistic, non-isothermal atmosphere, Fall Meeting, AGU, 3-7 Dec, (Abstract published in *EOS*, **71**:1496)

Makhlouf, V., Tuan, T-F, and Dewan , E., (1989) Further analysis of the hydrostatic and nonhydrostatic effects in gravity waves, AGU Spring Meeting, May 7-12, 1989, *EOS*, **70**(Addendum 4)

McIntyre, M. (1992) Comment made at NATO Advanced Research Workshop, Loen, Norway

Peterson, A. (1990) Color photographs of active OI (5577) and OH airglow with comparisons to video and fisheye pictures, presented at AGU spring meeting, *EOS*, **71**:571

Peterson, A. (1990) Analysis of an extensive, long wavelength OH wave packet generated by a thunderstorm, presented at AGU fall meeting, *EOS*, **70**:1244

Taylor, M.J., Avery, J. S., and Connor, L. (1989) Simultaneous radar and imaging observations at mesospheric heights, *EOS*, **70**:1244

B5 PUBLICATIONS AND PRESENTATIONS OF EDMOND DEWAN

Dewan, E. (1991) Similitude modeling of internal gravity wave spectra, *Geophys. Res. Lett.*, **18**: 1473-1476

Dewan, E. (1990) *Power Spectra of Internal Gravity Waves*, Geophysics Laboratory (AFSC), GL-TR-90-0233, Special Reports, No. 265, ADA 231596

Dewan, E.M. (1979) Stratospheric wave spectra resembling turbulence, *Science*, **204**:832-835

Dewan, E., and Good, R.E., (1986) Saturation and the universal spectrum for vertical profiles of horizontal scalar winds in the atmosphere, *J. Geophys. Res.*, **91**, D2:2,742-2,748

Dewan, E., Grossbard, N., Good, R.E., and Brown, J., (1988) Power spectral densities of zonal and meridional winds in the stratosphere, *Physica Scripta*, **37**:154-157

Dewan, E., Grossbard, N., Quesada, A., and Good, R.E. (1984) Spectral analysis of 10 m resolution scalar velocity profiles in the stratosphere, *Geophys. Res. Lett.*, **11**:624

Dewan, E., Pendleton, W., Grossbard, N., and Espy, P. (1992) Mesospheric OH airglow temperature fluctuations: A Spectral Analysis, *Geophys. Res. Lett.*, **19**:597-600

Dewan, E., and Shapiro, R., (1991) Are sunspot-weather correlations real?, *J. Atmos. Terr. Phys.*, **53**:171-174

Dewan, E.M. and Tuan, T.-F. (1988) On hydrostatic and non-hydrostatic changes of pressure caused by atmospheric gravity waves, AGU Fall Meeting, Dec 5-9, 1988, *Trans. Am. Geophys. Union*, **69**:1342

Good, R.E., Beland R., Murphy, E., Brown, J., and Dewan, E. (1988) Atmospheric models of optical turbulence, *SPIE Reports*, Vol. 928, *Modeling of the Atmosphere*, L. Rothman, Ed., pp. 165-186

Makhlouf, U., Dewan, E., Isler, J.R., and Tuan, T.-F., (1990) On the importance of the purely gravitationally induced density, pressure, and temperature variations in gravity waves: Their application to airglow observations, *J. Geophys. Res.*, **95**:(A4)4103-4111

Presentations

Dewan, E.(1992) Mesospheric dynamics and OH airglow temperature measurements, Invited paper, CEDAR Workshop, June 21-26, 1992, Boulder, CO

Dewan, E. (1992) Physical models for atmospheric gravity wave spectra and vertical transport implications, NATO Advanced Workshop, May 23-29, 1992, Loen, Norway

Dewan, E. (1992) Mesospheric dynamics and OH airglow temperature measurements, AGU Spring Meeting, May 1992

Dewan, E. (1991) On the question of interpretation of atmospheric gravity wave spectra from lidar and balloon measurements, AGU Fall Meeting, Dec 1991

Dewan, E. (1991) Ground-based measurements of mesospheric OH airglow temperature fluctuations, their PSD's and quantitative interpretation in terms of a gravity wave model, AGU Spring Meeting, May 1991

Dewan, E. (1990) A physical basis for the spatial and temporal gravity wave 'universal' spectrum, AGU Fall Meeting, Dec 1990

Dewan, E. (1989) The MAPSTAR mesospheric hydroxyl airglow 1988 field campaign - an overview, AGU Fall Meeting, Dec 1989

Dewan, E. (1989) Why do atmospheric gravity waves have a 'universal power spectral density'? Invited presentation at SUNY, Albany, NY, Apr 24, 1989

Dewan, E.M. (1988) Statistical test for causal correlation between time series having large autocorrelation: are sunspot-weather correlations real?, CEDAR Workshop, Boulder CO, June 6-10 1988

Dewan, E.M. (1987) New results concerning the saturation explanation of the universal gravity wave spectral model , GRATMAP Meeting, Adelaide, Australia, May 18-23, 1987

Dewan, E.M. (1986) Waves & Turbulence, the physical difference, Scripps workshop, San Diego, 3-5 Dec 1986

Dewan, E.M., and Fougere, P., (1987) Gravity waves and the maximum entropy method of spectral analysis, GRATMAP Meeting, Adelaide, Australia, May 18-23, 1987

Dewan, E. and Good, R.E., (1986) Explanations of the universal vertical wavenumber spectrum of gravity waves, Scripps Workshop, San Diego, 3-5 Dec 1986

Dewan, E., and Grossbard, N., (1987) Contrast between Fourier and Maximum Entropy spectral analysis applied to atmospheric wave data, AGU Fall Meeting, Dec 6-11, 1987

Dewan, E., Pendleton, W., Grossbard, N., and Espy, P., (1991) Gravity-wave spectra from ground-based OH mesospheric temperature measurements and interpretations via a cascade model, CEDAR Workshop, Boulder, CO, June 17-21, 1991

Grossbard, N., and Dewan, E., (1991) Methods for estimating the autocorrelation and power spectral density function when there are many missing data values, ASSP Workshop on Spectral Estimation and Modeling, Oct 10-12, 1991

B6 PUBLICATIONS OF M.J. TAYLOR AND COLLEAGUES

Chisham, G. (1990) Ph.D. Thesis, Physics Department, University of York, U.K.

Chisham, G., Orr, D., Taylor, M.A., and Luhr, H. (1990) The magnetic and optical signature of a Pg pulsation, *Planet. Space Sci.*, **38**:1443

Gadsden, M., and Taylor, M.J. (1992) Anweisungen fur die photographischen aufnahmen der leuchtenden nachtwolken - 103 years on, *J. Atmos. Terr. Phys.*, **56**:447-459

Simmons, D.A.R., Henriksen, K., Taylor, J.J., and Hermansen, D (1990) A remarkable outburst of solar activity and its geomagnetic effects, *J. Br. Astron. Assoc.*, **100**:280

Taylor, M.J. (1991) *MAPSTAR Final Report*, on sub contract 387-003 and C802640 [period covered, 1 October 1987 to 30 June 1991], between Utah State University and Southampton University, U.K. Presented at the final MAPSTAR workshop, University of western Ontario, London, Ontario, September 1991

Taylor, M.J. (1991) Final Report, on subcontract between Southampton University and University of Cincinnati, issued as part of Air Force Contract F19628-87-K-0023 (covering 3 May 1990 to 4 April 1991), Submitted to University of Cincinnati, June 1991, contributed to PL-TR-91-2193; ADA 244504

Taylor, M.J. (1989) *Comparison of Southampton Image Data and Thunderstorm Maps for the Colorado MAPSTAR Campaign, 1988*, MAPSTAR Report, June 1988

Taylor, M.J. (1989) *First Results from the MAPSTAR Colorado Campaign*, MAPSTAR Interim Report No. 4, submitted to USU February, 1989

Taylor, M.J. (1986) TV observations of mesospheric wave structure, in: Collections of the Works of the International Workshop of Noctilucent Clouds, *Valgus*, 153

Taylor, M.J. (1985) MAPSTAR Final Report, on subcontract 85-049, [period covered, 1 October 1985 to 30 September 1987] between Utah State University and Southampton University, U.K., submitted to USU November 1987

Taylor, M.J. (1985) MAPSTAR Final Report, on subcontract 85-049, [period covered, 1 January 1985 to 30 September 1985] between Utah State University and Southampton University, U.K., submitted to USU November 1985

Taylor, M.J. (1985) Observation and analysis of wave-like structures in the lower thermospheric nightglow emissions, Ph.D. Thesis, Southampton University, U.K.

Taylor, M.J., Chisham, G., and Orr, D. (1989) Pulsating auroral forms and their association with geomagnetic giant pulsations, *Planet. Space Sci.*, **37**:1477

Taylor, M.J., Avery, J. S., and Connor, L. (1989) Simultaneous radar and imaging observations at mesospheric heights, *EOS*, **70**:1244

Taylor, M.J., Connor, L., Avery, S.K., and Pendleton, Jr., W (1995) Simultaneous radar, imaging and interferometer measurements at mesospheric heights, *Submitted to J. Geophys Res.* (Presented at Winter AGU Meeting, San Francisco, q.v.)

Taylor, M.J., and Edwards, R. (1991) Observations of short period mesospheric wave patterns; *in situ* or tropospheric wave generation? *Geophys. Res. Lett.*, **18**:1337

Taylor, M.J., Espy, P.J., Baker, D.J., Sica, R.J., Neal, P.C., and Pendleton, Jr., W. (1991) Simultaneous temperature, intensity and imaging measurements of short period wave structure in the OH nightglow emission, *Planet. Space Sci.*, **39**:1172

Taylor, M.J., and Hapgood, M.A. (1990) On the origin of ripple-type wave structure in the OH nightglow emission, *Planet Space Sci.*, **38**:1421

Taylor, M.J., and Hapgood, M.A. (1988) Identification of a thunderstorm as a source of short period gravity waves in the upper atmospheric nightglow emissions, *Planet. Space Sci.*, **36**:975

Taylor, M.J., Hapgood, M.A., and Rothwell, P. (1987) Observations of gravity wave propagation in the OI (577.7 nm) and the near infra-red OH nightglow emissions, *Planet. Space Sci.*, **35**:413

Taylor, M.J., and Henriksen, K. (1989) Gravity wave studies at polar latitudes, in *Electromagnetic Coupling In the Polar Clefts and Caps*, P.E. Sandholt and A. Egeland, eds., Kluwer Academic Publishers, pp. 421-434

Taylor, M.J., and Hill, M.J. (1991) Near infrared imaging of hydroxyl wave structure over an ocean site at low latitudes, *Geophys. Res. Lett.*, **18**:1333-1336

Taylor, M.J., Lowe, R.P., and Baker, D.J. (1995) Hydroxyl temperature and intensity measurements during noctilucent cloud displays, *Annales Geophysicae*, in press, 1995

Taylor, M.J., Ryan, E.H., Tuan, T.-F., and Edwards, R. (1992) Evidence of preferential directions for gravity wave propagation due to wind filtering in the middle atmosphere, *J. Geophys. Res.*, **98**:6047-6057

Taylor, M.J., Ryan, E.H., and Tuan, T.-F. (1991) Effects of wind filtering on OH airglow observations of gravity wave propagation, American Geophysical Union meeting, San Francisco, CA, December 1991, *Trans. Am. Geophys. Union*, **72**:208

Taylor, M.J., Turnbull, D.N., and Lowe, R.P. (1991) Coincident imaging and spectrometric observations of zenith OH nightglow structure, *Geophys. Res. Lett.*, **18**:1349-1352

Taylor, M.J., van Eyken, A.P., Rishbeth, H., Witt, G., Witt, N., and Clilverd (1989) Simultaneous observations of noctilucent clouds and polar mesospheric radar echoes: evidence of non-correlation, *Planet. Space Sci.*, **37**:1013-1020

Ware, G., and Baker, D. (1990) Spatially separated observations of OH intensity and rotational temperature waves, *EOS*, **71**:573

Ware, G., Baker, D., and Taylor, M. (1993) High-altitude infrared emission "clouds:" structures and motions, Annual meeting of the Utah Academy of Sciences, Arts, and Letters, May 1993, (Submitted to ENCYLIA, Nov. 1993)

Ware, G., and Goode, D. (1988) *MAPSTAR Interferometer Piece-Part Drawings*, MAPSTAR Data Report No. 9

Presentations

Baker, D.J., Lowe, R.P., Ware, G., and Yoshimoto, H. (1986) Wave modulation transferrance to IR fluctuations in the mesosphere, *EOS*, **67**:1124

Espy, P., and Taylor, M.J. (1992) Break period of radiometric PSD vs structure in imager, presented at SOAR Workshop No. 2, 1 Oct 1992

Espy, P., and Taylor, M.J. (1991) Radiometric Measurements and PSD's vs. Taylor All-Sky-Structure-Cover-Percent-Parameter, MAPSTAR Workshop April 22-23, 1991, Hanscom AFB, MA

Taylor, M.J. (1991) High Latitude noctilucent clouds and low latitude airglow studies, Invited talk, The Auroral Observatory, University of Tromso, Norway, May 1991

Taylor, M.J. (1990) Observations of mesospheric wave structure over an ocean site at low latitudes, Special session on the ALOHA-90 Campaign, American Geophysical Union, San Francisco, December 1990

Taylor, M.J. (1990) Noctilucent cloud studies at Southampton, invited talk, Department of Physics, University of Tartu, Estonian SSR, USSR, November 1990

Taylor, M.J., (1990) Measurements of Wave Motions in the near infrared OH nightglow emission, 17th Annual Meeting on Atmospheric studies by Optical Methods, Abastumani Astrophysical Observatory, Georgian SSR, USSR, September 1990

Taylor, M.J. (1989) Studies of middle atmosphere motions as revealed by the airglow emissions, Invited talk, Arrhenius Laboratory, University of Stockholm, Sweden, March 1989

Taylor, M.J. (1988) On the optical signature of a giant auroral pulsation event, Magnetospheric, Ionospheric, Solar Terrestrial (MISTI) Meeting, Sheffield, U.K., April 1988

Taylor, M.J. (1988) TV measurements of hydroxyl nightglow structures, invited talk, Physics Dept., University of Western Ontario, London, Ontario, Canada, February 1988

Taylor, M.J. (1988) Analysis techniques for airglow image data, Invited talk, Electrical Engineering Department, Brigham Young University, Provo, Utah, USA, January 1988

Taylor, M.J. (1987) Infra-red imaging of gravity waves in the nightglow emissions, Invited talk, Geophysical Institute, University of Alaska, Fairbanks, Alaska, USA, August 1987

Taylor, M.J. (1986) Low Light TV measurements of OH wave structure, Invited talk for Progress in MAP-Related projects symposium, Royal Astronomical Society, London, U.K., Spring 1986

Taylor, M.J. (1985) Breaking long period waves as a source of OH airglow structure, Invited talk, Air Force Geophysics Laboratory, Hanscom AFB, Bedford, MA, December 1985

Taylor, M.J. (1985) On the morphology of OH airglow structure, Invited talk, American Geophysical Union, San Francisco, USA, December 1985

Taylor, M.J., and Henriksen, K. (1988) Gravity Wave studies at polar latitudes, Invited talk, NATO Advanced Workshop on Electromagnetic Coupling in the Polar Clefts and Caps, Lillehammer, Norway, September 1988

Taylor, M.J., Lowe, R.P., Baker, D.J., and Ulwick, J. (1989) On the association of the OH nightglow emission with noctilucent clouds, Proceedings, International Noctilucent Cloud Workshop, Tallinn, Estonia,

Taylor, M.J., Lowe, R.P., Baker, D.J., and Ulwick, J. (1988) On the association of the OH nightglow emission with noctilucent clouds, International workshop on noctilucent Clouds Tallinn, Estonia, 27-31 July 1988

Taylor, M.J., Lowe, R.P., and Ulwick, J. (1990) Coordinated measurements of noctilucent clouds and the hydroxyl nightglow emission, American Geophysical Union Meeting, Baltimore, MD, Spring 1990, *EOS*, **71**:572

B7 PUBLICATIONS OF R. LOWE AND COLLEAGUES

Gardner, C.S., Kane, T.J., Yeo, J.H., Niciejewski, R.J., Hecht, J.H., Walterschied, R.L., Lowe, R.P., and Turnbull, D.N. (1991) Formation characteristics of sporadic Na layers observed simultaneously by LIDAR and airglow instruments during ALOHA-90, *Geophys. Res. Lett.*, **18**:1369-1372

Gilbert, K.L., and Lowe, R.P. (1990) The effect of quenching on the correlation of hydroxyl airglow intensities and rotational temperatures, *EOS*, **70**:1245

Gilbert, K.L., and Lowe, R.P. (1988) Does the hydroxyl rotational temperature vary with vibrational level?, *EOS*, **69**:1343

Gilbert, K.L., and Lowe, R.P. (1987) A synthetic spectrum fitting technique for determining hydroxyl rotational temperature, *EOS* **68**:1389

Lowe, R.P., Gilbert, K.L., and Turnbull, D.N. (1991) High latitude summer observations of the hydroxyl airglow, *Planet. Space Sci.*, **39**:1263-1270

Lowe, R.P., Gilbert, K.L., and Turnbull, D.N. (1990) Hydroxyl airglow observations at high latitude under summer conditions, *EOS*, **70**:1245

Lowe, R.P., Turnbull, D.N., Meriwether, J.W., Dao, P.D., and McNutt, R.T. (1990) Simultaneous lidar and Fourier transform spectrometer observations of temperature fluctuations of the midlatitude mesopause region, *EOS*, **71**:573

Steed, A., Ulwick, J., Lowe, R.P., Turnbull, D.N., and Taylor, M.J. (1986) The association of noctilucent clouds with the OH airglow emission, *EOS*, **67**:1123

Turnbull, D.N., and Lowe, R.P. (1991) Temporal Variations in the hydroxyl nightglow observed during ALOHA-90, *Geophys. Res. Lett.*, **18**:1345-1348

Turnbull, D.N., and Lowe, R.P. (1990) A summary of the results obtained by the UWO ground-based MI during ALOHA '90', *EOS*, **71**:1501 (invited paper) See Yoshimoto et al

Turnbull, D.N., and Lowe, R.P. (1989) A review of the evidence for vertical separation of the emission heights of the vibrational levels of the hydroxyl airglow, *EOS*, **70**:1245

Turnbull, D.N., and Lowe, R.P. (1989) New hydroxyl transition probabilities and their importance in airglow studies, *Planet. Space Sci.*, **37**:723-738

Turnbull, D.N., and Lowe, R.P. (1988) An empirical determination of the dipole moment function of OH ($X_2\Pi$), *J. Chem. Phys.*, **89**:2763-2767

Turnbull, D.N., and Lowe, R.P. (1987) Effect of transition probabilities on the determination of rotational temperatures in OH, *EOS*, **68**:1389

Turnbull, D.N., and Lowe, R.P., (1986) A new dipole moment function for OH based on airglow and laboratory observations *EOS*, **67**:1124

Turnbull, D.N., Lowe, R.P., and Gilbert, K.L. (1988) The measurement and significance of hydroxyl vibrational level populations in the night airglow, *EOS*, **69**:1343

Yoshimoto, H., Lowe, R.P., and Turnbull, D.N. (1990) The detection and interpretation of internal gravity wave signatures in ground-based hydroxyl airglow data from ALOHA '90 and from the Delaware Observatory, *EOS*, **71**:1501

Presentations

Lowe, R.P. (1991) Presentation to Final MAPSTAR Workshop, University of Western Ontario, 24 September 1991

Lowe, R.P., (1991) Simultaneous measurements of the horizontal structure and spectrum of the hydroxyl in the zenith, Eighteenth Annual European Meeting on Atmospheric Studies by Optical Methods, Tromso, Norway, June 1991

Lowe, R.P. (1990) Recent observations of gravity wave effects in the hydroxyl airglow, Seventeenth Annual European Meeting on Atmospheric Studies by Optical Methods, Abastumani, Georgia, September 1990

Lowe, R.P., Gilbert, K.L., and Turnbull, D.N., (1988) High latitude summer observation of intensity and rotational tempeature of the hydroxyl airglow, Joint Symposium on a Middle Atmosphere Science IAGA/IAMAP, Exeter (UK), July 1988

Lowe, R.P., and Taylor, M.J. (1988) The implications of high hydroxyl rotational temperatures during noctilucent cloud displays, Noctilucent Cloud Symposium IAMAP, Reading (UK) August 1988

Turnbull, D.N., Lowe, R.P., and Gilbert, K.L. (1991) Temporal variations of the OH nightglow, IUGG General Assembly, Vienna, Austria, August 1991

B8 PUBLICATIONS OF T.-F. TUAN AND COLLEAGUES

Isler, J.R., Tuan, T.-F., Picard, R.H., and Makhlouf, U. (1991) On the nonlinear response of airglow to linear gravity waves, *J. Geophys. Res.*, **96A**:14,141-14,152

Isler, J., Makhlouf, U., Tuan, T.-F., and Picard, R.H. (1989) Lagrangian approach to airglow response, *EOS*, **70**:1242

Isler, J., Tuan, T.-F., He, F., and Dewan, E., (1990) Trajectories of linear gravity wave fluid elements, their possible observation with interferometers, AGU Fall Meeting, Dec 1990, *EOS*, **71**:1495

Isler, J.R., Tuan, T.-F., He, F., and Picard, R.H. (1994) Perturbation treatment of the nonlinear response of minor atmospheric species to linear gravity waves, *J. Geophys. Res.* (revision)

Isler, J., Tuan, T.-F., Makhlouf, U., and Picard, R.H. (1988) Perturbation treatment of nonlinear airglow response, *EOS*, **69**:1324

Makhlouf, V., Tuan, T-F, and Dewan , E., (1989) Further analysis of the hydrostatic and nonhydrostatic effects in gravity waves, AGU Spring Meeting, May 7-12, 1989, *EOS*, **70** (Addem 4)

Makhlouf, U., Wang, D.Y., Lin, J.J., and Tuan, T.-F. (1990) On the importance of the purely gravitationally induced density, pressure, and temperature variations in gravity waves: their application to airglow observations, *J. Geophys. Res.*, **95**:4103-4111

Makhlouf, U., Wang, D.Y., Lin, J.J., and Tuan, T.-F. (1987) Effects of different gravity-wave models and horizontal winds on the mesospheric emission, *EOS*, **68**:1394

Tuan, T.-F. (1991) *An Investigation in Atmospheric Dynamics and Its Effects on Optical Emission*, PL-TR-91-2193, Phillips Laboratory, Hanscom AFB, MA, Final Report, Contract F19628-87-K-0023, University of Cincinnati, NTIS No. ADA 244504

Tuan, T.-F. (1989) Nonlinear airglow response III, *EOS*, **70**(Addem 4)

Tuan, T.-F., Hedinger, R., Silverman, S., and Okuda, M. (1979) On gravity wave induced Brunt-Vaisala oscillations, *J. Geophys. Res.*, **84**:393-398

Tuan, T.-F., Isler, J., and Makhlouf, U. (1988) Nonlinear airglow response to linear gravity waves, *EOS*, **69**:1342

Tuan, T.-F., Lowe, R.P., Isler, J.R., Picard, R.H., and Bhattacharyya, A. (1995) Analysis of air parcel motions in the presence of gravity waves and winds; implications for direct optical wave observations, Submitted to *Can. J. Phys.*

Tuan, T.-F., and Wang, D.Y. (1984) Reply to Hines' 'Comments on "potential" treatment of atmospheric waves', *J. Geophys. Res.*, **89**:3965. N.B. This paper was written as part of the precursor to MAPSTAR.

Wang, D.Y., and Tuan, T.-F. (1988) Brunt-doppler ducting for small-period gravity waves, *J. Geophys. Res.*, **93**(A9):9916-9926

Wang, D.Y., and Tuan, T.-F. (1987) Effects of the variation of Brunt period with height on gravity waves, International Union of Geodesy and Geophysics (IUGG), XIX General Assembly, **3**:789

Wang, D.Y., and Tuan, T.-F. (1986) Effects of dissipation and instability on guided short-period gravity waves, *EOS*, **67**:319